Identification of Genes and Pathways Involved in Schwann Cell Tumor Initiation, Development and Progression to Develop Novel Drug Targets

A DISSERTATION
SUBMITTED TO THE FACULTY OF THE GRADUATE SCHOOL
OF THE UNIVERSITY OF MINNESOTA
BY

Adrienne Leigh Watson

IN PARTIAL FULLFILLMENT OF THE REQUIREMENTS
FOR THE DEGREE OF
DOCTOR OF PHILOSOPHY

Dr. David A. Largaespada

June 2013

Acknowledgements

I would first and foremost like to thank my graduate school advisor Dr. David Largaespada for instilling a passion for science and technology in me, inspiring me to be creative, and allowing me to grow into an independent scientist. I would also like to thank all of the current and former members of the Largaespada lab, including: Dr. Eric Rahrmann, Dr. Branden Moriarity, Dr. Vincent Keng, Sue Rathe, Caitlin Conboy, Barbara Tschida, Pauline Jackson, Micki Diers, and Dominic Beckmann for their immense scientific insight as well as friendship they were willing to share with me over the years. Finally, a huge thanks to the many young scientists who worked on my projects with me: Anna Meyer, Brian Wahl, David Daniels, Bernard Akem, Austin Haynesworth, Andrew Greeley, Leah Anderson, Amanda Halfond, Natasha Powell, and Rory Williams. We made a great team and I could not have done this without you.

Dedication

I would like to dedicate this thesis to those who have endured the toughest battle of their life, cancer. To those who are struggling, my uncle Mark and the bravest little boy I know, Zachary Bartz, keep fighting! To those who I have lost during my graduate career, my uncle Richard, a great friend Paula Austin, and a wonderful mentor Dr. John Ohlfest. You give me hope and inspiration.

Abstract

In 2012 in the United States alone, over 1.6 million people were diagnosed with cancer and nearly 600,000 people died as a result of cancer. Cancer is a disease in which inherited or acquired genetic changes endow cells with abnormal properties such as the ability to rapidly grow and proliferate, resist normal mechanisms of cell death and senescence, induce angiogenesis, invade surrounding tissues and eventually metastasize throughout the body. Malignant peripheral nerve sheath tumors (MPNSTs) are tumors composed of Schwann cells that have acquired these oncogenic characteristics. MPNSTs occur spontaneously in the general population at a rate of 1 in 100,000 people per year, but more commonly occur in the context of Neurofibromatosis Type 1 (NF1), an inherited genetic disease that occurs in 1 in 2,500 live births. NF1 patients develop neurofibromas, benign tumors derived from Schwann cells throughout the peripheral nerves of the body, due to loss of the tumor suppressor gene *Neurofibromin 1* (*NF1*). Ten percent of patients with NF1 will incur additional genetic mutations in *NF1* null cells that lead to the transformation of a benign neurofibroma into an MPNST. With little known about the genetic changes that cause sporadic MPNSTs or transformation from neurofibromas to MPNST, the current treatments for patients with MPNSTs are surgical resection and non-specific chemotherapy and the 5-year survival rate remains very low at less than 25%. In an attempt to better understand the genetic drivers of Schwann cell

tumors and identify potential pathways that could be targeted by small molecule inhibitors, we conducted a *Sleeping Beauty (SB)* unbiased, forward genetic screen in mice. This screen uncovered hundreds of genes that may play a role in Schwann cell tumor initiation, development, progression and maintenance. The following thesis will describe in detail, several of the important findings that came out of the *SB* screen including: the discovery and validation of canonical Wnt/β-catenin signaling as a pathway that plays a role in Schwann cell transformation, progression and tumor maintenance, and the profound clinical implications of co-targeting the MAPK and PI3K pathways, shown to be co-activated in the *SB* screen using small molecule, targeted therapies.

Table of Contents

List of Tables

List of Figures

Chapter 3 **Page**

Chapter 1: Introduction

I. Cancer in the United States

Cancer is a disease in which normal cells in the body acquire or inherit genetic mutations that endow them with abnormal properties, which lead to the formation of a tumor (Hanahan and Weinberg, 2011). In the United States, in 2012, over 1.6 million people were diagnosed with cancer, with an incidence rate of 465.2 per 100,000 men and women based on the National Cancer Institute Surveillance Epidemiology and End Results (SEER data)(Siegel et al., 2012). While detection, diagnosis, and treatment of cancer has been steadily improving over the past decade, nearly 600,000 people died of cancer in 2012 alone and cancer remains the second leading cause of death in the United States (SEER data)(Siegel et al., 2012). Clearly there are improvements that have yet to be made, and in the era of new technology and genetic tools, hopefully, our understanding and treatment of cancer will continue to improve.

II. Cancer is a Genetic Disease

Epidemiological data clearly shows that cancer is a disease of age (SEER data) (Siegel et al., 2012) (**Figure 1**). The reason that cancer incidence increases with age is because cells incur genetic mutations that can give a normal cell abnormal or oncogenic properties, and it often takes many years for a single cell to acquire the mutations necessary to become cancerous (Armitage and Doll, 2004). Epidemiological data and mathematical models in colorectal cancer has

suggested that it takes about 5 to 7 rate limiting "steps" for transformation to occur (Renan, 1993). It is thought that these steps are the occurrence of genetic mutations that are drivers of tumorigenesis (Renan, 1993). Recently, whole exome sequencing analysis in colorectal and breast cancer has shown that any given tumor has an average of 90 mutant genes, with 11 of these mutations being "cancer-causing" (Sjoblom et al., 2006). Genetic mutations have been found to be caused by mutagens, which can be further classified as chemical (i.e. benzene, asbestos, hydrocarbons, arsenic), physical (i.e. radiation), or biological (i.e. viruses) (Ames, 1979; Huang et al., 2003; zur Hausen, 1991) . While many genetic mutations seen in cancer are caused by environmental or biological mutagens, approximately 15% of cancers occur due to inherited genetic syndromes (Houlston et al., 1992). In these cases, defective genes are inherited and can predispose a person to the formation of cancer.

In addition to the genetic mutations described above, many other changes are known to occur to drive tumorigenesis. The role of epigenetics, or changes that do not involve variations in the underlying DNA sequence have been shown to play a role in many types of cancer (Esteller, 2008). Epigenetic changes include DNA methylation and histone modifications that result in changes in gene expression (Esteller, 2008). For example, while germline mutations in the tumor suppressor gene *BRCA1* are found in a small percentage of breast cancer patients, 13% of patients have CpG island methylation of the *BRCA1* gene, resulting in

reduced gene expression of *BRCA1* and an increased susceptibility to cancer (Bird, 2007).

Non-coding RNAs (ncRNAs) have recently been shown to play a role in many aspects of development and disease, and their role in cancer is beginning to be elucidated (Jansson and Lund, 2012). One important type of ncRNAs are micro-RNAs (miRNAs), which are 22 base pair, non-coding RNAs that function in transcriptional and post-transcriptional regulation of gene expression (Jansson and Lund, 2012). miRNAs can reduce gene expression by targeting an mRNA for destruction or repressing the translation of an mRNA (Jansson and Lund, 2012). One of the first human miRNAs to be discovered was mir-21, which targets many tumor suppressor genes, including *PTEN, TGFBR11,* and *RHOB* and deregulation of mir-21 has been identified in many cancer types including breast, colon, lung, liver, and brain cancer (Jansson and Lund, 2012).

Larger chromosomal abnormalities are also a common phenomenon in cancer (Albertson et al., 2003). These include whole chromosome gains or losses (aneuploidy), large chromosomal deletions, chromosomal translocations, and smaller copy number variations (CNVs) in which small regions of the chromosome are amplified or deleted (Albertson et al., 2003; Rajagopalan and Lengauer, 2004). Examples of aneuploidy include somatic trisomy 12 in chromonic lymphocytic leukemia and somatic trisomy 8 in acute myeloid leukemia, and in most cases, this is the result of genetic instability (Hassold and

Hunt, 2001). Individuals with genetic syndromes associated with chromosomal instability such as Fanconi Anemia patients, have a high risk of developing cancer due to the increased susceptibility to large chromosomal aberrations and aneuploidy (D'Andrea, 2010). CNVs are also commonly seen in cancer, and many recurrent CNVs have been identified, such as *EGFR* amplification in non-small cell lung cancer (Cappuzzo et al., 2005).

III. Proto-Oncogenes and Tumor Suppressor Genes

There are two types of genes that can acquire mutations and increase the likelihood of a cell becoming cancerous, proto-oncogenes and tumor suppressor genes (Hanahan and Weinberg, 2000). Proto-oncogenes control aspects of cellular biology such as growth rate and differentiation status, and their expression is tightly controlled in normal cells (Hanahan and Weinberg, 2000). When proto-oncogenes are activated in cancer, they become oncogenes, and drive the formation of cancer by allowing cells to rapidly proliferate, remain undifferentiated, and avoid normal mechanisms of cell death (Croce, 2008). Tumor suppressor genes are genes that under normal conditions, put a break on cell division, control DNA repair, and tell the cell when to undergo apoptosis (Weinberg, 1991). In cancer, tumor suppressor genes themselves, or their functions are often lost, contributing to the cells ability to become oncogenic (Weinberg, 1991).

IV. Hallmarks of Cancer

The abnormal properties that normal cells acquire to become cancer cells are known as oncogenic properties. These properties are acquired when genes and subsequent signaling pathways are activated or disrupted, that lead to several functional changes that characterize cancer cells. Historically, there have been six "hallmarks of cancer" that describe these functional changes (Hanahan and Weinberg, 2000) (**Figure 2A**) . First, cancer cells acquire the ability to actively proliferate, even in situations when proliferation should be halted, such as in adult tissues that are no longer developing (Hanahan and Weinberg, 2000). This is often accomplished by activating pathways that promote cellular proliferation such as the MAPK or PI3K pathways (Jiang and Liu, 2009; Zhang and Liu, 2002). Second, cancer cells attain the ability to evade growth suppressors, often by loss of proteins that function as gatekeepers of cell cycle progression, such as Retinoblastoma protein (Rb) (Hanahan and Weinberg, 2000; Murphree and Benedict, 1984). Third, cancer cells have the ability to evade cell death signals that would normally result in apoptosis of unhealthy or genetically damaged cells . The most common mechanism for evading cell death is loss of the *TP53* tumor suppressor gene which senses DNA damage and induces programmed cell death (Hanahan and Weinberg, 2000; Smith et al., 2003). Fourth, cells that are destined to become cancerous will also achieve replicative immortality . Under normal

circumstances, a cell only has the ability to pass through a limited number of growth and division cycles, as the telomere at the end of chromosomes shorten and signal for the cell to enter senescence, or a viable, non-proliferative state (Blasco, 2005; Hanahan and Weinberg, 2000). In order for a macroscopic tumor to form, cells must overcome this limitation, and often accomplish replicative immortality by activating telomerase, an enzyme which adds repetitive DNA to the end of chromosomes, allowing resistance to the induction of senescence (Blasco, 2005). A fifth hallmark of cancer is the induction of angiogenesis, in which a tumor is able to harness the vascular system to attain the required oxygen and nutrient supply necessary for its continued growth (Bergers and Benjamin, 2003; Hanahan and Weinberg, 2000). Finally, tumor cells are able to invade surrounding tissue, enter the circulatory system, and metastasize to a new location in the body (Klein, 2008). This process is known as epithelial to mesenchymal transition (EMT) and is often induced by activating pathways and transcription factors that are normally only on in developing tissues (Hanahan and Weinberg, 2000; Kong et al., 2011).

In addition to the 6 hallmarks of cancer described above, there are several features of cancer cells that have recently emerged as contributing to the ability of oncogenic cells to become tumors, as well as characteristics that enable cancer cells to attain the 6 hallmarks described above (**Figure 2B**) (Hanahan and Weinberg, 2011). The first emerging hallmark is the ability of cancer cells to

change cellular energetics to enable these cells to rapidly grow and divide (Hanahan and Weinberg, 2011). The second emerging hallmark of cancer cells is avoiding detection and/or destruction by the immune system (Hanahan and Weinberg, 2011). Because the immune system can detect and eliminate abnormal cells, this acquired capability is critical to ensure cancer cell survival (Hanahan and Weinberg, 2011; Whiteside, 2006). To enable cells to acquire the hallmarks of cancer described above, there are two "enabling" characteristics of cancer cells, genome instability and tumor-promoting inflammation (Hanahan and Weinberg, 2011). Genome instability is a trait that characterizes cells that have a high frequency of mutations, including aneuploidy, chromosomal inversions and translocations, deletions, and double-stranded breaks (Hanahan and Weinberg, 2011). The mutations that result from genome instability may contribute to the six hallmarks of cancer (Hanahan and Weinberg, 2011). Tumor-promoting inflammation is a phenomenon in which normal cells of the immune system contribute to tumorigenesis by promoting inflammation within the tumor (Hanahan and Weinberg, 2011). The result of this inflammation is a supply of growth factors, cytokines, angiogenic factors, extracellular matrix-modifying enzymes, and factors that can promote EMT, all of which promote tumor growth and progression (Hanahan and Weinberg, 2011).

V. The History of Cancer Treatments

Over the course of history, the treatment of cancer has largely depended on the available knowledge of cancer biology (**Figure 3**). The oldest known description of cancer comes from the Edwin Smith Papyrus that was written in 3000 BC (Sudhakar, 2009). This work describes tumors of the breast and the treatment of these masses by cauterization using a tool called a fire drill (Sudhakar, 2009). Surgical removal of the tumors continued to be the only treatment for cancer until the late 19th century, and is still used today, although many scientific and technological advances made in the late 19th and early 20th centuries had made surgery safer and more effective (Sudhakar, 2009). These advances include anesthesia, which became widely available in 1846, and allowed for major operations to take place, including the first mastectomy, performed in 1882 (Henderson and Canellos, 1980). Advanced imaging techniques and fiberoptic technology have allowed surgeons to more safely operate and remove tumors more precisely, in less invasive procedures. The advancement of surgical techniques has indeed improved the quality of life and chances of survival for patients after diagnosis.

In the late 19th century, other treatments of cancer were beginning to be explored and laid the foundation for non-surgical techniques that are still being used today. Radiation therapy was discovered in the late 19th century, and by the early 20th century, it was being used to destroy cancer cells by inflicting irreparable DNA damage to cancer cells, effectively killing them (Bucci et al.,

2005). Chemotherapy drugs were discovered in the mid 20th century, and it was later found that these drugs often act as alkylating agents that could kill rapidly growing cells by damaging their DNA (Hirsch, 2006). Chemotherapy began being used in 1949, and by 1958, combination chemotherapy was found to cure certain types of leukemia (DeVita and Chu, 2008; Gilman, 1963; Hirsch, 2006). By 1975, the combination of surgery and adjuvant chemotherapy had been shown to be very beneficial in the treatment of breast cancer (DeVita and Chu, 2008). As more data became available, it became clear to physicians and researchers that viruses played a role in oncogeneisis, and in 1981, the first vaccine against hepatitis B became available and dramatically reduced the incidence of liver cancer (zur Hausen, 1991). More targeted therapies also began to be developed including hormone therapy, in which hormone-dependent tumors such as breast, ovarian, and prostate tumors were treated by depriving them of the hormones required for their growth (Brawer, 2006; Jones and Buzdar, 2004; Riman et al., 1998). In 1986, tamoxifen, an estrogen antagonist, was first used as a hormone therapy for the treatment of breast cancer (Jones and Buzdar, 2004).

In recent decades, targeted therapeutics have become of great interest, as these drugs can specifically and effectively target cancer cells, while leaving normal cells in the body relatively unharmed (Ross et al., 2004). The downside to targeted therapies is that it requires in depth and precise knowledge about the genetic changes that drive the formation of any given tumor (Ross et al., 2004). A

hallmark example of targeted therapy is Gleevec (imantinib), which was developed in light of the finding that many patients with chronic myeloid leukemia (CML) harbored an abnormal chromosome known as the Philadelphia chromosome (Stegmeier et al., 2010). The Philadelphia chromosome was the result of a reciprocal chromosomal translocation between chromosome 9 and 22, resulting in an oncogenic gene fusion between the *BCR* and *ABL1* genes (Kurzrock et al., 2003). Gleevec is a small molecule that potently and specifically blocks the tyrosine kinase activity of *BCR-ABL (Stegmeier et al., 2010).* With the implementation of Gleevec and its FDA approval in 2001, patients diagnosed with CML saw a sharp increase in cytogenic responses and survival rates compared to previous therapies such as interferon combined with cytarabine (**Figure 4**) (O'Brien et al., 2003). Similar to Gleevec, there are hundreds of tyrosine kinase targeted therapies being designed and tested pre-clinically and in clinical trials and have often proven to be effective in patients and FDA approved (Miller et al., 2013; Ross et al., 2004).

In addition to tyrosine kinase inhibitors, several other molecular targeted therapies have been developed and are currently being tested for safety and efficacy in patients (Sawyers, 2004). These include monoclonal antibodies that target antigens that are expressed by cancer cells such as Bevacizumab (Avastin) which targets the Vascular Endothelial Growth factor Receptor (VEGF-R) (Rini, 2007). Avastin works by inhibiting angiogenesis, effectively cutting off nutrient

supply to the tumor, and was FDA approved in 2004 for several types of cancer (Rini, 2007).

Immunotherapy is also being implemented as a cancer therapy (Miller et al., 2013). Immunotherapy works by harnessing the immune system to attack cancer cells (Miller et al., 2013). One type of immunotherapy is to block immune checkpoints to allow persistent and prolonged anti-tumor immune response (Miller et al., 2013). Examples of checkpoint blockade drugs are PD-1 inhibitors which entered clinical trials in 2013, and CTLA-4 inhibitors such as Ipilimumab, which was FDA approved for malignant melanoma in 2011 (Pardoll, 2012).

With the advancement of cancer treatments, the United States saw a record number of cancer survivors in 2012, of over 12 million people, a four-fold increase since 1971 (**Figure 3**) (Siegel et al., 2012). The overall survival rates of most cancer types have also been steadily improving over the last 40 years (**Figure 5)** (SEER data) (Siegel et al., 2012).

VI. The Future of Targeted Cancer Therapeutics

While the design and development of targeted therapies has been rapid in the past 20 years, and will continue to revolutionize cancer therapy, many problems have arisen with their use that will need to be addressed in the future. The main problem with targeted therapies is that, undoubtedly, most patients will eventually develop resistance to targeted agents (Daub et al., 2004; Ellis and

Hicklin, 2009). The development of resistance to targeted therapies has been well studied in CML patients given Gleevec, in which nearly half of patients develop resistance to targeting the *BCR-ABL* kinase (Gambacorti-Passerini et al., 2003). To address this problem, researchers are now trying to unravel the mechanisms by which resistance develops, and design new drugs or combinations of targeted agents that reduce the occurrence of resistance (Ellis and Hicklin, 2009). Agents designed to overcome multi-drug resistance are also being developed and tested (Persidis, 1999). There is also research being conducted to address drug delivery methods that may make these therapies more effective (Moses et al., 2003). Finally, new approaches to targeted therapies are being developed to more selectively target cancer cells, while leaving normal, healthy cells untouched. These approaches include liposomal therapy, in which drugs are embedded in liposomes, which selectively target cancer cells, and monoclonal antibody therapies directed towards an antigen that is enriched in cancer cells (Adams and Weiner, 2005; Noble et al., 2004).

VII. Schwann Cell Tumor Biology

Schwann cells are glial cells of the peripheral nervous system and play a role in supporting neurons and transmitting nerve impulses along axons (Bhatheja and Field, 2006). They are derived from neural crest cells during embryogenesis, and begin the process of development into Schwann cell precursors when they associate with axons of the peripheral nervous system (**Figure 6**) (Jessen and

Mirsky, 2005). They then develop into immature Schwann cells, and eventually into mature Schwann cells which can be either myelinating or non-myelinating. Myelin is a material composed of water, lipids, and proteins that surrounds axons and facilitates the conduction of nerve impulses (Hartline and Colman, 2007). This process of Schwann cell development has been well studied, and many of the pathways and molecules involved have been elucidated (Jessen and Mirsky, 2005). These include important developmental pathways such as BMP/TGFβ, Notch, PI3K/AKT, and growth factor receptor signaling pathways (Jessen and Mirsky, 2005). It is thought that Schwann cell precursors, or immature Schwann cells are the cell of origin for Schwann cell tumors, and it is likely that many of the pathways that control Schwann cell development and differentiation may also play a role in the path to malignancy (Carroll and Ratner, 2008).

Schwann cell tumors include benign neurofibromas, plexiform neurofibromas, and malignant peripheral nerve sheath tumors (MPNSTs) (Carroll, 2012; Uhlmann and Plotkin, 2012). These tumors can arise sporadically in the general population, but are more often associated with the genetic disorder Neurofibromatosis Type 1 (NF1), which will be described in the following section (Uhlmann and Plotkin, 2012). Benign neurofibromas are seen in 99% of patients with NF1 and arise when a Schwann cell precursor or immature Schwann cell incurs a genetic mutation that gives it a proliferative advantage, usually loss of the wild type *NF1* allele (Ferner, 2010; Zhu et al., 2002). This results in nerve

hyperplasia, and eventual macroscopic, grade 1 tumor formation (**Figure 7**) (Brossier and Carroll, 2012). Neurofibromas can occur on any peripheral nerve of the body but are most often associated with dermal nerves, the sciatic nerves, and nerves of the brachial plexus (Ferner, 2010). While Schwann cells are the cell of origin for these tumors, they also contain many other cell types including fibroblasts, macrophages and mast cells (Brossier and Carroll, 2012; Prada et al., 2013). Neurofibromas are associated with severe pain and discomfort and are often result in disfigurement in patients (Uhlmann and Plotkin, 2012). Plexiform neurofibromas are similar to benign neurofibromas, but are often associated with multiple nerve bundles, and have a high likelihood of malignant transformation into MPNSTs (Carroll and Ratner, 2008). MPNSTs are the result of malignant transformation of neurofibromas due to additional genetic changes (**Figure 7**) (Brossier and Carroll, 2012). These tumors are classified as soft tissue sarcomas, arising from Schwann cells associated with peripheral nerves (Carroll and Ratner, 2008). MPNSTs are notoriously difficult to treat, as surgery is often not an option due to the association of these tumors with nerves (Widemann, 2009). In addition, MPNSTs tend to be highly chemo-resistant and very aggressive tumors (Widemann, 2009).

VIII. Neurofibromatosis Type 1

Neurofibromatosis Type 1 (NF1) is one of the most common genetic disorders known, occurring in 1 in 2,500 live births (Uhlmann and Plotkin, 2012).

NF1 an inherited autosomal dominant disorder, which is characterized by loss of one copy of the tumor suppressor gene *Neurofibromin (NF1)* (Cichowski and Jacks, 2001). While half of patients with NF1 inherit the mutant *NF1* gene from a parent, the other half of NF1 patients have new *NF1* mutations (Ferner, 2010). The *NF1* gene was cloned in 1990 and was discovered to encode the protein Neurofibromin (Cichowski and Jacks, 2001). Neurofibromin is a negative regulator of Ras signaling, and functions to keep Ras in its inactive GDP-bound state by acting as a Ras GTPase activating protein (Ras-GAP) (**Figure 8**) (Cichowski and Jacks, 2001). This hyperactive Ras signaling leads to activation of the MAPK and PI3K pathways, giving cells proliferative and survival advantages (Cichowski and Jacks, 2001; Johannessen et al., 2005).

Loss of *NF1*, and subsequent hyperactive PI3K and MAPK signaling leads to severe clinical manifestations in NF1 patients (Uhlmann and Plotkin, 2012). The most prominent feature of patients with NF1, and one of the diagnostic indicators of this disorder is café au lait spots, or darkened pigmentation of the skin (Ferner, 2010). Café au lait spots appear in 99% of NF1 patients by 5 years of age (Ferner, 2010). Other complications of NF1 include epilepsy, cerebral malformations, cognitive problems, cardiovascular disease, respiratory problems and bone abnormalities (Uhlmann and Plotkin, 2012). In addition to these symptoms, NF1 patients are at very high risk for developing cancer (Carroll, 2012). Tumors of the brain and optic pathway are quite common,

occurring in 15% of patients (Gutmann et al., 2006). Additionally, there is a 99% penetrance of neurofibromas in NF1 patients (Carroll, 2012). These tumors, while benign, can cause debilitating pain and neurological symptoms and are often quite difficult to surgically remove, as they are closely associated with nerves (Widemann, 2009). Sixty percent of NF1 patients will also develop a plexiform neurofibroma, which is characterized as a more aggressive benign tumor with a higher likelihood of transforming into a malignant tumor (Brems et al., 2009). 10% of NF1 patients will go on to develop a malignant peripheral nerve sheath tumor (MPNST), and these aggressive tumors remain the leading cause of death for NF1 patients (Carroll and Ratner, 2008).

IX. Known Genetic Drivers of Schwann Cell Tumorigenesis

The most common genetic change associated with Schwann cell tumors is loss of the tumor suppressor *NF1* (Laycock-van Spyk et al., 2011). The majority of benign neurofibromas and plexiform neurofibromas arise in patients with NF1, and 50% of MPNSTs are also NF1-associated (Widemann, 2009). While loss of *NF1* is sufficient for the development of benign neurofibromas, secondary genetic changes are required for the transformation to malignancy (**Figure 7**) (Miller et al., 2006).

Many mouse models have been developed to try to understand the genetic changes that lead to neurofibromas and MPNST development (**Table 1**) (Brossier

and Carroll, 2012). The first mouse model of neurofibroma was developed in 1999, in which *Nf1* null chimeric embryos were generated and led to the presence of plexiform neurofibromas in every animal (Cichowski et al., 1999; Vogel et al., 1999). The first mouse model of MPNST was also made in 1999 in which *Nf1* and *p53*, two tumor suppressor genes that are highly linked on mouse Chromosome 11, were knocked out in *cis*, resulting in MPNST formation in 81% of animals (Cichowski et al., 1999; Vogel et al., 1999). These two mouse models demonstrated that while loss of *Nf1* is sufficient for plexiform neurofibromas formation, secondary genetic changes are required for the development of MPNSTs, and that the P53 pathway represents a major barrier to MPNST development (Cichowski et al., 1999; Vogel et al., 1999).

Many mouse models have been developed to identify genes that cooperate with loss of *Nf1* in the formation of MPNSTs (Brossier and Carroll, 2012). In a *Sleeping Beauty* screen conducted in our lab to identify novel drivers of Schwann cell tumorigenesis, we identified *Nf1* and *Pten* as two tumor suppressor genes that were often co-mutated in MPNSTs. In this screen, while either *Nf1* or *Pten* were often mutated in benign neurofibromas, nearly every tumor that had both *Nf1* and *Pten* mutated were high grade MPNSTs. To model the cooperation of these two genes, our lab developed a mouse model showing that biallelic loss of *Nf1* and *Pten* in Schwann cells and their precursors is sufficient for rapid, high grade tumor formation in 100% of mice (Keng et al., 2012a). *CDKN2A* is a tumor

suppressor gene also found highly mutated in human MPNSTs, and when this locus ($p16^{Ink41}/p19^{Arf}$) is homozygously deleted in the context of *Nf1* heterozygous mice, 26% of animals develop MPNSTs (Kourea et al., 1999b; Nielsen et al., 1999).

Other mouse models have been developed to investigate the genetic changes that lead to spontaneous MPNSTs (Brossier and Carroll, 2012). Overexpression of *EGFR* in Schwann cells and their precursors was sufficient to cause nerve hyperplasia and hypercellularity, and at a low rate, neurofibromas (Ling et al., 2005). Our lab demonstrated that when *EGFR* is overexpressed in the context of biallelic *Pten* deletion, aggressive peripheral nerve sheath tumors are formed in 100% of mice (Keng et al., 2012b).

X. Current Challenges in Understanding and Treating Schwann Cell Tumors

The standard treatment for Schwann cell tumors has historically been surgery, radiation, and chemotherapy (Widemann, 2009). Unfortunately, surgical excision is often impossible, as these tumors are highly associated with nerves. High dose radiation and chemotherapy, while modestly effective, have many unwanted and negative side effects (Widemann, 2009). With these current treatments, the 5-year survival rates for MPNSTs remain very low at less than 25% (Brekke et al., 2010). There is an urgent need for new, more effective therapies to treat these tumors.

With the increased understanding of the genetic drivers of Schwann cell tumors over the past decade, as well as new genetic and genomic technologies available, the discovery and use of targeted therapies to treat these tumors will hopefully increase survival and quality of life for patients. Unfortunately, to date, no targeted therapies that have entered clinical trials for neurofibromas or MPNSTs have been very successful (Packer and Rosser, 2002; Widemann, 2009). For example, one of the first biologic-based therapies was a randomized phase II trial using either *cis*-retinoic acid or interferon-α (Packer et al., 2002). It was hypothesized that retinoic acid, as a maturation agent, may be effective in slowing or stopping tumor cell growth (Packer et al., 2002). Interferon-α has been shown to have both anti-inflammatory and anti-angiogenic properties, and was thought that this agent may also be effective at treating these tumors (Packer et al., 2002). At the end of this trial, 86% of patients on retinoic acid and 96% of patients on interferon-α were stable, although no patients demonstrated a radiographic response. Importantly, 14% (8 patients) did show symptomatic improvements, including resolution of bradycardia (1 patient) and orthopnea (1 patient) and reduction in pain (6 patients) (Packer et al., 2002). A phase I clinical trial was conducted in which patients were given thalidomide, another antiangiogenic therapy (Gupta et al., 2003). Although this was a relatively small study, with only 20 patients, 4 patients showed a decrease in tumor size, and five patients had symptomatic improvements (Gupta et al., 2003). Another phase I clinical trial

tested the use of a farnesyl protein transferase inhibitor, in an attempt to block the function of RAS proteins (Yan et al., 1995). This was the first study to target a molecular change known to occur in transformed Schwann cells (Packer et al., 2002). Unfortunately, no patients showed a radiographic response (Yan et al., 1995).

While much has been learned about the genetic changes that occur in Schwann cells as they become malignant, the success of targeted therapies has lagged (Widemann, 2009). There are likely several reasons for this. First, while large-scale genetic approaches such as cytogenetics to look for large chromosomal abnormalities, comparative genome hybridization to find gene copy number changes, whole exome sequencing to identify genetic mutations, gene expression microarray, and RNA sequencing to look for gene expression changes have uncovered a myriad of genetic changes, it is difficult to determine which genetic changes are simply "passengers" and which changes are "drivers" (Bignell et al., 2010). It is important to determine the "driver" mutations in order to design targeted therapies that will have functional consequences to malignant tumor cells (Bignell et al., 2010). Another problem that has arisen is that although some driver mutations have been discovered, such as loss of *NF1*, it is often quite difficult to target these changes (Downward, 2003). There has been a lot of work done to identify and implement Ras-targeted therapies, but most, including farnesyl transferase inhibitors described above, have proven to be ineffective

(Downward, 2003). An additional problem in treating Schwann cell derived tumors is tumor heterogeneity, in which subsets of cells within a single tumor may harbor different genetic mutations that each may need to be targeted (Gerlinger et al., 2012). Not only are neurofibromas and MPNSTs composed of malignant Schwann cells, but there are also other cell types that are highly associated with thee tumors, including fibroblasts, mast cells and macrophages, and targeting these tumor-associated cells may be necessary for the successful treatment of these tumors (Brossier and Carroll, 2012). Finally, while targeted therapies have been shown to be quite effective in many cancer types, it is very clear that the likelihood of a patient developing resistance to these therapies is quite high (Sierra et al., 2010). It is therefore necessary to begin to investigate the mechanisms of targeted therapy resistance, and develop new drugs or combinations of drugs that may overcome this acquired resistance.

XI. *Sleeping Beauty* Mutagenesis as a Tool to Understand the Genes and Pathways Involved in Schwann Cell Tumorigenesis and Develop Better Treatments

Sleeping Beauty (*SB*) mutagenesis is a tool used to identify genetic drivers of cancer, and in our recently published study, we used *SB* to uncover genes, pathways, and drugable targets in Schwann cell tumors (Largaespada, 2009; Rahrmann et al., 2013). *SB* is a two part system composed of an oncogenic

transposon, known as *T2/Onc* and the transposase enzyme S*leeping Beauty* (**Figure 9**) (Collier and Largaespada, 2005). The oncogenic transposon contains a murine stem cell virus (MSCV) 5' LTR, splice acceptor (SA)/splice donor (SD), and polyadenylation (pA) sequences (Dupuy et al., 2009). Therefore, if the *T2/Onc* transposon lands upstream of an oncogene, it can drive its overexpression, and if it lands within a tumor suppressor gene, it can disrupt the gene or cause a truncated product (Collier and Largaespada, 2005). Once a tumor forms, DNA can be extracted, and linker-mediated PCR can be performed to identify the *T2/Onc* genomic junctions using an Illumina sequencing platform (Largaespada, 2009). After bioinformatic distillation, a list of common transposon insertion sites (CIS) is generated (Sarver et al., 2012). These are regions of the genome that harbor transposons at a frequency higher than expected by random chance, and are therefore likely genetic drivers of tumorigenesis (Largaespada, 2009).

In the *SB* screen to identify genetic drivers of Schwann cell tumors, we used a *CNPase* promoter driving *Cre Recombinase* expression which, in combination with a Cre/Lox-regulated *Rosa26-SB11*^{LSL} transgene, allowed for *T2/Onc* mutagenic transposon mobilization in Schwann cells and their precursors, the cell of origin for peripheral nerve sheath (Carroll and Ratner, 2008; Rahrmann et al., 2013). It is known that a high percentage of human MPNSTs have expression of *EGFR* and 75% have deletion or mutations in *P53* (Frahm et al., 2004; Holtkamp et al., 2008; Spurlock et al., 2010; Tabone-Eglinger et al., 2008;

Tawbi et al., 2008). To predispose mice to the development of Schwann cell tumors, we used a *CNP-EGFR* transgene to drive the overexpression of EGFR, and a dominant negative *Tp53* allele (*$p53^{R270H}$*) in combination with *SB* transposition (de Vries et al., 2002; Ling et al., 2005).

This *SB* screen resulted in a spectrum of peripheral nerve disease including nerve hyperplasia, grade 1 neurofibromas, grade 2 Schwannomas, and grade 3 peripheral nerve sheath tumors (**Figure 10**) (Rahrmann et al., 2013). These murine tumors highly resembled human tumors in both location and histo-pathology analysis (Rahrmann et al., 2013). While overexpression of EGFR and loss of *Tp53* alone resulted in the development of Schwann cell tumors, the addition of transposition increased the frequency of tumor development, resulted in higher grade tumors, and reduced latency, suggesting that we were in fact identifying drivers of tumor development and progression (**Figure 11**) (Rahrmann et al., 2013). A list of CIS-associated genes was generated for 269 neurofibromas and 106 MPNSTs and resulted in the identification of 695 and 87 statistically significant sites of recurrent transposon integration (Rahrmann et al., 2013). When compared to human data sets, this *SB* screen in fact revealed both known and novel genes that function in the formation and/or progression of MPNSTs (Rahrmann et al., 2013). Additionally, an analysis of transposon integration co-occurrence revealed cooperating genes that were enriched for in the Wnt/β-

catenin, PI3K/AKT/mTOR, and growth factor receptor signaling pathways (Rahrmann et al., 2013).

XII. Using Genetic Information to More Effectively Treat Schwann Cell Tumors

The *SB* screen that we conducted to identify genetic drivers of Schwann cell tumor development and progression gave us a wealth of new information. The goal of my research was to use the genetic information derived from this screen to develop and pre-clinically test new targeted therapies for MPNSTs. Using the data from the forward genetic screen, I was able to address some of the difficulties associated with targeted therapies as cancer treatments. First, this screen allowed us to differentiate between "driver" and "passenger" mutations that other genetic approaches are unable to do. We set the parameters for CIS calling stringent enough to exclude potential non-driver mutations that are found in minor sub-clones or due to artifacts (Sarver et al., 2012). Second, we found enough driver mutations to choose which genes or pathways would be potentially drugable targets, and exclude those that are likely difficult or impossible to design drugs to (Rahrmann et al., 2013). Third, the co-occurrence analysis allowed us to find cooperating pathways that could potentially be co-targeted with small molecules to avoid the rapid development of resistance (Rahrmann et al., 2013).

XIII. Thesis Statement

The following thesis will describe my hypothesis that the *SB* screen we conducted for Schwann cell tumor initiation, development, and progression may identify genes and pathways that could be used as novel drug targets for therapy of Schwann cell tumors. Specifically, I will describe the identification and validation of canonical Wnt/β-catenin signaling in Schwann cell tumor development, progression and maintenance, and the use of small molecule inhibitors of Wnt signaling in combination with mTor inhibitors to successfully induce apoptosis in MPNST cell lines. I will also describe the results of co-targeting the MAPK and PI3K pathways in two *in vivo* genetically engineered mouse models of MPNSTs as a means to increase the efficacy and overcome resistance that often occurs when treating tumors with a single targeted agent.

Figure 1: Cancer incidence increases with age. The National Cancer Institute Surveillance Epidemiology and End Results (SEER) analysis of cancer incidence by age (Siegel et al., 2012) . These data show that in the United States, the rate of cancer is relatively low for younger populations and increases with age, with ages 70-74 having the highest incidence of cancer. This is due to the fact that cancer is a genetic disease that requires multiple mutations and selection for a tumor to form. Based on the rate of mutations, epidemiological studies, and whole exome sequencing analysis, it is predicted that 6-11 driver mutations must occur for cancer to form (Sjoblom et al., 2006). This figure was generated from the National Cancer Institute Surveillance Epidemiology and End Results (SEER database) (Siegel et al., 2012).

Figure 1

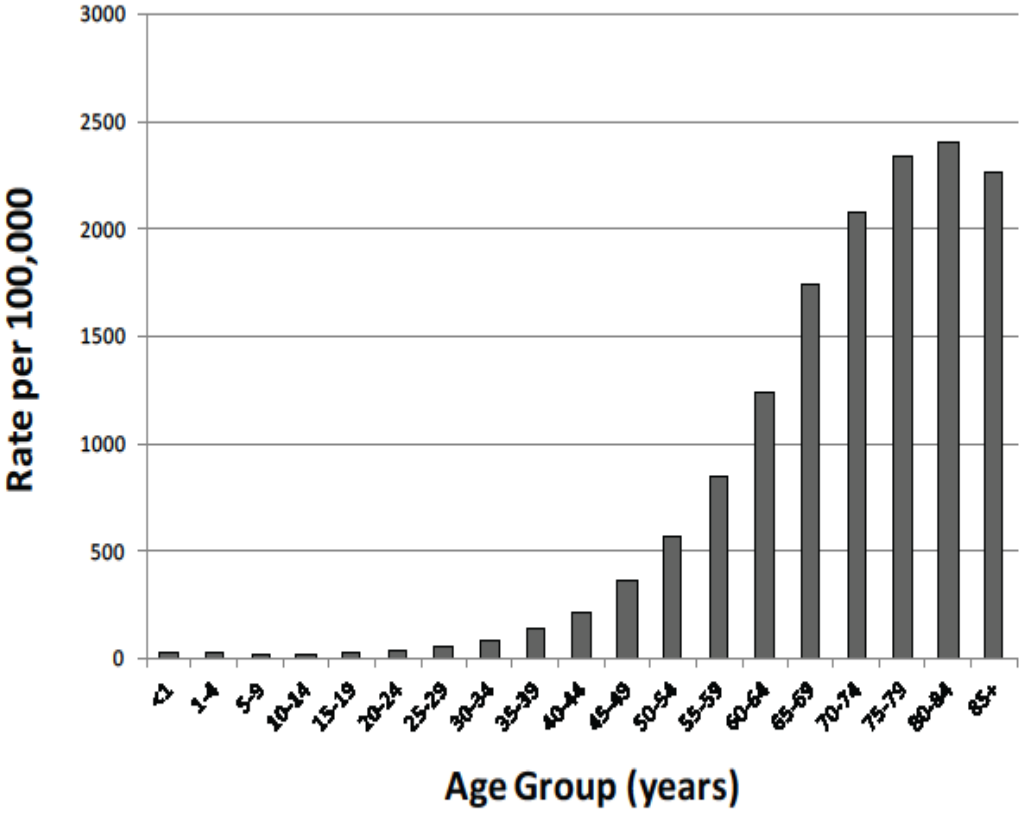
Rate per 100,000
3000
2500
2000
1500
1000
500
0
<1
1-4
5-9
10-14
15-19
20-24
25-29
30-34
35-39
40-44
45-49
50-54
55-59
60-64
65-69
70-74
75-79
80-84
85+
Age Group (years)

Figure 2: Hallmarks of cancer. A. The 6 hallmarks of cancer describe the functional changes that occur in cells or tumors during the process of oncogenesis. These hallmarks include sustained proliferative signaling, avoiding growth suppressors, resisting cell death, enabling replicative immortality, inducing angiogenesis, and activating invasion and metastasis. B. Over the past decade, two "emerging" hallmark of cancer have been described including deregulating cellular energetics and avoiding immune destruction. In addition, it has become clear that there are enabling characteristics of cancer cells that allow them to attain the hallmarks of cancer. These include genome instability and mutation as well as tumor-promoting inflammation (Hanahan and Weinberg, 2000; Hanahan and Weinberg, 2011). This figure was adapted from Hanahan and Weinberg, 2000 and Hanahan and Weinberg, 2011.

Figure 2

A

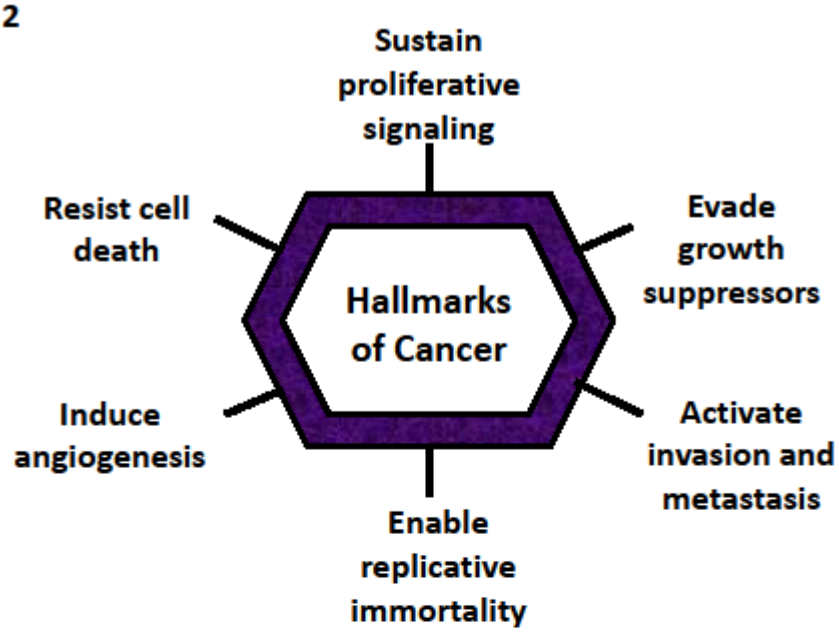
Sustain proliferative signaling
Resist cell death
Evade growth suppressors
Hallmarks of Cancer
Induce angiogenesis
Activate invasion and metastasis
Enable replicative immortality

B

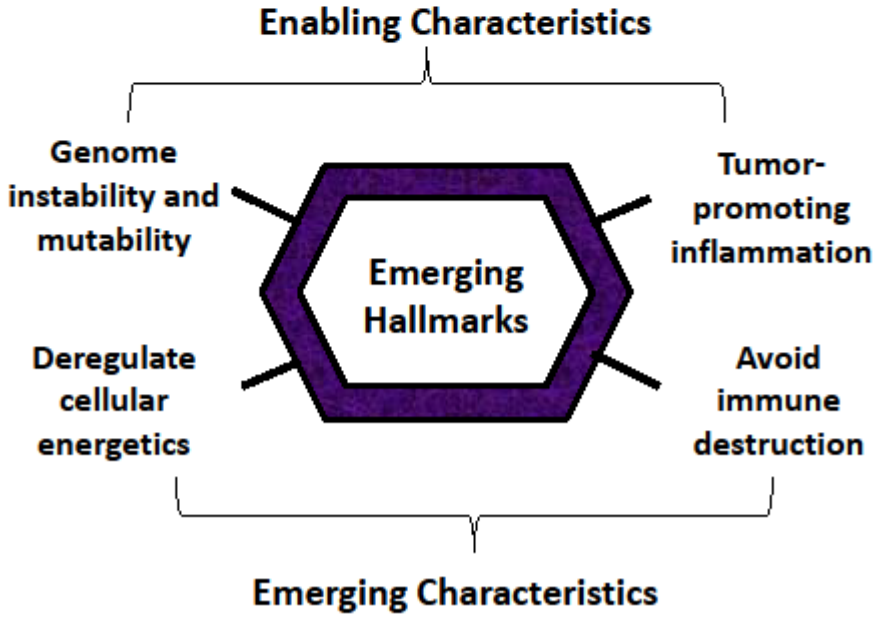
Enabling Characteristics
Genome instability and mutability
Tumor-promoting inflammation
Emerging Hallmarks
Deregulate cellular energetics
Avoid immune destruction
Emerging Characteristics

Figure 3: History of cancer treatment. Cancer treatments have evolved dramatically over the past century. Cancer was first described in 3000 BC in the Edwin Smith Papyrus, and the treatment for these tumors was surgical removal with a device referred to as a fire drill. Surgery remained the only available treatment for cancer into the 20th century, although surgical techniques and patient outcome improved with the advent of anesthesia in 1846. In 1882, the first mastectomy was performed as a treatment for breast cancer. With the discovery of X-rays, came with first use of radiation to kill cancer cells in 1903, a technique that has been optimized, but is still in use today. In 1949, the first chemotherapeutic agent, nitrogen mustard was approved as a cancer therapy, and by 1958, combination chemotherapy had been implemented and could cure certain types of leukemia. In 1975 adjuvant chemotherapy in combination with surgery was developed and improved survival in breast cancer. In the mid to late 1900s, a viral basis for cancer became known, and the development of the hepatitis B vaccine in 1981 dramatically reduced the incidence of liver cancer. Hormone-dependent cancers were identified, and in 1986, tamoxifen was first used to treat estrogen-dependent breast cancer. It was also in the 1980's when targeted therapies began to be investigated. Researchers and physicians sought to identify cancer cell-specific changes that could be used to design treatments that targeted oncogenic cells in the body. The first targeted therapy, rituximab was approved in 1997, and many other monoclonal antibody therapies have been designed and implemented in the clinic since. Gleevec, a therapy that targets the *BCR-ABL* fusion product became available in 2001, and revolutionized the outcome for patients diagnosed with CML. In 2004, the FDA approved Avastin, a drug that targets the VEGF Receptor and inhibits angiogenesis, effectively shrinking and/or killing macroscopic tumors. With the vast increase in knowledge about the genetic changes that cause cancer and the advancements in cancer treatments, by 2012 there were over 12 million cancer survivors in the United States, a four-fold increase from 1971.

Figure 3

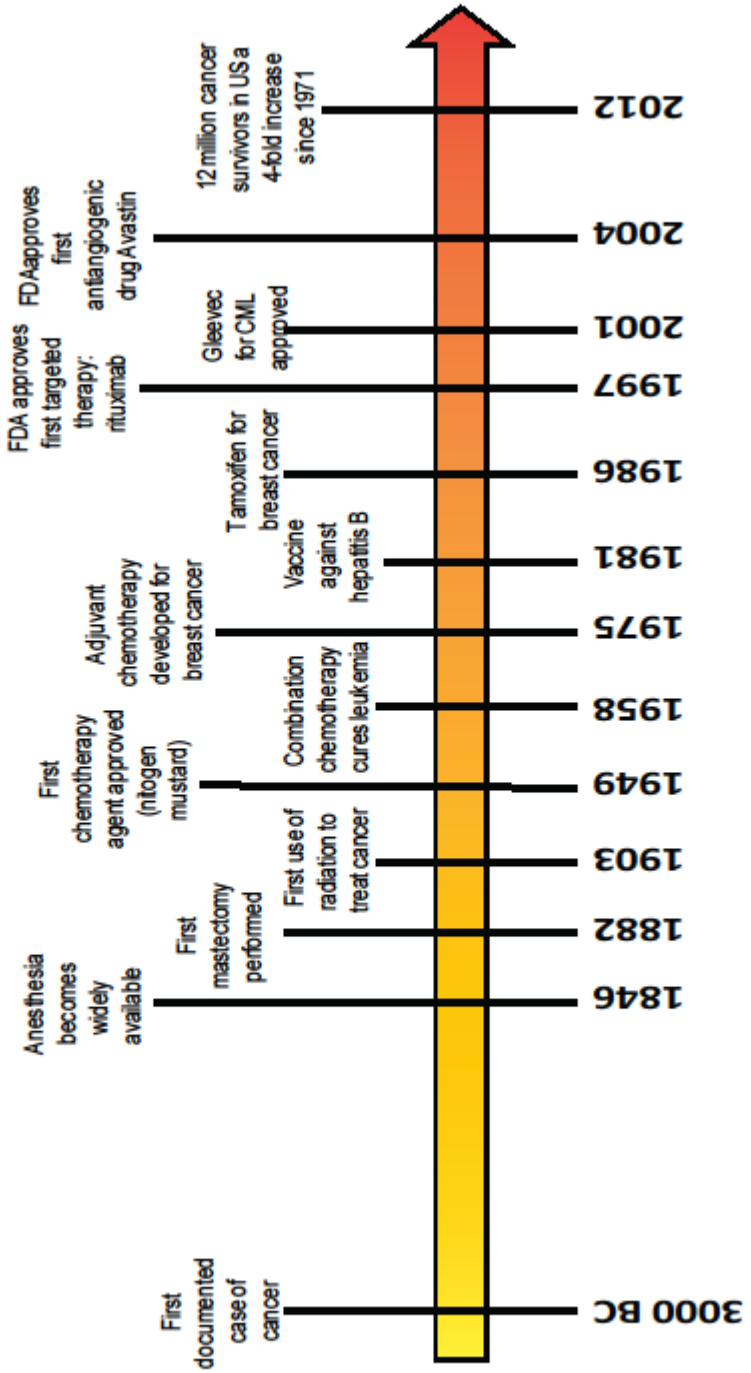
3000 BC
First documented case of cancer
1846
Anesthesia becomes widely available
1882
First mastectomy performed
1903
First use of radiation to treat cancer
1949
First chemotherapy agent approved (nitogen mustard)
1958
Combination chemotherapy cures leukemia
1975
Adjuvant chemotherapy developed for breast cancer
1981
Vaccine against hepatitis B
1986
Tamoxifen for breast cancer
1997
FDA approves first targeted therapy: rituximab
2001
Gleevec for CML approved
2004
FDAapproves first antiangiogenic drug Avastin
2012
12 million cancer survivors in USa 4-fold increase since 1971

Figure 4: Gleevec has dramatically improved Chronic Myeloid Leukemia (CML) responses. Historically, CML has been a very deadly disease. With the implementation of Gleevec as a targeted therapy patients observed an increase in major cytogenic response (A), complete cytogenic response (B), freedom from progression at 18 months (C), and progression-free survival at 24 month (D) compared to interferon and cytarabine combination treatment (O'Brien et al., 2003). This figure was generated from data cited in O'Brien et al., 2003.

Figure 4

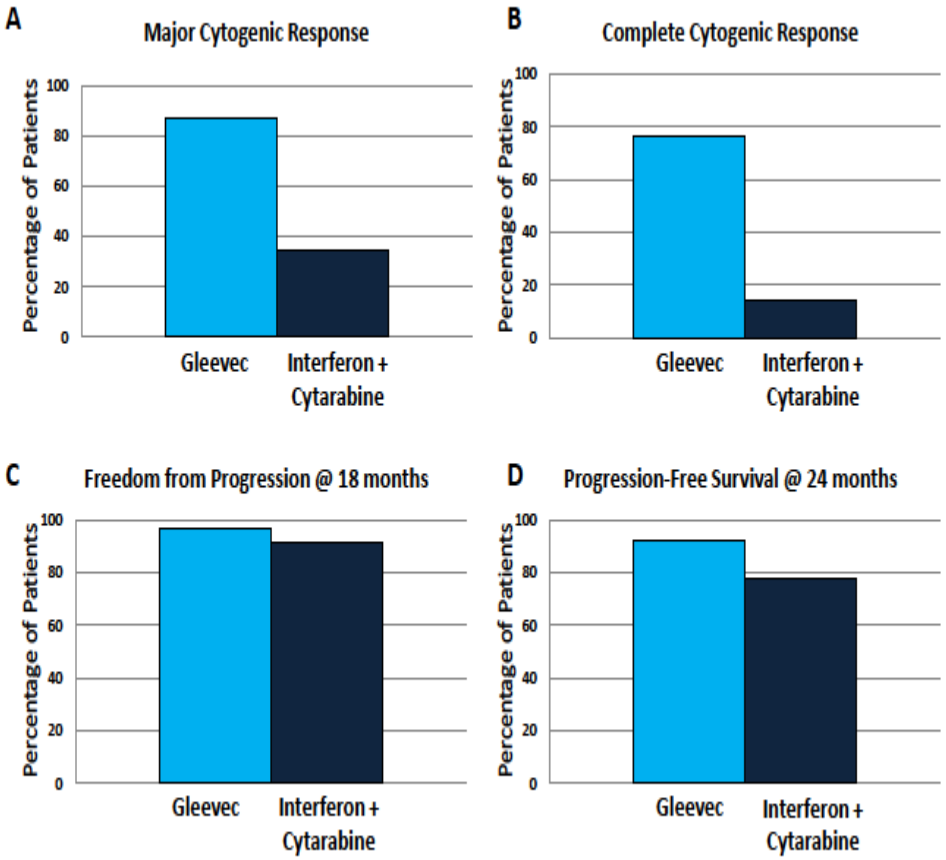
A
Major Cytogenic Response
Percentage of Patients
100
80
60
40
20
0
Gleevec
Interferon + Cytarabine
B
Complete Cytogenic Response
Percentage of Patients
100
80
60
40
20
0
Gleevec
Interferon + Cytarabine
C
Freedom from Progression @ 18 months
Percentage of Patients
100
80
60
40
20
0
Gleevec
Interferon + Cytarabine
D
Progression-Free Survival @ 24 months
Percentage of Patients
100
80
60
40
20
0
Gleevec
Interferon + Cytarabine

Figure 5: Cancer survival rates are improving. The National Cancer Institute Surveillance Epidemiology and End Results (SEER database) of cancer survival based on cancer type (Siegel et al., 2012). Nearly all cancer types have shown an increase in survival over the past 3 decades. This is due to a better understanding of the causes of cancer, cancer prevention strategies, improved diagnostic techniques, and better treatment strategies. This figure was generated from the National Cancer Institute Surveillance Epidemiology and End Results (SEER database) (Siegel et al., 2012).

Figure 5

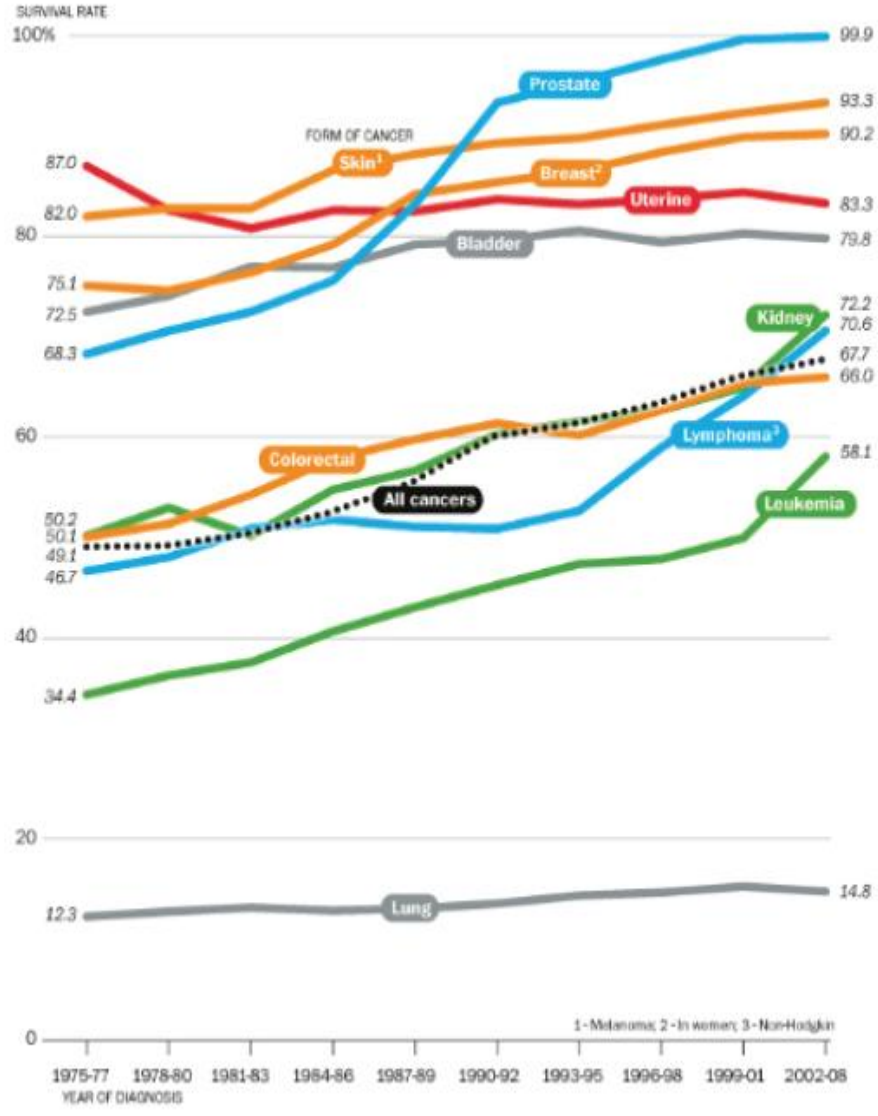
SURVIVAL RATE
100%
80
60
40
20
0
FORM OF CANCER
Prostate
Skin¹
Breast²
Uterine
Bladder
Kidney
Colorectal
All cancers
Lymphoma³
Leukemia
Lung
99.9
93.3
90.2
87.0
82.0
83.3
79.8
75.1
72.5
68.3
72.2
70.6
67.7
66.0
58.1
50.2
50.1
49.1
46.7
34.4
14.8
12.3
1-Melanoma; 2-In women; 3-Non-Hodgkin
1975-77
1978-80
1981-83
1984-86
1987-89
1990-92
1993-95
1996-98
1999-01
2002-08
YEAR OF DIAGNOSIS

Figure 6: Schwann cell development. Schwann cells are derived from neural crest cells. A subset of neural crest cells become Schwann cell precursors after migration to the periphery of the body and association with axons. Schwann cell precursors develop into immature Schwann cells under the influence of Notch signaling and FGF signals. Immature Schwann cells the mature into either myelinating or non- myelinating (not shown) Schwann cells. This maturation process is controlled by many different secreted factors and transcription factors. Myelinating Schwann cells are highly associated with axons of the peripheral nervous system, where they function to help in the conduction of nerve impulse, as well as support neurons (Jessen and Mirsky, 2005). This figure was adapted from Jessen and Mirsky, 2005.

Figure 6

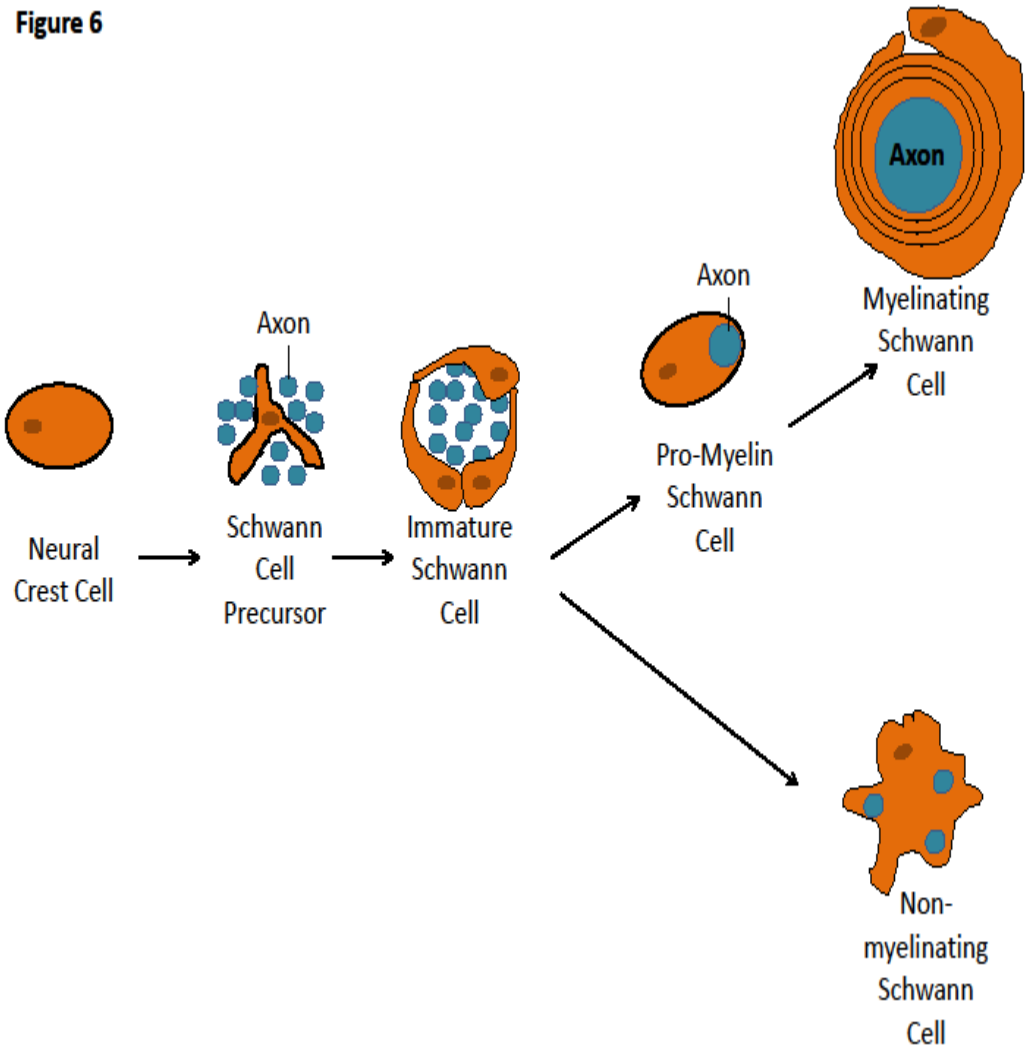
Axon
Axon
Axon
Myelinating Schwann Cell
Pro-Myelin Schwann Cell
Neural Crest Cell
Schwann Cell Precursor
Immature Schwann Cell
Non-myelinating Schwann Cell

Figure 7: Development of neurofibromas and MPNSTs. Nerve hyperplasia is often seen in patients with NF1. When patients with NF1 lose the second copy of the *NF1* allele in Schwann cells, neurofibromas develop. Neurofibromas are grade 1 benign tumors that are highly associated with peripheral nerves and contain a variety of cell types including Schwann cells, fibroblasts, and mast cells. When secondary genetic changes occur in addition to the loss of *NF1*, an MPNST can develop. These secondary genetic changes include loss of *p16* expression, mutation or deletion of *p53*, overexpression of *EGFR*, and loss of PTEN. 50 % of MPNSTs form sporadically, or in the absence of NF1 syndrome, and are often characterized by similar genetic changes (Brossier and Carroll, 2012). This figure was adapted from Brossier and Carrol, 2012.

Figure 7

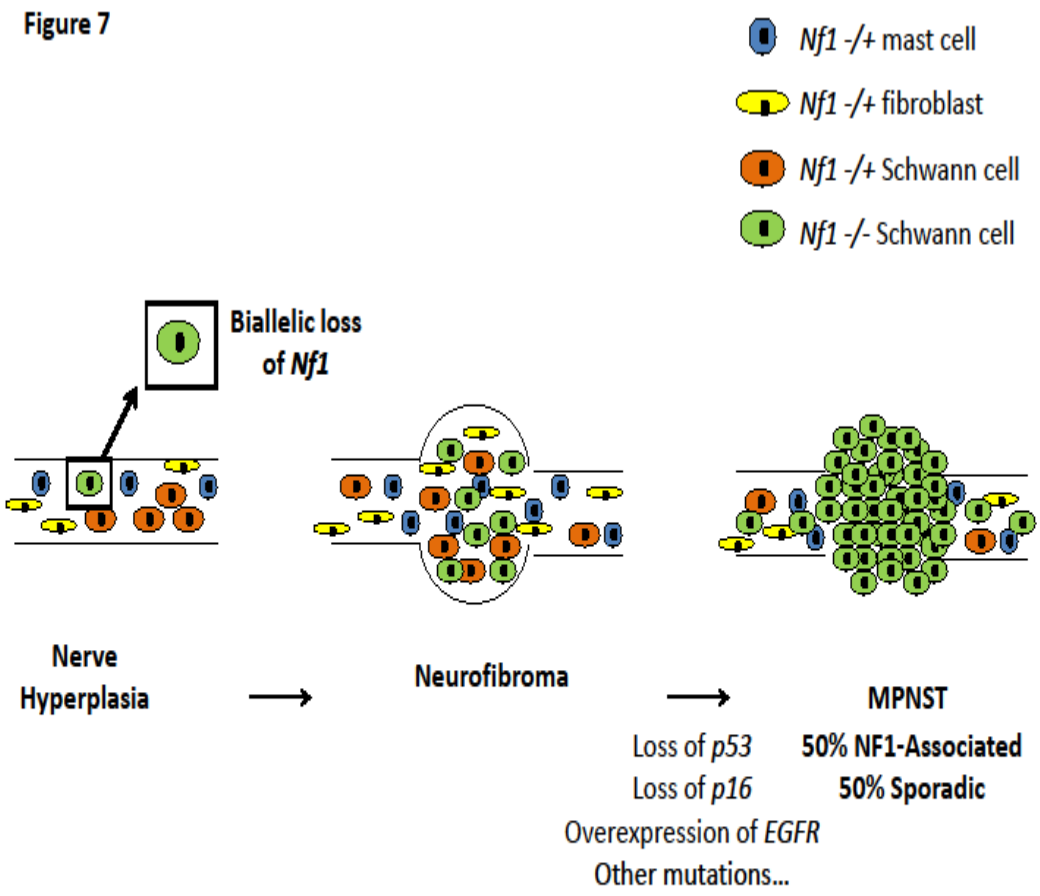
Nf1 -/+ mast cell
Nf1 -/+ fibroblast
Nf1 -/+ Schwann cell
Nf1 -/- Schwann cell
Biallelic loss of Nf1
Nerve Hyperplasia
Neurofibroma
MPNST
Loss of p53
Loss of p16
Overexpression of EGFR
Other mutations...
50% NF1-Associated
50% Sporadic

Figure 8: NF1 is a negative regulator of RAS. *NF1* is a gene that encodes for the protein Neurofibromin. This protein is a Ras GTPase-activating protein, or RAS-GAP. Neurofibromin functions as a negative regulator of Ras signaling by keeping Ras in its GDP bound state. When *NF1* is mutated or deleted, constitutive Ras signaling occurs, and the MAPK and PI3K/AKT/mTOR pathways are hyperactivated. This results in a proliferative and survival advantage in cells that are *NF1* null. This figure was adapted from mycancergenome.org.

Figure 8

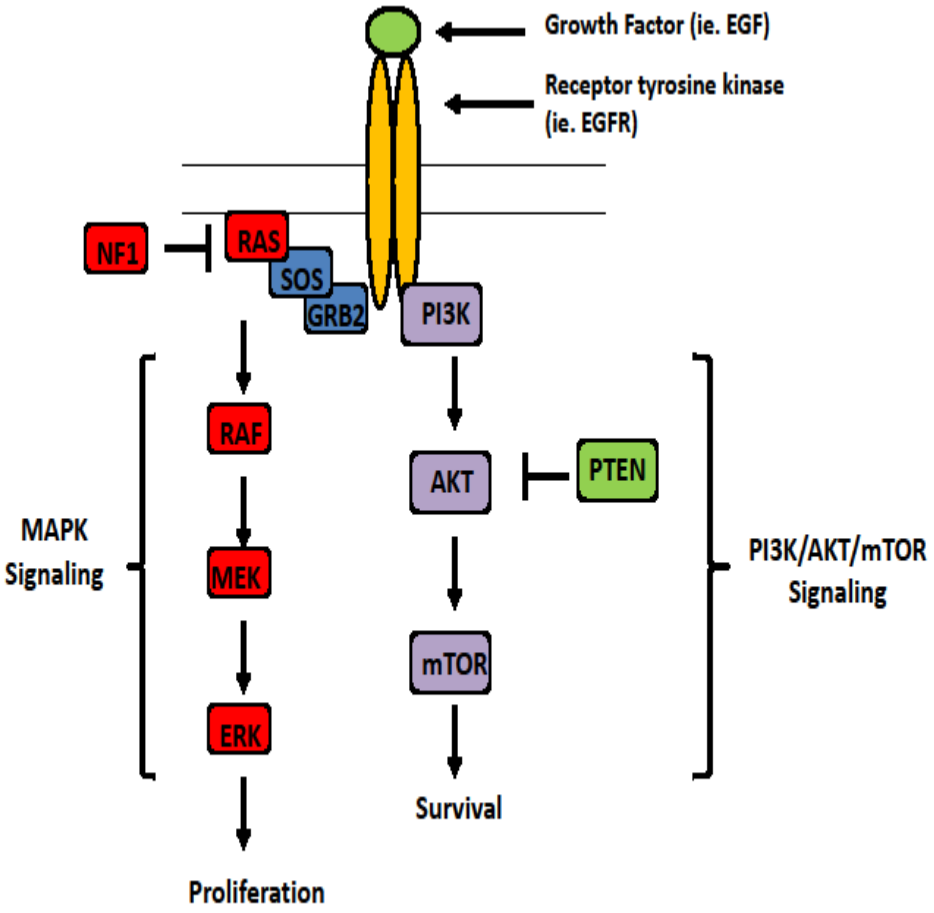
Growth Factor (ie. EGF)
Receptor tyrosine kinase
(ie. EGFR)
NF1
RAS
SOS
GRB2
PI3K
RAF
AKT
PTEN
MAPK
Signaling
MEK
mTOR
PI3K/AKT/mTOR
Signaling
ERK
Survival
Proliferation

Figure 9: *T2/Onc* identifies oncogenes and tumor suppressor genes. A. *T2/Onc* is a mutagenic transposon which is flanked by inverted repeat/direct repeat (IR/DR) sequences that the *SB* enzyme can recognize, allowing excision from the donor locos and insertion randomly into the genome. *T2/Onc* has been genetically engineered to be an oncogenic transposon, containing splice donor (SD)/splice acceptor (SA) sequences, polyadenylation (pA) sequences, and a murine stem cell virus 5' LTR (MSCV 5' LTR) sequence. B. The *T2/Onc* transposon can identify oncogenes by integrating in the genome upstream of proto-oncogenes. The MSCV 5'LTR allows the transposon to cause overexpression of genes downstream of the integration site. C. The *T2/Onc* transposon can identify tumor suppressor genes (TSG) by integrating within a TSG. If the transposon lands within an exon of a TSG, it can disrupt the gene, and if it lands within an intron, it can cause a truncated product due to the presence of the SD/SA and pA sequences (Collier and Largaespada, 2005; Dupuy et al., 2009). This figure was adapted from Collier and Largaespada, 2005.

Figure 9

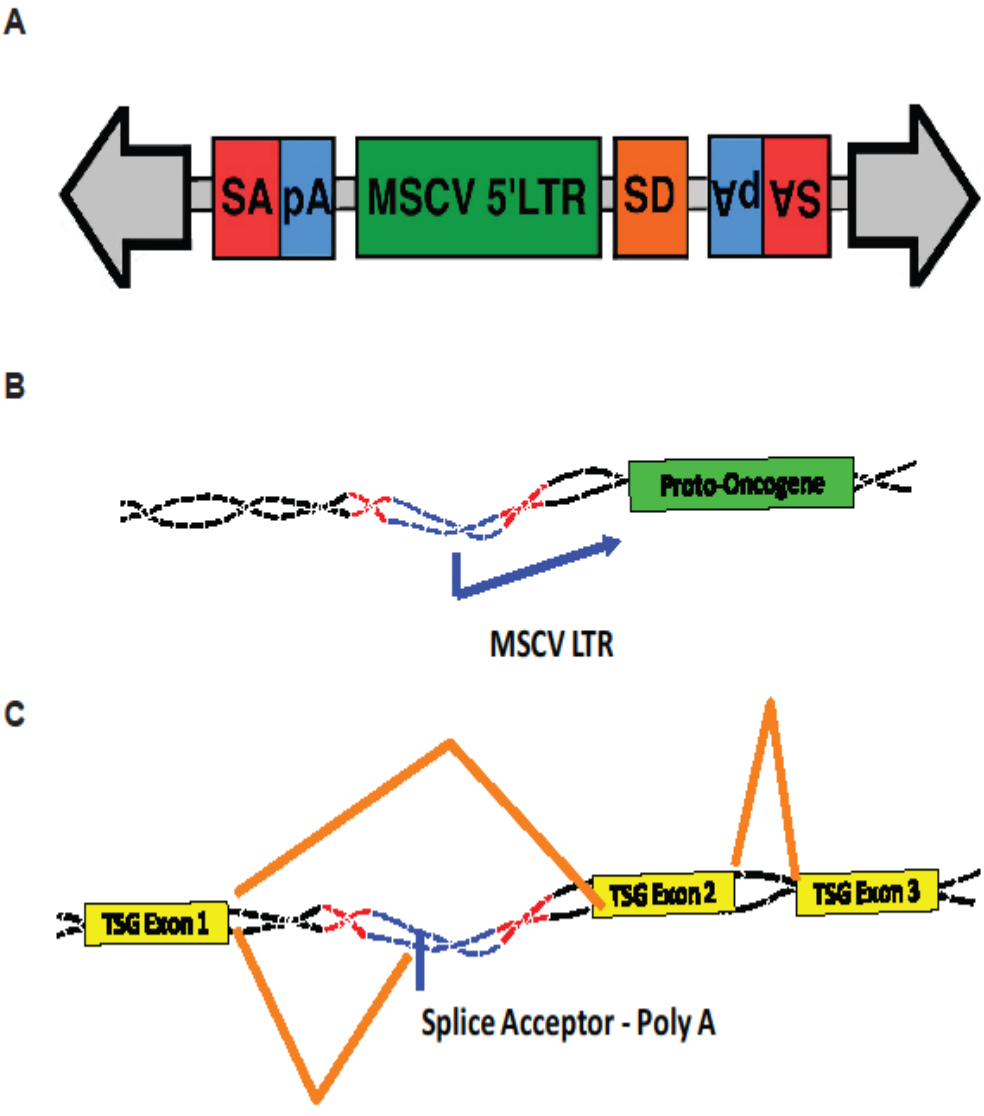
A
SA
pA
MSCV 5'LTR
SD
pA
SA
B
Proto-Oncogene
MSCV LTR
C
TSG Exon 1
TSG Exon 2
TSG Exon 3
Splice Acceptor - Poly A

Figure 10: *SB* mutagenesis results in the development of Schwann cell tumors. Schwann cell tumors were derived from animals with *EGFR* overexpression, expression of a *p53* dominant negative allele, and *SB* transposition in Schwann cells. The resulting tumors occurred in locations in which resemble the locations seen in patients including the brachial plexus, lumbar plexus, sciatic nerve, and nerves of the dorsal root ganglia. Histological analysis also revealed that these tumors microscopically resemble human tumors with high cellularity and spindle-shaped cells. Hematoxylin and eosin (H & E) staining and immunohistochemistry for proliferation (Ki67) allowed tumor grades to be determined, and we found nerve hyperplasia, grade 1 neurofibromas, grade 2 Schwannomas, and grade 3 PNSTs. S100 staining, a marker of Schwann cells, confirmed that the tumors seen were derived from a Schwann cell origin (Rahrmann et al., 2013).

Figure 10

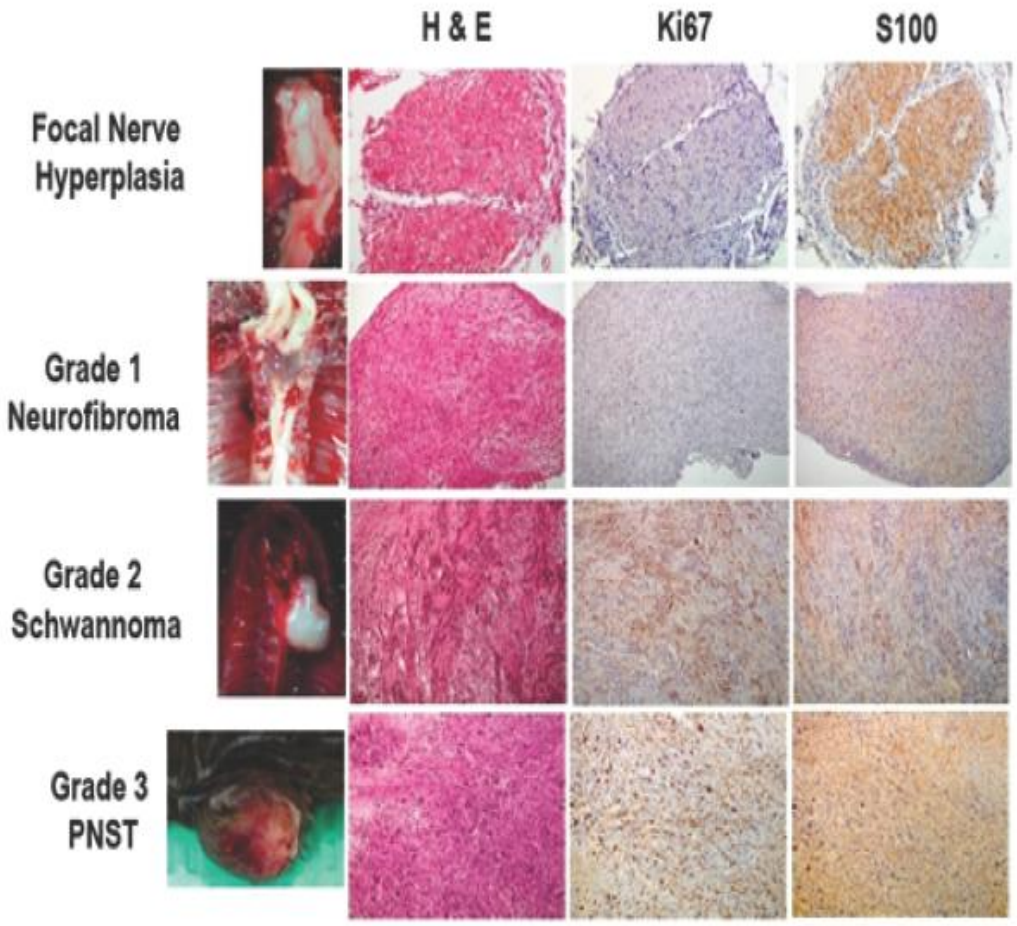
H & E
Ki67
S100
Focal Nerve Hyperplasia
Grade 1 Neurofibroma
Grade 2 Schwannoma
Grade 3 PNST

Figure 11: *SB* mutagenesis increase tumor burden and grade while decreasing latency. Wild type mice or mice with transposition alone did not form tumors at a significant frequency. When *EGFR* was overexpressed and a dominant negative allele of *p53* was expressed in Schwann cells, over 70% of mice developed tumors. The majority of these tumors were benign neurofibromas that occurred with an average latency of 362 days. In contrast, when *SB* transposition was induced in the context of *EGFR* overexpression and loss of *p53* function, over 80% of mice developed tumors. These tumors were mostly high grade PNSTs with an average latency of 299 days. Because *SB* transposition increased tumor frequency, increased tumor grade, and decreased latency, we concluded that we were in fact identifying genetic drivers of Schwann cell tumorigenesis by transposon mutagenesis (Rahrmann et al., 2013). This figure was adapted from Rahrmann et al., 2013.

Figure 11

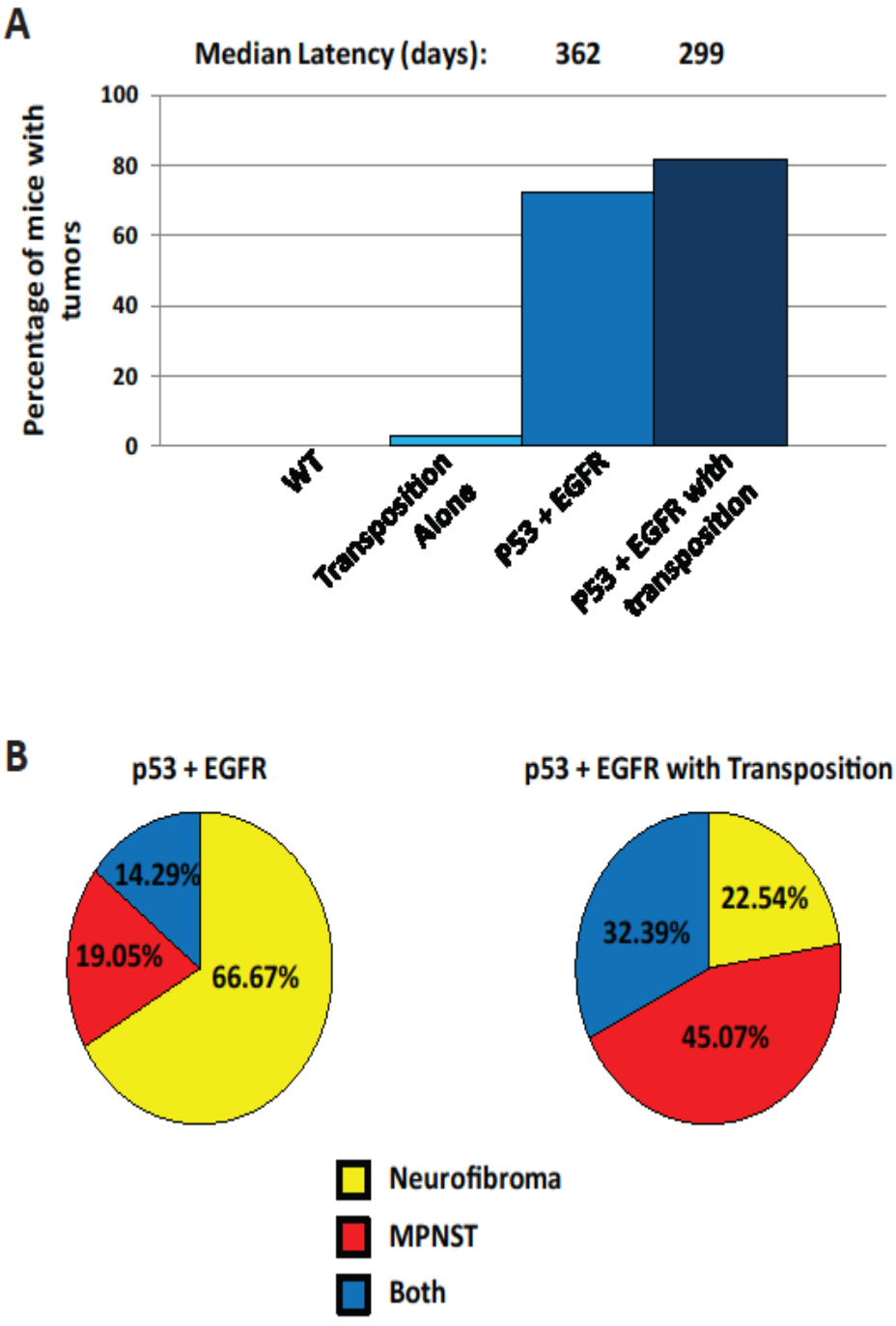
A
Median Latency (days):
362
299
Percentage of mice with tumors
100
80
60
40
20
0
WT
Transposition Alone
P53 + EGFR
P53 + EGFR with transposition
B
p53 + EGFR
p53 + EGFR with Transposition
14.29%
19.05%
66.67%
22.54%
32.39%
45.07%
Neurofibroma
MPNST
Both

Table 1: Mouse models of peripheral nerve tumors. The following table describes many of the genetically engineered mousse models available to study the development and progression of peripheral nerve tumors. The phenotype and limitation of each model is also described (Brossier and Carroll, 2012). This table was adapted from Brossier and Carroll et al., 2012.

Table 1: Mouse models of peripheral nerve tumors.

Transgenic mouse model	Phenotype
Nf1$^{\Delta 31/\Delta 31}$	Die by E13.5 due to cardiac failure
Nf1$^{\Delta 31/+}$	Develop pheochromocytomas (15% incidence); show accelerated development of other non-NF1 tumors as compared to wild-type mice
Nf1$^{-/-}$; *Nf1*$^{+/-}$ chimeras	Multiple plexiform neurofibromas present in animals with intermediate level of chimerism
Nf1$^{flox/flox}$; *Krox20-Cre*	Schwann cell hyperplasia
Nf1$^{flox/-}$; *Krox20-Cre*	Plexiform neurofibroma development by 1yr of age (demonstrating importance of both *Nf1*$^{+/-}$ and *Nf1*$^{-/-}$ cells in neurofibroma formation)
Nf1$^{flox/flox}$; *Krox20-Cre* transplanted with *Nf1*$^{+/-}$ bone marrow	Developed plexiform neurofibromas infiltrated by donor mast cells (demonstrating importance of Nf1 haploinsufficiency in hematopoietic lineage for neurofibroma formation)
Nf1$^{flox/flox}$; *Krox20-Cre* transplanted with *Nf1*$^{+/-}$; *c-Kit*$^{W41/W41}$ bone marrow	No neurofibromas developed (demonstrating importance of c-Kit signaling in Nf1 haploinsufficient cells in the hematopoietic lineage)
Nf1$^{flox/+}$; *Krox20-Cre* transplanted with *Nf1*$^{+/+}$ bone marrow	No neurofibromas developed (demonstrating importance of Nf1 haploinsufficiency in hematopoietic lineage for neurofibroma formation)
Nf1$^{flox/-}$; *Wnt1-Cre*,	Died at birth; no neurofibromas developed
Nf1$^{flox/-}$; *Mpz-Cre*	
Nf1$^{flox/-}$; *Pax3-Cre*	
Nf1$^{flox/-}$; *3.9Periostin-Cre*	Died by 4 weeks after birth; no neurofibroma development observed
Nf1$^{flox/-}$; *P*$_{0a}$*-Cre*	Plexiform neurofibroma formation observed by 15–20 months
Nf1$^{flox/flox}$; *Dhh-Cre*	Plexiform and subcutaneous neurofibroma development (demonstrating that an *Nf1*$^{+/-}$ microenvironment might not be strictly required for neurofibroma formation)
Nf1$^{flox/-}$; *CMV-CreERT2*; *Rosa26*	Dermal neurofibromas generated ~6 months following topical tamoxifen administration
trans-linked *Nf1*$^{+/-}$*;p53*$^{+/-}$	Developed non-MPNST sarcomas characteristic of *p53* LOH
cis-linked Nf1 $^{+/-}$*;p53*$^{+/-}$	Developed MPNSTs (~30% incidence)
Nf1$^{+/-}$*p16*$^{Ink4a-/-}$	Accelerated development of tumors characteristic of p16 ^{INK4a} loss

Transgenic mouse model	Phenotype
Nf1$^{+/-}$*p19*$^{Arf-/-}$	Accelerated development of tumors characteristic of p19 ^{Arf} loss
Nf1$^{+/-}$*p16*^{Ink4a}*/p19*$^{Arf-/-}$	Developed MPNSTs (~30% incidence)
^{LSL}*Nras*$^{G12V/+}$; *CAMK2-Cre*	Pigmentary abnormalities of skin and dermal neurofibromas observed
^{LSL}*Kras2B*$^{G12D/+}$; *mGFAP-Cre*	No obvious phenotype
^{LSL}*Kras2B*$^{G12D/+}$*Pten*$^{flox/+}$; *mGFAP-Cre*	Plexiform neurofibroma development by 4 months of age with progression to MPNSTs by 7 months
P_0-*GGF*β *3*	Neurofibroma formation with progression to MPNSTs by 6–10 months
CNPase-EGFR	Schwann cell hyperplasia with mast cell recruitment and fibrosis
Dhh-Cre; Nf1 $^{fl/fl}$*; Pten* $^{fl/fl}$	>20 high grade peripheral nerve sheath tumors in 100% of animals, mice moribund by day 15.
Dhh-Cre; Pten $^{fl/fl}$*; EGFR*	10-15 high grade peripheral nerve sheath tumors in 100% of animals, mice moribund by day 28.

Chapter 2: Canonical Wnt/β-catenin Signaling Drives Human Schwann Cell Transformation, Progression, and Tumor Maintenance

Adrienne L. Watson[1,2,3,4], Eric P. Rahrmann[1,2,3,4], Branden S. Moriarity[1,2,3,4], Kwangmin Choi[9,11], Caitlin B. Conboy[1], Andrew D. Greeley[1,2], Amanda L. Halfond[5], Leah K. Anderson[2], Brian R. Wahl[2], Vincent W. Keng[1,2,3,4,13], Anthony E. Rizzardi[7], Colleen L. Forster[8], Margaret H. Collins[10,11], Aaron L. Sarver[1], Margaret R. Wallace[12], Stephen C. Schmechel[6,7,8], Nancy Ratner[9,11], and David A. Largaespada[1,2,3,4,5]

Adapted by permission from the American Association for Cancer Research:

Adrienne L. Watson et al., Canonical Wnt/β-catenin Signaling Drives Human Schwann Cell Transformation, Progression, and Tumor Maintenance, *Cancer Discovery*, 2013, Epub ahead of print.

[1]Masonic Cancer Center, [2]Department of Genetics, Cell Biology and Development, [3]Center for Genome Engineering, [4]Brain Tumor Program, [5]Health and Natural Sciences Department, [6]Department of Pediatrics, [7]Department of Laboratory Medicine and Pathology, [8]BioNet, Academic Health Center, University of Minnesota, Minneapolis, MN 55455, USA. [9]Division of Experimental Hematology and Cancer Biology, [10]Division of Pathology and Laboratory Medicine, **[11]**Department of Pediatrics, Cincinnati Children's Hospital Medical Center, Cincinnati, OH 45229, USA. [12]Department of Molecular Genetics and Microbiology, University of Florida, Gainesville, FL 32611, USA. [13]Department of Applied Biology and Chemical Technology, The Hong Kong Polytechnic University, Hung Hom, Kowloon, Hong Kong.

Running title: Canonical Wnt/β-catenin signaling in MPNST

This work was supported by the National Institutes of Health (P50 NS057531), The Children's Tumor Foundation, The Zachary NF Fund, and The Jacqueline Dunlap NF Fund. A.L.W is funded by the 2011 Children's Tumor Foundation Young Investigators Award (2011-01-018). K.C. is funded by the National Cancer Institute Training Grant 5T32CA059268-15. C.B.C is funded by NIH F30 CA171547 and NIH MSTP grant T32 GM008244. These studies utilized BioNet

histology and digital imaging core facilities which are supported by NIH grants P30-CA77598 (D Yee), P50-CA101955 (D Buchsbaum), and KL2-RR033182 (B Blazar), and by the University of Minnesota Academic Health Center.

Correspondence should be addressed to David A. Largaespada (larga002@umn.edu)

Keywords: Malignant peripheral nerve sheath tumors, Schwann cells, neurofibromatosis type 1 syndrome, neurofibromin 1, neurofibromatosis 1, Wnt signaling, β-catenin, targeted therapies, Sleeping Beauty transposon system, forward genetic screen, murine models

Conflict of interest statement: Dr. Largaespada is the co-founder and part owner of two biotechnology companies, NeoClone Biotechnology, Inc. and Discovery Genomics, Inc. No company resources or personnel were involved in this research, which is unrelated to the goals of these companies.

Author Contributions:

Adrienne L. Watson: Her work contributed to the majority of the data published. She designed and optimized the majority of the experiments including the analysis of mouse tumors and human cell lines, the analysis of the human tissue microarray results, the functional studies using gene knockdown and overexpression, the analysis of *RSPO2* expression and functional outputs, and the assessment of small molecule inhibitors in MPNST cell lines. She also did the majority of data analysis and writing of the manuscript.

Eric P. Rahrmann: He assisted in experimental design and interpretation. He performed the *Sleeping Beauty* screen to identify genes that contribute to MPNST development and progression. He performed the β-catenin immunohistochemistry on mouse tumors from the *Sleeping Beauty* screen. He was also an integral part of optimizing experiments and conditions to allow functional assay to be performed.

Branden S. Moriarity: He developed the constructs used for gene overexpression, including the *GSK3B* overexpression cassette and the *Luciferase* control. He assisted with optimizing and validating gene knockdown and overexpression in cells, allowing for functional assays to be performed.

Kwangmin Choi: He compiled, interpreted, and made the figure for the microarray gene expression data.

Caitlin B. Conboy: She assisted with the experimental design and constructs used in the *RSPO2* experiments. Additionally, she provided the *β-catenin* overexpression and *dsred* control constructs.

Andrew D. Greeley: He maintained mice and performed immunohistochemistry on the mouse tumors from previously published MPNST models. He also helped in collecting data from xenograft mouse models.

Amanda L. Halfond: She maintained cells in culture and assisted in setting up soft agar assays. She also contributed to the QPCR results presented in the manuscript.

Leah K. Anderson: She helped conduct QPCR and western blots shown in the figure. She also played a significant role in maintaining xenograft mice and harvesting their tumors.

Brian R. Wahl: He maintained cells in culture and assisted in setting up proliferation assays.

Vincent W. Keng: He designed, developed, and provided two novel mouse models of MPNST used in this work.

Anthony E. Rizzardi: He assisted in analysis and interpretation of the human tissue microarray.

Colleen L. Forster: She performed the immunohistochemistry on the human tissue microarray.

Margaret H. Collins: She performed all pathological analyses of all mouse Schwann cell-derived tumors that were generated in the *Sleeping Beauty* screen.

Aaron L. Sarver: He performed the bioinformatic distillation of genes identified in the *Sleeping Beauty s*creen.

Margaret R. Wallace: She made and provided the immortalized human Schwann cells used in this work.

Stephen C. Schmechel: He oversaw work done on the tissue microarray.

Nancy Ratner: She was a co-principal investigator on the grant for this work.

David A. Largaespada: He was a co-principal investigator on the grant for this work.

Genetic changes required for the formation and progression of human Schwann cell tumors remain elusive. Using a *Sleeping Beauty* forward genetic screen, we identified several genes involved in canonical Wnt signaling as potential drivers of benign neurofibromas and malignant peripheral nerve sheath tumors (MPNSTs). In human neurofibromas and MPNSTs, activation of Wnt signaling increased with tumor grade and was associated with down-regulation of β-catenin destruction complex members or overexpression of a ligand that potentiates Wnt signaling, R-spondin 2 (RSPO2). Induction of Wnt signaling was sufficient to induce transformed properties to immortalized human Schwann cells, and down-regulation of this pathway was sufficient to reduce the tumorigenic phenotype of human MPNST cell lines. Small molecule inhibition of Wnt signaling effectively reduced viability of MPNST cell lines, and synergistically induced apoptosis when combined with an mTOR inhibitor, RAD-001, suggesting that Wnt inhibition represents a novel target for therapeutic intervention in Schwann cell tumors.

I. Introduction

Malignant peripheral nerve sheath tumors (MPNSTs) are soft tissue sarcomas that are believed to originate in the Schwann cell or Schwann cell precursors (Carroll and Ratner, 2008). These tumors can occur in the context of Neurofibromatosis Type 1 Syndrome (NF1), which occurs in 1 in 3,000 live births, but can also occur spontaneously in the general population (Uhlmann and Plotkin, 2012; Widemann, 2009). Due to the incomplete understanding of the genes and pathways driving MPNST development and progression, the current treatment for patients is surgical resection of the tumor, if possible, followed by non-specific, high-dose chemotherapy (4,5). These therapies often prove ineffective, and subsequently, patients with MPNSTs suffer very poor 5-year survival rates of less than 25% (Katz et al., 2009; Widemann, 2009). This demonstrates the urgent need for a more complete understanding of the genetic events that drive these tumors, in order to develop novel targeted therapies to treat these patients.

It is known that biallelic loss of the *Neurofibromin 1* gene (*NF1*) in Schwann cells is the pathological cause of the benign neurofibromas seen in NF1 patients, but secondary genetic changes, many of which remain unknown, must occur for these benign tumors to transform into MPNSTs (Carroll, 2012; Carroll and Ratner, 2008; Gregorian et al., 2009; Kourea et al., 1999a; Kourea et al., 1999b). Ten percent of NF1-associated neurofibromas will undergo malignant transformation, the leading cause of death in adult NF1 (Katz et al., 2009).

MPNSTs can also form spontaneously, in the absence of *NF1* loss, and the genes responsible for spontaneous MPNST formation are also largely unknown (Katz et al., 2009; Widemann, 2009). Loss of Phosphatase and Tensin Homolog (PTEN) expression and overexpression of Epidermal Growth Factor Receptor (EGFR) are two changes often seen in both spontaneous MPNSTs and NF1-associated MPNSTs, but there are likely many other important genetic changes and signaling pathways yet to be identified (Carroll, 2012; Gregorian et al., 2009; Holtkamp et al., 2008; Keng et al., 2012a; Ling et al., 2005; Mawrin, 2010; Tawbi et al., 2008; Vincent W. Keng, 2012).

Canonical Wnt/β-catenin signaling has been shown to play a role in many types of cancer, including colorectal, lung, breast, ovarian, prostate, liver and brain tumors (MacDonald et al., 2009). However, this pathway has not been directly implicated in neurofibromas or MPNSTs. In other cell types, Wnt signaling can be activated in cancer through a variety of mechanisms, including activating mutations in β-catenin (*CTNNB1*), overexpression of Wnt ligand genes, inactivating mutations in *AXIN1*, *GSK3B*, and *APC* (all members of the β-catenin destruction complex), and promoter hypermethylation of negative regulators of Wnt signaling (Curtin and Lorenzi, 2010). Another mechanism of Wnt pathway activation recently shown in colorectal cancer is overexpression of R-spondins due to gene fusions (Seshagiri et al., 2012). R-spondins are secreted ligands that can potentiate Wnt signaling in the presence of Wnt ligands (Jin and Yoon, 2012).

Wnt signaling can also be activated via crosstalk with other signaling pathways including the PI3K/AKT/mTOR pathway, where loss of PTEN can activate PKB/AKT, causing the phosphorylation and inactivation of GSK3B, resulting in stabilization of β-catenin protein (Gehrke et al., 2009). Growth factor signaling pathways can also activate Wnt signaling; such as the case of Epidermal Growth Factor (EGF) stimulation of the receptor (EGFR), which results in the activation of β-catenin/TCF/LEF-dependent transcription of genes such as *CyclinD1 (CCND1), C-Myc (MYC),* and *Survivin (BIRC5)* (Emami et al., 2004; Hu and Li, 2010). Notably, some human MPNSTs have been shown to have loss of PTEN expression and/or express high levels of active EGFR (Holtkamp et al., 2008; Ling et al., 2005; Mawrin, 2010; Vincent W. Keng, 2012). β-catenin-dependent transcription can promote progression through the cell cycle, stem cell self-renewal, and epithelial to mesenchymal transition, all of which play a role in tumor initiation and progression (Barker, 2008; Curtin and Lorenzi, 2010; MacDonald et al., 2009). Due to the importance of this pathway in driving tumorigenesis in many types of cancer, the development of small molecule inhibitors that target Wnt signaling is rapidly underway and has the potential for profound clinical benefits for patients with Wnt-driven tumors (Curtin and Lorenzi, 2010; Ischenko et al., 2008; Yao et al., 2011).

We have implicated canonical Wnt signaling in the development and progression of peripheral nerve tumors by using a murine *Sleeping Beauty (SB)*

forward genetic screen (Rahrmann et al., 2013). Additionally, we demonstrate that several well-established murine models of neurofibromas and MPNST development also exhibit activation of the Wnt signaling pathway. Activation of this pathway has been confirmed in human patient samples by gene expression microarray analysis and tissue microarray (TMA) studies. Activation of Wnt signaling occurs in human tumors through multiple mechanisms including down-regulation of β-catenin destruction complex members and overexpression of R-spondin 2 (*RSPO2*). We demonstrate that activating canonical Wnt signaling is sufficient to induce transformed properties in immortalized human Schwann cells *in vitro*. We also show that down-regulating canonical Wnt signaling reduces the oncogenic and tumorigenic phenotypes observed in human NF1-associated and sporadic MPNST cell lines as measured by cell viability, colony formation, and xenograft tumor growth. Further, we find that small molecule inhibitors of Wnt signaling inhibit MPNST cell viability with little effect on normal human Schwann cells. These inhibitors show marked synergistic effects when combined with the mammalian target of rapamycin (mTOR) inhibitor, RAD-001, which has previously shown to be moderately effective in preclinical MPNST models (Johannessen et al., 2008; Johansson et al., 2008; Wu et al., 2012). These results suggest that Wnt/β-catenin signaling is a novel drug target for patients with MPNSTs.

II. Results

Diverse mouse models implicate canonical Wnt signaling in Schwann cell tumor development and progression

To identify genes and pathways that drive Schwann cell tumor development and progression, a forward genetic screen using the *SB* transposon system was conducted in mice, similar to many that have been previously published (Largaespada, 2009). The full details of this screen will be published separately (Rahrmann et al., 2013). This screen identified several members of the canonical Wnt/β-catenin signaling pathway in the development of benign neurofibromas and MPNSTs (**Supplementary Table 1**). This screen was conducted using a *CNPase* promoter driving *Cre* expression which, in combination with a Cre/Lox-regulated *Rosa26-SB11*^{LSL} transgene, allows for T2/Onc mutagenic transposon mobilization in Schwann cells and their precursors, the cell of origin for peripheral nerve sheath tumors (Lappe-Siefke et al., 2003). A common transposon insertion site (CIS) associated gene list was generated independently for benign neurofibromas and MPNSTs, as diagnosed by histopathological examination (Rahrmann et al., 2013). We required that integrations map uniquely to the murine genome with a sequence length that would preclude random mapping. Further, we required that each integration be present at greater than 1/10,000 of the total sequences present to exclude potential

non-driver mutations that are found in minor sub-clones or due to artifacts (Sarver et al., 2012). When the entire CIS gene list for MPNSTs was analyzed using Ingenuity Pathway Analysis (IPA, Ingenuity ® Systems, www.ingenuity.com), we found enrichment for genes that are present in the Wnt/β-catenin pathway (p= 3.93E-4). Further, when immunohistochemistry (IHC) analysis was performed on murine tumors from this *SB* screen at various stages of progression, the level and nuclear localization of β-catenin increased with tumor progression (**Figure 1A**). In addition to tumors from mice induced with *SB,* four other well-established mouse models of MPNST showed nuclear β-catenin expression (**Figure 1B**) (Cichowski et al., 1999; Keng et al., 2012a; Mayes et al., 2011; Vincent W. Keng, 2012; Vogel et al., 1999). These mouse models represent both NF1-associated and sporadic MPNST development by a variety of genetic mechanisms. Interestingly, tumors from the rapidly forming, highly aggressive models, *Dhh-Cre; Nf1* $^{fl/fl}$*; Pten* $^{fl/fl}$ and *Dhh-Cre; Pten* $^{fl/fl}$*; CNP-EGFR* stained very strongly for nuclear β-catenin, while the slower forming *NPcis* and *PLP-Cre; Nf1* $^{fl/fl}$ tumors had less total β-catenin, but still highly nuclear staining. Thus, the intensity of nuclear β-catenin staining may correlate with and indeed drive tumor aggressiveness.

To determine the role of Wnt/β-catenin signaling in human Schwann cell tumors, we assayed expression and localization of β-catenin and expression of known Wnt target genes in human Schwann cells and MPNST cell lines.

Activated β-catenin is found in the nucleus where it can be transcriptionally active, while inactive β-catenin is cytoplasmically localized or membrane-bound (Barker, 2008). In a *TERT/CDK4*^{R24C} immortalized human Schwann cell line (iHSC2λ, Margaret Wallace, manuscript in preparation), β-catenin was expressed, but localized primarily in the cytoplasm (**Figure 1C**). In contrast, both sporadic and NF1-associated MPNST cell lines (STS-26T and ST8814, respectively) expressed a similar level of β-catenin, but with predominantly nuclear localization. Western blot analysis showed that in all 4 MPNST cell lines analyzed, the level of MYC protein was increased, and in 2 out of 4 MPNST cell lines, CCND1 protein was increased compared to the immortalized human Schwann cell line (**Figure 1D)**. These data suggest that known β-catenin outputs are increased in MPNST cell lines compared to immortalized human Schwann cells.

Canonical Wnt signaling is activated in a subset of human neurofibromas and MPNSTs

To characterize whether alterations in regulators of Wnt signaling underlie pathway activation in MPNST cell lines, we assayed Wnt regulators by gene expression microarray in purified Schwann cells taken from human peripheral nerve, neurofibromas, and MPNSTs, as well as solid tumors at various stages of disease (Miller et al., 2009) (**Figure 2**). Several members of the β-catenin

destruction complex, including *APC* and *GSK3B*, showed down-regulation with tumor progression, in a subset of cases. The Wnt ligands *WNT2*, *WNT5A*, and *WNT5B* showed an increase in many or most samples. These data suggest that multiple mechanisms activate canonical Wnt signaling in human Schwann cell tumors.

To further investigate activation of Wnt signaling in human tumors, and to account for regulation of Wnt signaling by post-translational mechanisms such as protein degradation or localization, we constructed a human tissue microarray (TMA) composed of 30 benign dermal neurofibromas (dNF), 32 plexiform neurofibromas (pNF), and 31 MPNSTs. The fraction of tumors positive for β-catenin increased with tumor progression (55.9% dNF, 86.2% pNF, 96.9% MPNSTs, p=0.0001 Fisher's Exact Test) (**Figure 3A**). Additionally, the percentage of tumors with nuclear β-catenin was higher in the MPNSTs than in the neurofibromas (**Figure 3B & C**). As a transcriptional output of Wnt signaling, we also quantified the percentage of CCND1 positive tumors and found that it also increased in the higher grade tumors (67.6% dNF, 64.7% pNF, 94.1% MPNST, p=0.0051 Fisher's Exact Test) (**Figure 3D**). Further, the intensity of CCND1 staining increased with tumor progression (p=0.0356 Fisher's Exact Test) (**Figure 3E & F**). As an additional transcriptional output of Wnt signaling, we assessed C-MYC staining intensity and found that it too showed a trend towards increased expression with tumor progression (p=0.1603 Fisher's Exact

Test) (**Supplementary Figure 1A & B**). This suggests that the acquisition of nuclear β-catenin in these tumors is activating known β-catenin-targets, and correlates with tumor progression. To confirm this, we assessed β-catenin and CCND1 staining on a plexiform neurofibroma which transformed into an MPNST. While there was only a single patient represented on our TMA with a paired plexiform neurofibroma and MPNST, we found that indeed, β-catenin level and nuclear localization increased in the MPNST. Further, while the plexiform neurofibroma was negative for CCND1, the MPNST was positive for CCND1 (**Figure 3G**).

Activation of Wnt/β-catenin signaling is sufficient to induce transformed phenotypes in immortalized Schwann cells

We next functionally validated a subset of the β-catenin regulatory genes identified in our *Sleeping Beauty* screen that were also implicated in human tumors (**Supplementary Table 1 & Figure 2**). We hypothesized that if Wnt/β-catenin signaling played a role in the development of peripheral nervous system tumors, then activation of this pathway in immortalized human Schwann cells may be sufficient to drive a more transformed phenotype in these cells. To activate Wnt signaling, we expressed an activated form of *CTNNB1 (CTNNB1*^{S33Y}) in immortalized human Schwann cells (iHSC1λ and iHSC2λ). Cells overexpressing *CTNNB1*^{S33Y} showed increased levels of total β-catenin protein,

but interestingly, only the iHSC1λ cells showed increased activated β-catenin (**Figure 4A**). Expression of *CTNNB1*^{S33Y} resulted in increased expression of *MYC, CCND1, AXIN2, LEF1,* and *BIRC5* in both iHSC1λ and iHSC2λ cell lines, demonstrating activation of genes that have been shown to be β-catenin targets (**Supplementary Figure 2A & B**). *CTNNB1*^{S33Y} expression also resulted in increased cell viability (**Figure 4B**), but did not change soft agar colony formation (**Figure 4C**). However, we did observe that cells overexpressing *CTNNB1*^{S33Y} stopped growing as a monolayer, as seen in non-transformed cells, and began growing as three-dimensional colonies (**Figure 4D**).

In addition to activating Wnt signaling by overexpressing *CTNNB1*^{S33Y}, we used shRNA to knock down *AXIN1* and *GSK3B*, both members of the β-catenin destruction complex identified in our *SB* screen (**Supplementary Table 1**) and known tumor suppressor genes in other types of cancers (MacDonald et al., 2009). These genes were knocked down in both immortalized human Schwann cell lines (iHSC1λ and iHSC2λ) using short hairpin RNAs (shRNAs), and validated by QPCR analysis (**Figure 4E & Supplementary Figure 2I)** and western blot analysis (**Supplementary Figure 2C & F**). We show that knockdown of either *AXIN1* or *GSK3B* activated genes that have been shown to be to be targets of β-catenin including *CCND1, MYC, AXIN2, LEF1,* and *BIRC5* (**Supplementary Figure 2D, E, G & H**). Knockdown of *AXIN1* or *GSK3B* was sufficient to induce oncogenic properties in immortalized human Schwann cells as

demonstrated *in vitro* by a significant increase in cell viability (**Figure 4F & Supplementary Figure 2J**) and anchorage-independent growth (**Figure 4G & Supplementary Figure 2K**) . When the immortalized human Schwann cells that expressed either *AXIN1* or *GSK3B* shRNAs were injected into immunodeficient mice, they were unable to induce tumor formation (data not shown), suggesting that while activation of Wnt signaling is sufficient to induce some oncogenic properties in Schwann cells *in vitro*, it is not sufficient to induce tumorigenic properties *in vivo.*

Inhibition of Wnt signaling can reduce the tumorigenic phenotype of MPNST cells

We next sought to determine whether inhibition of Wnt/β-catenin signaling in MPNST cell lines was sufficient to reduce cellular viability and anchorage-independent growth. To reduce Wnt signaling, we knocked down *CTNNB1* and *TNKS* in two MPNST cell lines, S462-TY (NF1-associated MPNST cell line (Mahller et al., 2008)) and STS-26T (sporadic MPNST cell line (Dahlberg et al., 1993)) using shRNA vectors. We chose to knockdown *CTNNB1* since it plays a direct role in the transcription of Wnt-dependent genes by binding TCF/LEF in the nucleus and acting as a transcriptional activator (22,23). *TNKS* was also knocked down because it was identified in our forward genetic screen and inhibition of *TNKS* is known to stabilize AXIN1, leading to the degradation of β-catenin protein (Huang et al., 2009). TNKS is also the target of many small

molecule inhibitors of the Wnt pathway (Huang et al., 2009). Knockdown of *CTNNB1* and *TNKS* by shRNA was confirmed by QPCR (**Figure 5A & D**). Reduction in either *β-catenin* or *TNKS* was sufficient to decrease expression of β-catenin transcriptional targets, as demonstrated by a reduction in the expression of *MYC, CCND1, AXIN2, LEF1,* and *BIRC5* (**Supplementary Figure 3A, B, C & D**). Knockdown of either *CTNNB1* or *TNKS* reduced cell viability (**Figure 5B & E**) and anchorage-independent growth (**Figure 5C & F**) in both S462-TY and STS-26T cells.

Overexpression of *GSK3B*, a member of the β-catenin destruction complex, also was sufficient to reduce the oncogenic properties of both the NF1-associated and sporadic MPNST cell lines. *GSK3B* overexpression was confirmed by western blot and QPCR and resulted in reduced β-catenin total protein levels (**Figure 5G, Supplementary Figure 3E & F**). The reduction in known Wnt signaling outputs was also shown by a decrease in *MYC, CCND1, AXIN2, LEF1*, and *BIRC5* transcript levels (**Supplementary Figure 3E & F**). *GSK3B* overexpression resulted in a decrease in cell viability (**Figure 5H**) and a significant decrease in soft agar colony formation in both cell lines (**Figure 5I**). These results suggest that these MPNST cell lines depend on Wnt signaling for rapid proliferation and robust colony forming abilities, and reduction in Wnt signaling can reduce these oncogenic properties.

To investigate the role of Wnt/β-catenin signaling *in vivo*, the S462-TY and STS-26T cell lines expressing either the *CTNNB1* shRNA or *GSK3B* cDNA were injected into immunodeficient mice, which were monitored for the rate of tumor formation and growth. Reduction in *CTNNB1* by shRNA delayed the rate of tumor growth in the NF1-asociated cell line (**Supplementary Figure 4A & B**). Tumor sections derived from cells expressing the *CTNNB1* shRNA showed fewer Ki67 positive cells compared to tumors derived from NS shRNA expressing cells (**Supplementary Figure 4C**). Overexpression of *GSK3B* resulted in reduction in tumor growth in the spontaneous MPNST cell line (**Supplementary Figure 4D & E**). Tumor sections from cells overexpressing *GSK3B* also showed fewer Ki67 positive cells compared to tumors derived from non-silencing (NS) shRNA expressing cells (**Supplementary Figure 4F**). Despite a significant delay in tumor onset, tumor volume at 40 days post-injection was similar in control and experimental groups. Evaluation of gene expression in these tumors indicated that knockdown of *CTNNB1* and overexpression of *GSK3B* was not maintained over the course of the experiment (data not shown).

R-spondin 2 is overexpressed in a subset of Schwann cell tumors and is a driver of Wnt signaling and MPNST cell growth

R-spondins are secreted ligands that potentiate Wnt signaling when Wnt ligand is available (Jin and Yoon, 2012). Microarray analysis showed that R-

spondin 2 (*RSPO2*) was highly expressed in 2 of 6 MPNST cell lines and 2 of 13 primary MPNSTs evaluated, compared with purified normal human Schwann cells or normal nerve (**Figure 6A**). Further, it has been shown that one mechanism for *RSPO2* overexpression is a deletion-mediated gene fusion between exon 1 of *EIF3E* and exon 2 of *RSPO2*, resulting in the overexpression of native RSPO2 protein (Seshagiri et al., 2012). To determine whether similar gene fusions occur in Schwann cell tumors, primers were designed to amplify any fusion transcripts between *EIF3E* and *RSPO2* in cDNA libraries made from 5 human MPNST cell lines and 2 immortalized human Schwann cell lines. We identified a fusion transcript expressed by the S462 MPNST cell line that was not present in any of the other MPNST or immortalized human Schwann cell lines (**Figure 6B**). Expression of this fusion correlated with a 1295-fold increase in *RSPO2* expression in the S462 cell line (**Figure 6C**). The fusion transcript that was identified included exon 1 of *EIF3E* fused to a 122 base pair region of chromosome 8 located between *EIF3E* and *RSPO2,* fused to exon 2 of *RSPO2* (**Figure 6D**). To determine if S462 cells require *RSPO2,* we used an shRNA construct to knock down its expression. Depletion of *RSPO2* significantly reduced expression of Wnt target genes and cell viability (**Figure 6E & F**). These data suggest that overexpression of *RSPO2* may drive a subset of human MPNSTs, and further support the model that Wnt signaling is activated in Schwann cells by multiple mechanisms.

Wnt inhibitors effectively reduce cellular viability in vitro

Our functional data suggested that targeting Wnt/β-catenin signaling with small molecule inhibitors, might be effective at reducing MPNST cell viability and tumor forming properties. To test this hypothesis, we exposed a panel of 5 MPNST cell lines (S462, S462-TY, ST8814, T265, and STS-26T) and 2 immortalized human Schwann cell lines (iHSC1λ and iHSC2λ) to two compounds that inhibit Wnt signaling, XAV-939 and IWR-1. These compounds both function to stabilize AXIN1 by inhibiting TNKS, resulting in an increase in β-catenin phosphorylation and subsequent degradation (Huang et al., 2009). We find normal Schwann cells are highly resistant to proliferation inhibition and cell death by these two compounds as demonstrated by high IC50 values, while the MPNST cell lines were quite sensitive with relatively low IC50s of 0.047uM to 2.22uM for XAV-939 and 0.055uM to 186.87uM for IWR-1 (**Figure 7A**) (CalcuSyn Version 2.1, BioSoft).

Wnt inhibitors synergize with an mTOR inhibitor to induce apoptosis of MPNST cells

We next conducted a screen to identify targeted therapies that synergized with Wnt signaling inhibitors to induce apoptosis in MPNST cell lines. Several drugs were screened, including inhibitors of PI3K (PI-103), mTOR (RAD-001

and Rapamycin), and MEK (PD-901 and AZD-6244). Of these drugs, the most significant synergism was seen with RAD-001. It has been shown that RAD-001 is modestly effective in several preclinical models of peripheral nerve tumors, but the effects of this drug are largely cytostatic (Johansson et al., 2008; Wu et al., 2012). In most cases, treatment of the S462, T265, and STS-26T MPNST cell lines with RAD-001, IWR-1, or XAV-939 as single agents at their IC50 concentrations resulted in less than 50% TUNEL-positive cells, demonstrating that while 50% of proliferation was inhibited, only a minority of cells underwent apoptosis (**Figure 7B & C**). In contrast, when the MPNST cell lines were treated with their IC25 dose of RAD-001 in combination with either IWR-1 or XAV-939 also at their IC25 dose, the percentage of TUNEL positive cells often went above 50%, and in the S462 cell line, even approached 100%, demonstrating that co-targeting the Wnt and mTOR pathways is synergistic in inducing apoptosis.

III. Materials and Methods

Mouse Tumor Immunohistochemistry (IHC)

Formalin fixed, paraffin embedded tissues were sectioned at 5 microns, mounted, and heat-fixed onto glass slides to be used for IHC analyses. Briefly, the glass section slides were de-waxed and rehydrated through a gradual decrease in ethanol concentration. The antigen epitopes on the tissue sections were then unmasked using a commercially available unmasking solution (Vector Laboratories) according to the manufacturer's instructions. The tissue section slides were then treated with 3% hydrogen peroxide to remove endogenous peroxidases. Blocking was performed at room temperature in normal goat serum (5% serum in PBS) in a humidified chamber for one hour. Sections were then incubated overnight at 4°C in a humidified chamber with primary antibody (β-catenin, 1:100, Cell Signaling). After primary incubation, sections were washed thoroughly in PBS before incubating with goat anti-rabbit horseradish peroxidase conjugated-secondary antibody (Santa Cruz Biotechnology). After 3 washes with PBS, the sections were treated with freshly prepared DAB substrate (Vector Laboratories) and allowed to develop before stopping the reaction in water once adequate signal was obtained. Finally, sections were then lightly counter-stained with hematoxylin, dehydrated through gradual increase in ethanol concentration,

cleared in Citrosol (Fisher Scientific) and mounted in Permount (Fisher Scientific).

Tissue culture reagents and cell lines

Cultured immortalized Schwann cells (iHSC1λ and iHSC2λ) were both derived from a patient's normal sciatic nerve, are *NF1* wild-type, and were immortalized by *hTERT* and $CDK4^{R24C}$ to allow *in vitro* studies (Dr. Margaret Wallace, manuscript in preparation). Immortalized human Schwann cell and MPNST cell lines (S462 (Frahm et al., 2004), S462-TY (Mahller et al., 2008), ST8814 (Fletcher et al., 1991), T265 (Badache and De Vries, 1998), and STS-26T (Dahlberg et al., 1993)) were maintained in Dulbecco's Modification of Eagle Medium (DMEM) supplemented with 10% fetal bovine serum and penicillin/streptomycin (Cellgro) and cultured on tissue culture-treated plates under standard conditions of 37 degrees Celsius and 5% CO2 . No authentication of cell lines was done by the authors.

Immunofluorescence and TUNEL staining

For immunofluorescence assays, cells were grown to 80% confluency on 8 chambered slides (Lab-TekII). Cells were fixed in 10% formalin and washed with phosphate-buffered saline (PBS) with 0.1% Tween-20 (PBST). Cells were incubated in β-catenin primary antibody (1:100, Cell Signaling) at 4 degrees Celsius overnight, followed by 1 hour room temperature incubation in anti-rabbit

AlexaFluor 488 secondary antibody (Invitrogen). TUNEL staining was performed using the In Situ Cell Death Detection Kit, POD (Roche). Slides were mounted using Prolong Gold Antifade Reagent with DAPI (Invitrogen) and images using a Zeiss Axiovert 25 inverted microscope. For analysis of cell death, total cells and TUNEL positive cells were counted and averaged over three independent frames with 50-100 cells per frame.

Western blot analysis

1 million cells were lysed using an NP-40 buffer (50mM Tris-HCl pH 7.6, 150mM NaCl, 1% NP-40, 5mM NaF, 1mM EDTA) containing a protease inhibitor (Roche) and phosphatase inhibitors (Sigma). Whole cell lysates were cleared by centrifugation. Protein samples were prepared in an SDS solution with reducing agent (Invitrogen) and run on 10% Bis-Tris pre-made gels (NuPage, Invitrogen). Gels were transferred onto PVDF membranes using the iBlot system (Invitrogen) and activated in 100% methanol. Membranes were blocked in filtered 5% Bovine Serum Albumin (BSA) for 2 hours at room temp followed by a 4 degrees Celsius overnight incubation in primary antibody. The primary antibodies used in this study were activated β-catenin (1:1000), total β-catenin (1:100), GSK3B (1:1000), AXIN1 (1:1000), and GAPDH (1:2000) (Cell Signaling). Following primary antibody incubation, membranes were thoroughly washed in TBS with 0.1% Tween-20 (TBST) and incubated in goat anti-rabbit IgG-HRP

conjugated secondary antibody (Santa Cruz, 1:4000 in 0.5% BSA, 1 hour at room temperature). Blots were thoroughly washed in TBST and developed using the SuperSignal WestPico Chemiluminescence Detection Kit (Thermo Scientific). Densitometry quantification was done using ImageJ software and normalized to GAPDH (Rasband, 1997-2012).

Microarray gene expression analysis

We used the published data (GEO accession #:GSE14038, Affymetrix GeneChip HU133 Plus 2.0) [38] for gene microarray analysis. This dataset used custom CDF (custom GeneChip library file) based on RefSeq target definitions (Hs133P REFSEQ Version 8) for accurate interpretation of GeneChip data (Dai et al., 2005). The dataset in Figure 2 includes 86 microarrays on purified human Schwann cells and primary tissues taken from a normal sciatic nerve, dermal neurofibromas, plexiform neurofibromas, and MPNST cell lines. The heatmap was generated using CRAN's pheatmap package (http://cran.r-project.org/web/packages/pheatmap/index.html) and Refseq IDs were replaced with corresponding HGNC official gene symbols. Statistical comparisons were done using R/Bioconductor's Limma package (http://www.bioconductor.org) and GeneSpring GXv7.3.1 (Agilent Technologies). Differentially expressed (DE)-genes were defined as genes with expression levels at least three-fold higher or

lower in target groups (MPNST) compared to NHSC after applying Benjamini and Hochberg false discovery rate correction (FDR/BH $p \leq 0.05$).

Tumor microarray (TMA) construction and immunohistochemistry

Representative areas of disease were identified on hematoxylin and eosin-stained sections for 30 neurofibromas, 32 plexiform neurofibromas, and 31 MPNSTs. TMA blocks consisting of duplicate 1.0 mm core samples were constructed with a manual tissue arrayer (MTA-1, Beecher Inc, WI) and limited to 64 cores per recipient block. Immunohistochemistry for CCND1 (SP4) monoclonal antibody (Neomarkers, Thermo Scientific, 1:50) and β-catenin (6B3) monoclonal antibody (Cell Signaling; 1:200) was performed utilizing an automated immunohistochemical staining platform (Nemesis 7200, Biocare) following standard IHC protocols (DeRycke et al., 2009). Digital images of IHC stained TMA slides were obtained as previously described (Rizzardi et al., 2012). P-values were determined using a 3x2 (staining positivity) or 3x3 (staining intensity or localization) Fisher's Exact Test to determine differences in staining between the three tumor types.

Gene knockdown and overexpression

GSK3B and *Luciferase* cDNA (Invitrogen) were each cloned into a vector containing a *CAGGS* promoter to drive cDNA expression followed by an *IRES-GFP*. These plasmid vectors were transfected into cells using the NEON

transfection system, according to manufacturer's protocol (Invitrogen). Three independent shRNAs targeting *AXIN1*, *GSK3B*, *CTNNB1*, *TNKS*, *RSPO2*, and a non-silencing (NS) control shRNA were purchased from OpenBiosystems. Lentiviral particles containing the shRNAs were produced in 293T cells using the Trans-Lentiviral Packaging Kit (Thermo Scientific). A *dsRed* control and $CTNNB1^{S33Y}$ were cloned into a vector containing a *CAGGS* promoter to drive cDNA expression followed by an *IRES-GFP* and also transduced into cells using lentiviral particles. Viral supernatant was collected after 24 hours of viral production, cleared, and applied directly to the cells for 6 hours. Following viral transduction, cells underwent selection in 4ug/mL puromycin (Invitrogen). shRNA expression was validated by GFP expression, western blot and QPCR. Data is shown for the one shRNA construct that gave the greatest knockdown as determined by western blot analysis and/or QPCR.

Quantitative Real-Time PCR (QPCR)

RNA was extracted from 1 million cells using the High Pure RNA Isolation Kit (Roche). RNA was analyzed by nanodrop (Thermo Scientific) and by agarose gel electrophoresis for quantification and quality control. 1ug of RNA was used to synthesize cDNA using the Transcriptor First Strand Synthesis (Roche) with both random hexamer and oligo dT primers. QPCR reactions were conducted using LightCycler 480 SYBR I Green (Roche) and run on an Eppendorf Mastercycler ep gradient S. Primer sequences can be found in **Supplementary Table 2**

(Biechele et al., 2009; Cui et al., 2007; Emami et al., 2004). Data were analyzed using RealPlex software, calibrated to *ACTB* levels and normalized to either over-expression control cells (expressing *CAGGS>Luciferase-IRES-GFP or dsRed*) or NS shRNA expressing cells and averaged over three experimental replicates.

Cellular Viability assays

Cellular viability assays were set up in a 96-well format with 100 cells plated per well in DMEM full media containing 4ug/mL puromycin (Invitrogen). Readings were taken every 24 hours over 6 days by the MTS assay (Promega). Absorbance was read at 490nm to determine viability and 650nm to account for cellular debris on a BioTek Synergy Mx automated plate reader.

Anchorage-independent growth assay

6-well plates were prepared with bottom agar composed of 3.2% SeaPlaque Agar (Lonza) in DMEM full media) and allowed to solidify before 10,000 cells in top agar (0.8% SeaPlaque Agar in DMEM full media) were plated and allowed to solidify. DMEM full media with 4ug/mL puromycin (Invitrogen) was plated over the cells and cells were incubated under standard conditions (5% CO2, 37 degrees Celsius) for 14 days. Top media was removed and cells were fixed in 10% formalin (Fisher Scientific) containing 0.005% crystal violet (Sigma) for 1 hour at room temperature. Formalin was removed and colonies were imaged on a Leica S8 AP0 microscope. 12 images per cell line were taken and automated colony

counts were done using ImageJ software (Rasband, 1997-2012). Results shown are a representative example of at least three independent experiments.

Xenografts

1.5 million cells in serum-free DMEM with 33% Matrigel Basement Membrane (BD Biosciences) were injected into the back flanks of athymic *Foxn1*$^{nu/nu}$ mice (Charles Rivers Laboratory). Each mouse was injected on the right flank with cells expressing a specific shRNA or a cDNA and on the left flank with control cell lines expressing a non-silencing (NS) shRNA or a *Luciferase* cDNA with at least 4 mice per experiment. Tumor volume was measured bi-weekly using calipers and mice were sacrificed when the tumor reached approximately 10% of the total body weight or 40 days post injection. Tumors were harvested for immunohistochemistry and western blot analysis. All animal work was conducted according to the University of Minnesota's approved animal welfare protocol.

In Vitro Drug Studies to Determine IC50

RAD-001, IWR-1, and XAV-939 were solubilized in DMSO and then subsequently diluted in sterile PBS. 1,200 cells per well of a 96-well plate were treated with varying concentration of drug in quadruplicate and assayed for cell viability using the MTS assay (Promega) to determine the IC50 values. All data analysis was done using Calcusyn software (CalcuSyn Version 2.1, BioSoft).

IV. Discussion

Analysis of MPNST tumor genomes has demonstrated a wide variety of genetic changes ranging from point mutations to entire chromosome gains and losses (Kobayashi et al., 2006). Determining which of these changes contribute to tumorigenesis and which changes are simply "passenger" mutations is crucial in identifying targets for therapeutic intervention (Brekke et al., 2010; Carroll and Ratner, 2008; Kobayashi et al., 2006). Prior studies have focused on NF1 and p53/Rb regulated pathways in MPNSTs, yet there remains a need to broaden our understanding of the genetic alterations that contribute to Schwann cell tumorigenesis. The *SB* transposon system is an unbiased, powerful tool to identify oncogenes and tumor suppressor genes (Largaespada, 2009). In an *SB* screen conducted to find genetic drivers of MPNSTs and neurofibromas, we uncovered many alterations that affect canonical Wnt/β-catenin signaling, suggesting this pathway is a likely driver of Schwann cell tumor development, progression and maintenance (**Supplementary Table 1**) (Rahrmann et al., 2013). We show that murine tumors from both the *SB* screen and from four other established MPNST models show nuclear-localized β-catenin, suggesting that they have activated canonical Wnt signaling (**Figure 1**). Additionally, we identified activation of Wnt signaling in a majority of human MPNST cell lines and primary human tumors investigated (**Figure 1-3)**.

In this study, we show that multiple genetic alterations correlate with activation of the canonical Wnt/β-catenin pathway, and that these alterations can induce oncogenic properties in human Schwann cells, and are required for tumor maintenance in MPNST cells. A subset of human Schwann cell tumors show down-regulation of β-catenin destruction complex components, such as *APC* and *GSK3B* (**Figure 2**). Microarray analysis also demonstrated overexpression of several Wnt ligands and *RSPO2,* a secreted ligand that can potentiate Wnt signaling, in a subset of human tumors (**Figure 6**). Interestingly, we find that while CCND1 protein levels correlate with tumor progression, *CCND1* mRNA expression is not as convincing (**Figure 2 & 3)**. It should be noted that the microarray data suggests that in whole tumors *CCND1* may be decreased, but in purified cells it seems to be unchanged or slightly up-regulated. This may be due to the effects of contaminating cells within the whole tumor such as fibroblasts, macrophages, and endothelial cells. In addition, we believe that the discrepancy seen between the TMA and the microarray gene expression of *CCND1* may be due to the fact that the *CCND1* transcript is highly regulated at the translational level. Due to the long 5' untranslated region and secondary structure of *CCND1* mRNA, it is often poorly translated, although many factors, including PI3K/mTOR signaling can increase the translation of this transcript (Gera et al., 2004). Based on the mRNA expression data, *MYC* may be a more consistent

marker for activated Wnt signaling, while CCND1 may be a better marker of Wnt signaling activation by immunohistochemistry.

We tested the functional importance of Wnt pathway activation in Schwann cell tumorigenesis through gain- and loss-of-function studies *in vitro.* Using gene overexpression and knockdown in immortalized human Schwann cells and MPNST cell lines, we showed that aberrant expression of Wnt regulators resulted in phenotypic and functional changes in these cells. Down-regulation of *GSK3B* and *AXIN1* and overexpression of *CTNNB1* were sufficient to induce transformed properties in immortalized human Schwann cells and down-regulation of *CTNNB1* and *TNKS,* as well as overexpression of *GSK3B* reduced the oncogenic properties of MPNST cell lines and delayed tumor growth *in vivo* (**Figure 4, Figure 5, Supplementary Figure 2 & Supplementary Figure 4)**.

Recently, a novel mechanism for activating Wnt signaling was demonstrated in colorectal cancer in which gene fusions occurred between *EIF3E* and *RSPO2* due to a deletion on chromosome 8, resulting in the overexpression of native RSPO2 protein (Seshagiri et al., 2012). We identified a similar fusion transcript in a human MPNST cell line with elevated *RSPO2* expression, and showed that knockdown of *RSPO2* was sufficient to reduce Wnt signaling outputs and cellular viability in this cell line (**Figure 6**). Further work is needed to determine the frequency of R-spondin fusion transcript expression in primary human Schwann cell tumors. It will also be necessary to identify whether expression of R-spondin

fusion transcripts in MPNSTs is mediated by chromosome 8 deletions similar to those seen in colorectal cancer, or if there is another mechanism by which this occurs, such as transcription-mediated gene fusion. Based on our results, a drug that could block the function of RSPO2 may be therapeutically beneficial for patients with MPNSTs overexpressing *RSPO2.*

In addition to the mechanisms described above, there are likely other mechanisms by which this pathway is activated in human tumors. For example, activation of PKB/AKT, a common phenomenon in MPNSTs, leads to the phosphorylation and inactivation of GSK3B, resulting in stabilization of β-catenin protein (Gehrke et al., 2009; Persad et al., 2001). Loss of *PTEN* expression has been demonstrated in human MPNSTs, and this could activate Wnt signaling through activation of AKT (Keng et al., 2012a; Mawrin, 2010). It has also been shown that in cells expressing EGFR, EGF stimulation can result in the activation of β-catenin/TCF/LEF-dependent transcription, and EGFR expression has been implicated in MPNST development as well (Holtkamp et al., 2008; Hu and Li, 2010; Ling et al., 2005). Recently, Mo et al. demonstrated a novel mechanism of NF1-associated MPNST progression in which autocrine activation of CXCR4 by CXCL12 mediates tumor progression through PI3K and β-catenin (Mo et al., 2013). Although no insertions were identified in *Cxcr4 or Cxcl12* in our *SB* screen, gene expression data from human tumors showed statistically significant differential regulation of *CXCR4* in MPNST tumor-to-nerve comparison (fc=5.3x,

p-value = 0.016), but not in MPNST cell-to-NHSC comparison (fc=0.85x, p-value=0.16). In contrast, *CXCL12* showed statistically differential expression pattern in MPNST cell-to-NHSC comparison (fc=2.7x, p-value=0.02), but not in MPNST tumor-to-nerve comparison (fc=4.7x, p-value = 0.15). This study by Mo et al. compliments our work in showing yet another mechanism by which human Schwann cell-derived tumors activate Wnt signaling, leading to tumor progression. Additional work will be required to determine the contribution of each of these pathways to Wnt activation in human MPNSTs.

It is unclear from this study whether Wnt pathway activation is important for tumor initiation or for tumor progression, but it seems likely that it may play a role in both processes. It is clear that a subset of benign human neurofibromas exhibit activated Wnt signaling, which may play a role in the initiation of these benign tumors (**Figure 3 & Supplementary Figure 1**). A larger percentage of high grade tumors (MPNSTs) have activation of this signaling pathway, making it plausible that this pathway also plays a role in progression from a benign tumor to malignancy. It is also likely that this pathway may cooperate with other pathways that play a role in the development or progression of MPNSTs. For example, Wnt signaling activation is an initiating event for colorectal cancer, leading to hyperplasia, but other genetic changes must occur for a tumor to (Fearon, 2011). Future work will need to focus on identifying cooperating mutations or signaling pathways that function in concert with Wnt signaling in MPNST formation.

Indeed, loss of *NF1* expression is a good candidate cooperating alteration, and future experiments in which *NF1* is lost and the Wnt pathway is activated in normal Schwann cells will be critical for our understanding of cooperating genes and pathways.

While the Wnt pathway is known to play a critical role in oncogenesis, the development of clinically beneficial targeted therapies has lagged. The discovery of small molecule inhibitors of the Wnt/β-catenin pathway is being aggressively pursued, as these therapies have the potential to benefit patients suffering from a wide variety of cancers (Curtin and Lorenzi, 2010; Ischenko et al., 2008; Yao et al., 2011). Wnt/β-catenin signaling is critical for many normal developmental and cellular processes, thus, inhibition of this pathway may have many unwanted and negative side effects (Curtin and Lorenzi, 2010; Gonsalves et al., 2011). To this end, inhibitors targeting the specific Wnt pathway molecules (such as RSPO2) and functions in tumorigenesis may be the key to identifying a successful targeted therapy (Curtin and Lorenzi, 2010; Gonsalves et al., 2011)**.** We show that inhibiting Wnt signaling *in vitro* is an effective cytostatic therapy, but when combined with RAD-001, they create a potent cytotoxic therapy (**Figure 7**). Further work will need to be done to investigate the use of Wnt pathway inhibitors using *in vivo* models of MPNST, as these may be a valuable new class of targeted therapies for patients with MPNSTs.

Figure 1: Murine peripheral nerve tumors and human MPNST cell lines show an increase in nuclear β-catenin and Wnt pathway outputs. A. Mouse tumors from the *SB* screen (Rahrmann et al., 2013) were stained by IHC for β-catenin. High grade tumors showed an increased level and nuclear localization of β-catenin compared to normal nerve or benign neurofibromas. B. Tumor sections from 4 established mouse models demonstrate nuclear β-catenin staining by IHC. C. Immortalized human Schwann cells (iHSC2λ) stain positive for β-catenin by immunofluorescence, but it is mainly localized in the cytoplasm. In contrast, MPNST cell lines (STS-26T and ST8814) show more nuclear-localized β-catenin. D. Compared to immortalized human Schwann cells (iHSC1λ), some MPNST cell lines show higher levels of C-MYC and CCND1 protein by western blot.

Figure 1

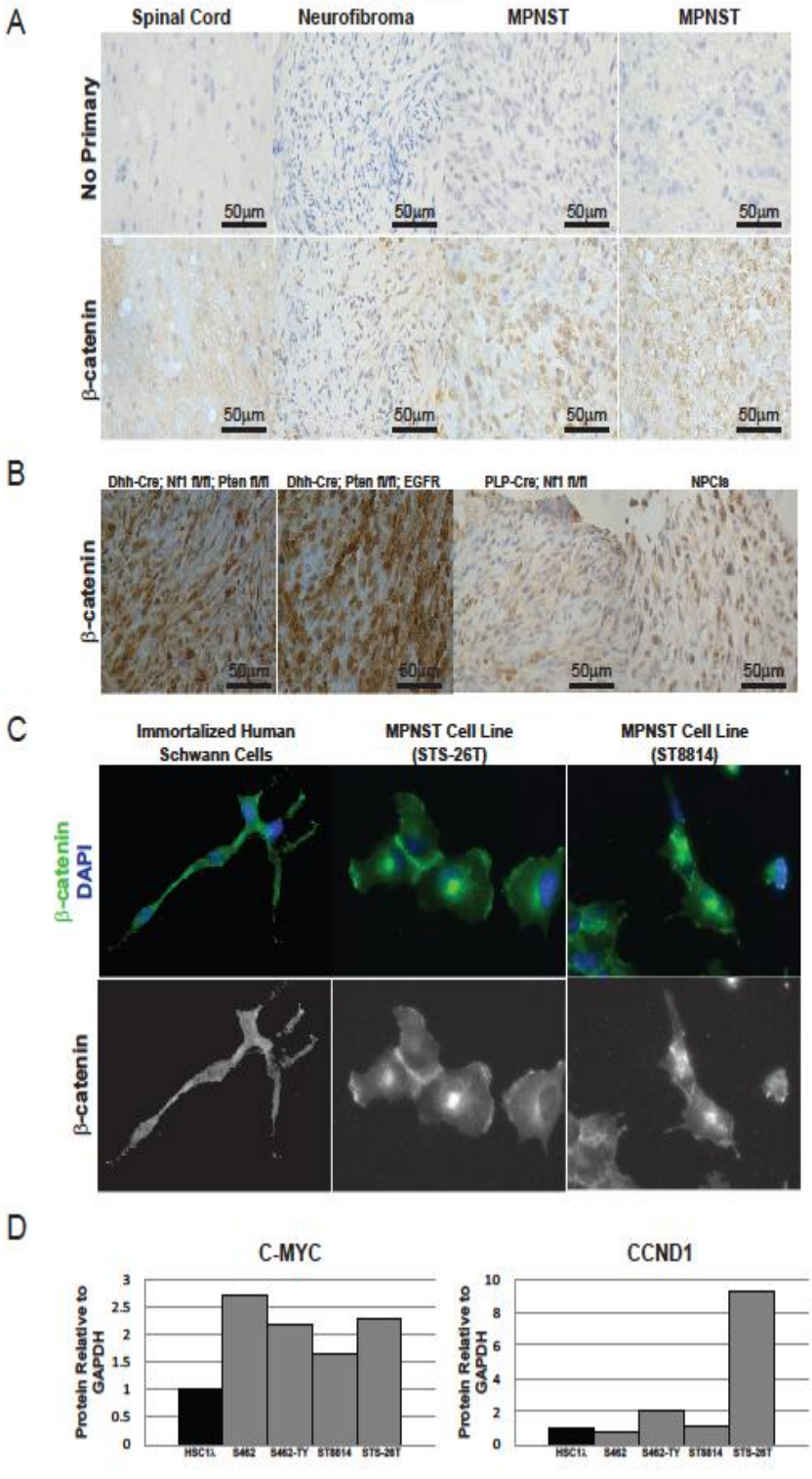
A
Spinal Cord
Neurofibroma
MPNST
MPNST
No Primary
β-catenin
50μm
B
Dhh-Cre; Nf1 fl/fl; Pten fl/fl
Dhh-Cre; Pten fl/fl; EGFR
PLP-Cre; Nf1 fl/fl
NPCIs
β-catenin
50μm
C
Immortalized Human Schwann Cells
MPNST Cell Line (STS-26T)
MPNST Cell Line (ST8814)
β-catenin
DAPI
β-catenin
D
C-MYC
CCND1
Protein Relative to GAPDH
3
2.5
2
1.5
1
0.5
0
10
8
6
4
2
0
HSC1λ
S462
S462-TY
ST8814
STS-26T

Figure 2: Microarray expression of Wnt signaling regulators and pathway members. Heat-map depicting microarray expression analysis for Wnt signaling regulators and pathway members. NHSC = purified normal human Schwann cells, dNFSC= purified dermal neurofibroma Schwann cells, pNFSC = purified plexiform-neurofibroma Schwann cells, MPNST cell = human MPNST cell lines, NV = normal human nerve, dNF = dermal neurofibroma, pNF = plexiform-neurofibroma, MPNST = bulk MPNST tumor.

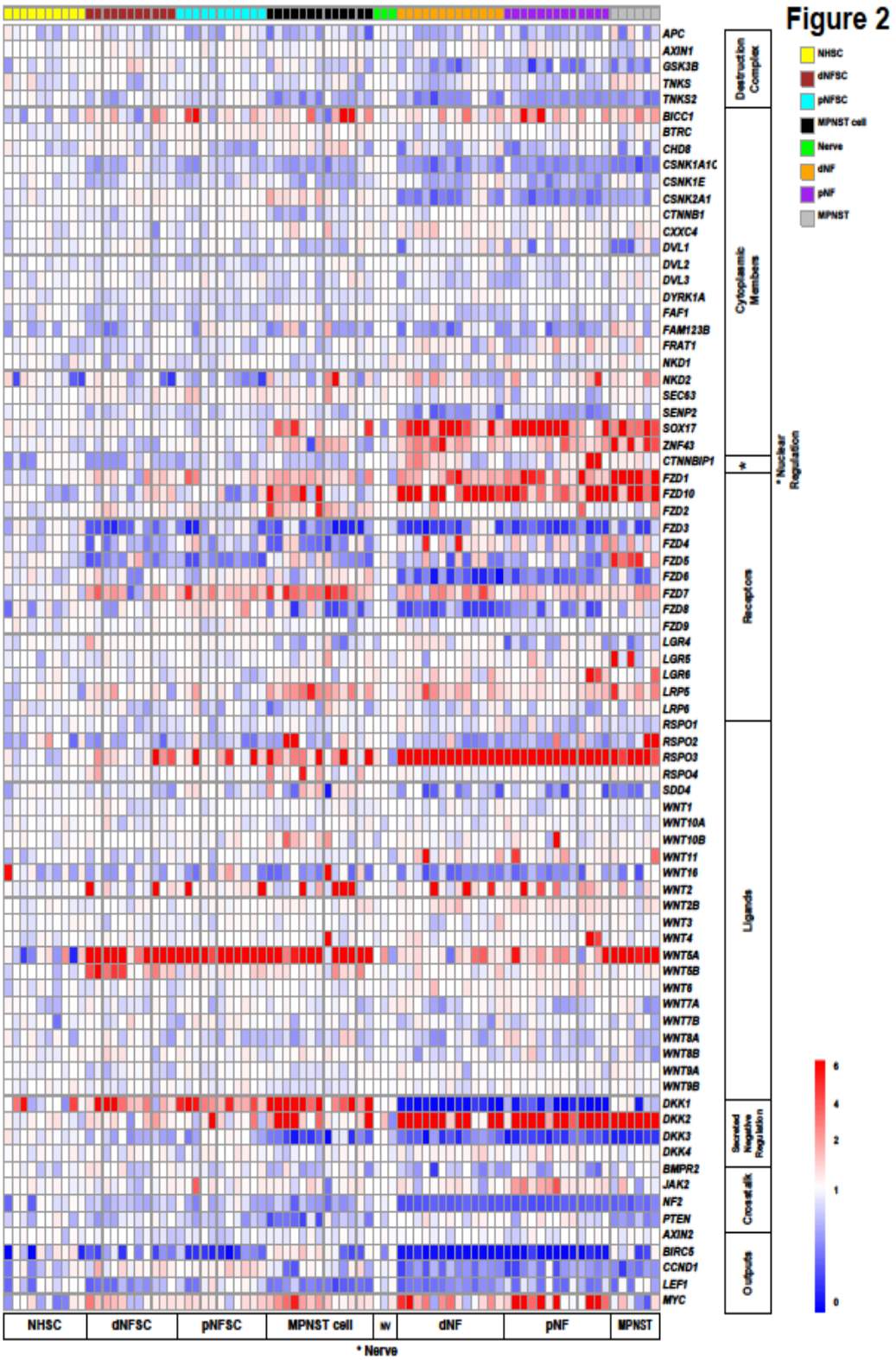
Figure 2
NHSC
dNFSC
pNFSC
MPNST cell
Nerve
dNF
pNF
MPNST
APC
AXIN1
GSK3B
TNKS
TNKS2
BICC1
BTRC
CHD8
CSNK1A1C
CSNK1E
CSNK2A1
CTNNB1
CXXC4
DVL1
DVL2
DVL3
DYRK1A
FAF1
FAM123B
FRAT1
NKD1
NKD2
SEC63
SENP2
SOX17
ZNF43
CTNNBIP1
FZD1
FZD10
FZD2
FZD3
FZD4
FZD5
FZD6
FZD7
FZD8
FZD9
LGR4
LGR5
LGR6
LRP5
LRP6
RSPO1
RSPO2
RSPO3
RSPO4
SDD4
WNT1
WNT10A
WNT10B
WNT11
WNT16
WNT2
WNT2B
WNT3
WNT4
WNT5A
WNT5B
WNT6
WNT7A
WNT7B
WNT8A
WNT8B
WNT9A
WNT9B
DKK1
DKK2
DKK3
DKK4
BMPR2
JAK2
NF2
PTEN
AXIN2
BIRC5
CCND1
LEF1
MYC
Destruction Complex
Cytoplasmic Members
*
* Nuclear Regulation
Receptors
Ligands
Secreted Negative Regulation
Crosstalk
Outputs
6
4
2
1
0
NHSC
dNFSC
pNFSC
MPNST cell
sv
dNF
pNF
MPNST
* Nerve

Figure 3: Human tissue microarray shows a subset of human neurofibromas and MPNSTs have activated Wnt/β-catenin signaling. A. A large subset of Schwann cell tumors stain positive for β-catenin by IHC. The fraction of β-catenin positive tumors increases from benign neurofibromas (neurofibroma) to plexiform neurofibromas (plex), to MPNSTs. B. The fraction of tumors staining positive for nuclear β-catenin increases from benign neurofibroma to MPNSTs as well. C. Example staining of β-catenin localization. D. Large subsets of Schwann cell tumors are positive for CCND1, an output of canonical Wnt/β-catenin signaling. A larger fraction of MPNSTs are CCND1 positive compared to the benign neurofibromas and plexiform neurofibromas. E. The level of CCND1 increases from benign neurofibromas to plexiform neurofibromas and is the greatest in MPNSTs. F. Example of CCND1 staining intensity. G. A patient-matched plexiform neurofibroma which transformed into an MPNST shows higher total and nuclear β-catenin staining with transformation. The plexiform neurofibroma stained negative for CCND1, while the MPNST was CCND1 positive.

Figure 3

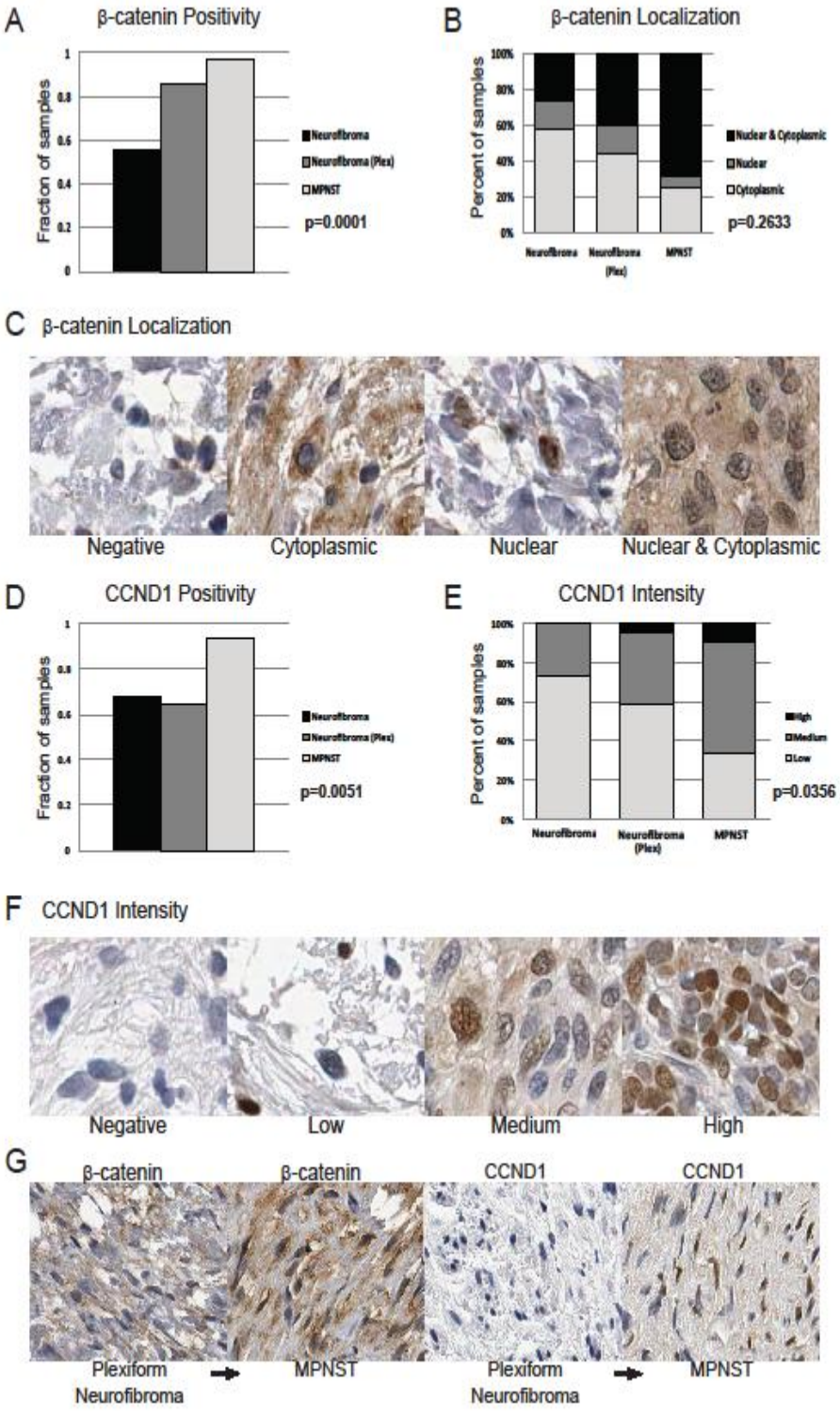
A
β-catenin Positivity
Fraction of samples
Neurofibroma
Neurofibroma (Plex)
MPNST
p=0.0001
B
β-catenin Localization
Percent of samples
Nuclear & Cytoplasmic
Nuclear
Cytoplasmic
p=0.2633
Neurofibroma
Neurofibroma (Plex)
MPNST
C
β-catenin Localization
Negative
Cytoplasmic
Nuclear
Nuclear & Cytoplasmic
D
CCND1 Positivity
Fraction of samples
Neurofibroma
Neurofibroma (Plex)
MPNST
p=0.0051
E
CCND1 Intensity
Percent of samples
High
Medium
Low
p=0.0356
Neurofibroma
Neurofibroma (Plex)
MPNST
F
CCND1 Intensity
Negative
Low
Medium
High
G
β-catenin
β-catenin
CCND1
CCND1
Plexiform Neurofibroma
MPNST
Plexiform Neurofibroma
MPNST

Figure 4: Immortalized human Schwann cells show an increase in transformed properties when Wnt/β-catenin signaling is activated. A. Overexpression of a *CTNNB1*^{S33Y} construct in the immortalized human Schwann cell line, iHSC1λ, results in an increase in total and activated β-catenin, while expression in iHSC2λ cells results in only an increase in total β-catenin. B. Expression of activated *β-catenin* increases cell viability in immortalized human Schwann cells. C. Expression of *CTNNB1*^{S33Y} has no effect on soft agar colony formation in iHSC2λ cells. D. Expression of *CTNNB1*^{S33Y} results in altered morphology when iHSC2λ cells are grown in 2-dimensional culture. E. The immortalized human Schwann cell line, iHSC2λ, has reduced *AXIN1* and *GSK3B* transcript levels, respectively, when treated with shRNA constructs against these genes (AXIN 67 and GSK3β 90). F. Knockdown of *AXIN1* and *GSK3B* in iHSC2λ cells increases cell viability. G. Reducing the expression of *AXIN1* and *GSK3B* in iHSC2λ cells is sufficient to increase soft agar colony formation.* $p<0.05$, **$p<0.0001$ unpaired T-test. Error bars represent SEM.

Figure 4

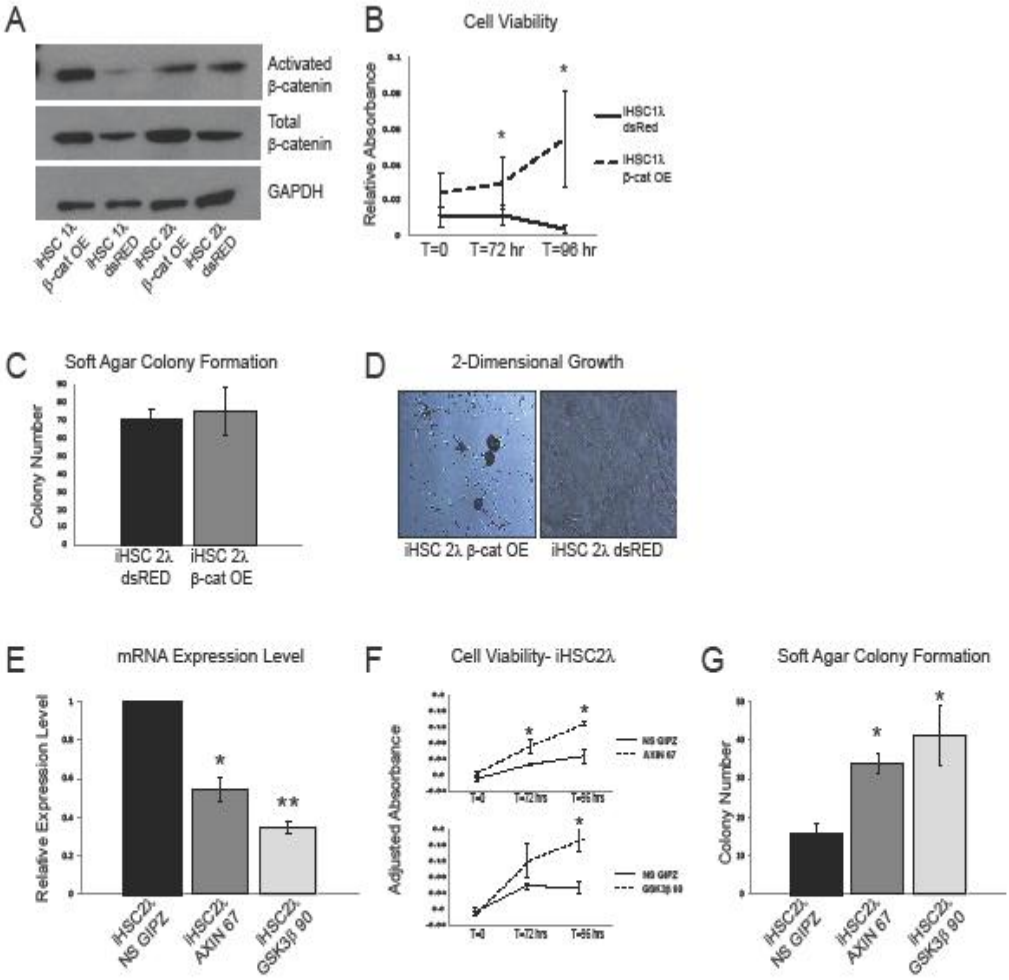
A
Activated β-catenin
Total β-catenin
GAPDH
iHSC 1λ β-cat OE
iHSC 1λ dsRED
iHSC 2λ β-cat OE
iHSC 2λ dsRED
B
Cell Viability
Relative Absorbance
iHSC1λ dsRed
iHSC1λ β-cat OE
T=0
T=72 hr
T=96 hr
C
Soft Agar Colony Formation
Colony Number
iHSC 2λ dsRED
iHSC 2λ β-cat OE
D
2-Dimensional Growth
iHSC 2λ β-cat OE
iHSC 2λ dsRED
E
mRNA Expression Level
Relative Expression Level
iHSC2λ NS GIPZ
iHSC2λ AXIN 67
iHSC2λ GSK3β 90
F
Cell Viability- iHSC2λ
Adjusted Absorbance
G
Soft Agar Colony Formation
Colony Number

Figure 5: NF1-associated and sporadic MPNST cell lines show a decrease in cell viability, soft agar colony formation, and xenograft tumor growth when Wnt/β-catenin signaling is down-regulated. A. shRNA reduces *β-catenin* (β-cat 23) and *TNKS* (*TNKS* 920) expression levels in an NF1-associated MPNST cell line (S462-TY) compared to non-silencing shRNA (NS GIPZ) treated cells. B. Knockdown of *β-catenin* or *TNKS* results in a reduction in cell viability in the S462-TY cell line. C. Soft agar colony formation is reduced in an NF1-associated cell line (S462-TY) when *β-catenin* or *TNKS* levels are reduced. D. shRNA treatment results in a reduction of *β-catenin* (β-cat 22) and *TNKS* (*TNKS* 920) levels in a cell line derived from a sporadic MPNST (STS-26T) compared to non-silencing shRNA (NS GIPZ) treated controls. E. Knockdown of *β-catenin* or *TNKS* is sufficient to reduce cell viability in STS-26T cells. F. A reduction in *β-catenin* or *TNKS* expression reduces soft agar colony formation in this spontaneous MPNST cell line. G. Western blot analysis shows that overexpression of *GSK3B* results in the degradation of β-catenin protein in both an NF1-associated and sporadic MPNST cell lines (S462-TY and STS-26T). H. Overexpression of *GSK3B* decreases cell viability in S462-TY and STS-26T MPNST cell lines. I. Overexpression of *GSK3B* reduces soft agar colony formation in S462-TY and STS-26T MPNST cell lines. * $p<0.05$, ** $p<0.0001$ unpaired T-test. Error bars represent SEM.

Figure 5

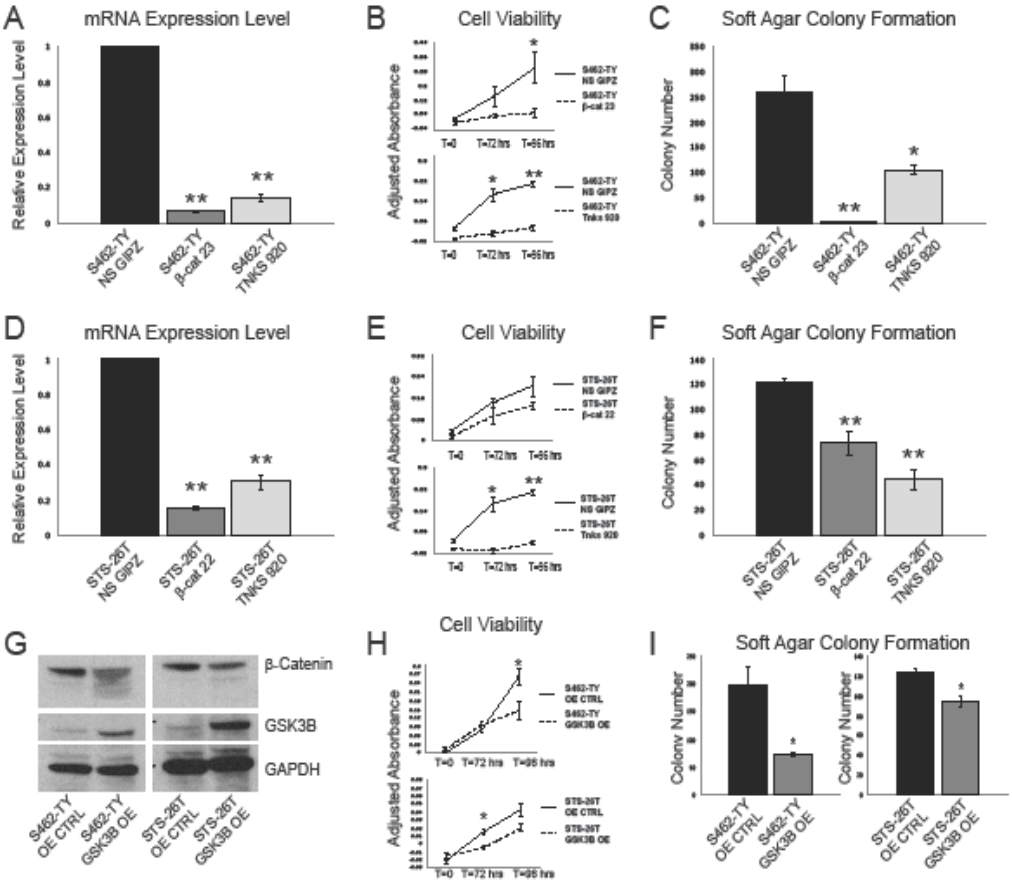
A
mRNA Expression Level
Relative Expression Level
S462-TY NS GIPZ
S462-TY β-cat 23
S462-TY TNKS 920
B
Cell Viability
Adjusted Absorbance
T=0
T=72 hrs
T=96 hrs
C
Soft Agar Colony Formation
Colony Number
D
mRNA Expression Level
STS-26T NS GIPZ
STS-26T β-cat 22
STS-26T TNKS 920
E
Cell Viability
F
Soft Agar Colony Formation
G
β-Catenin
GSK3B
GAPDH
S462-TY OE CTRL
S462-TY GSK3B OE
STS-26T OE CTRL
STS-26T GSK3B OE
H
Cell Viability
I
Soft Agar Colony Formation

Figure 6: The secreted Wnt/β-catenin activator *RSPO2* is highly expressed in a subset of human Schwann cell tumors and can be detected as a fusion transcript with the upstream *EIF3E* gene. A. Gene expression microarray shows that a subset of plexiform neurofibromas and MPNSTs from both purified Schwann cells (top) and primary tumors (bottom) have high *RSPO2* expression. B. cDNA libraries derived from human MPNST cell lines were screened for *EIF3E-RSPO2* fusion transcripts (fusion transcripts verified by sequencing are denoted by an arrow). C. 5 MPNST cell lines were screened for *RSPO2* expression levels and normalized to an immortalized human Schwann cell line (iHSC1λ). The S462 cell line showed very high *RSPO2* expression and was found to contain a fusion between *EIF3E* and *RSPO2*. D. The S462 cell line has a fusion between *EIF3E* exon 1, followed by a 122 base pair chromosome 8 intergenic sequence and *RSPO2* exon 2. This fusion results in the production of a native RSPO2 protein. E. The S462 cell line was transduced with a lentivirus expressing an *RSPO2* shRNA. This resulted in a decrease in *RSPO2* expression, as well as a decrease in expression of known Wnt signaling outputs *MYC*, *AXIN2*, *LEF1*, *CCND1*, and *BIRC5*, as compared to S462 cells treated with a non-silencing shRNA (NS GIPZ). F. Knockdown of *RSPO2* in S462 cells significantly reduces cell viability. Error bars represent standard error of the mean. * $p<0.05$, **$p<0.0001$ unpaired T-test. Error bars represent SEM.

Figure 6

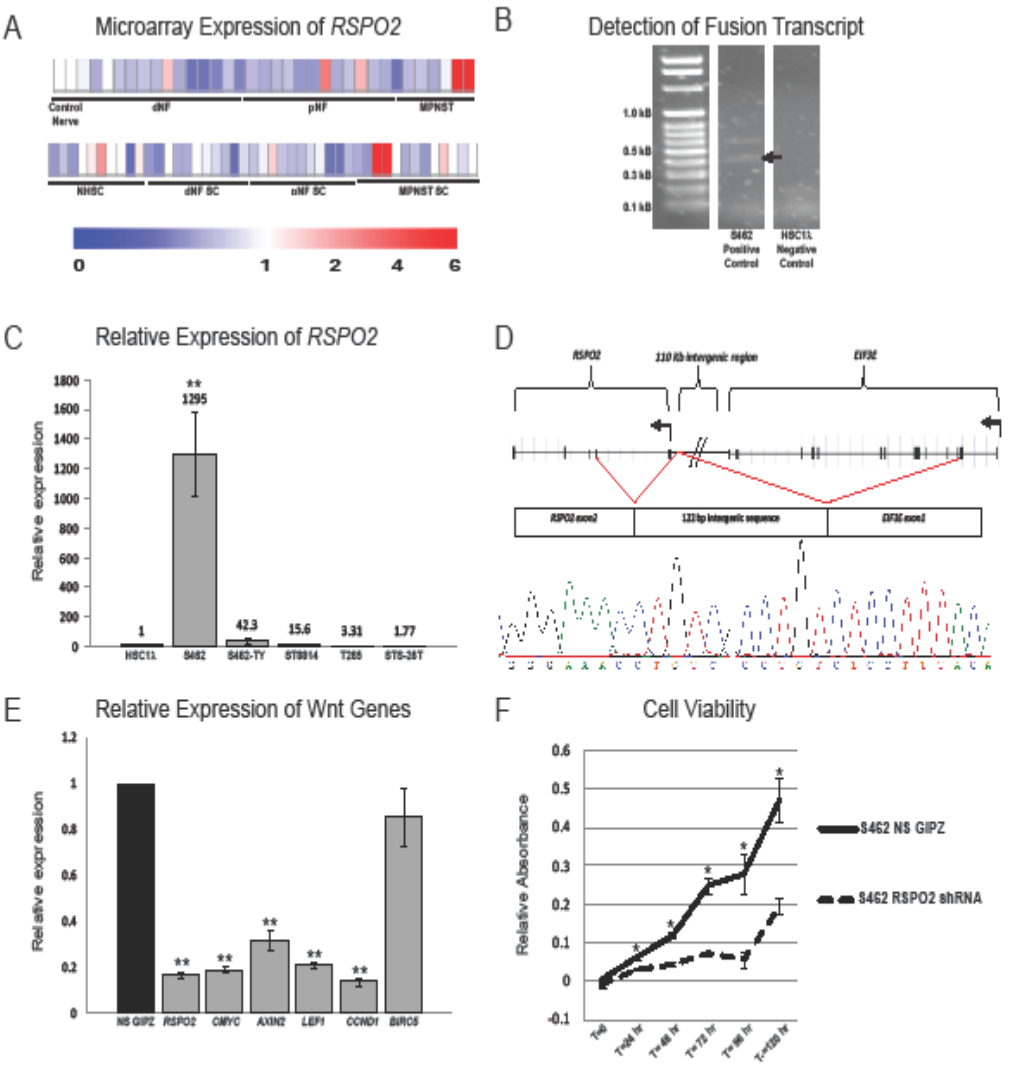
A
Microarray Expression of RSPO2
Control Nerve
cNF
pNF
MPNST
NHSC
cNF SC
pNF SC
MPNST SC
0
1
2
4
6
B
Detection of Fusion Transcript
1.0 kB
0.5 kB
0.3 kB
0.1 kB
S462 Positive Control
HSC11 Negative Control
C
Relative Expression of RSPO2
Relative expression
1800
1600
1400
1200
1000
800
600
400
200
0
**
1295
1
42.3
15.6
3.31
1.77
HSC11
S462
S462-TY
ST8814
T265
STS-26T
D
RSPO2
110 Kb intergenic region
EIF3E
RSPO2 exon2
123 bp intergenic sequence
EIF3E exon1
E
Relative Expression of Wnt Genes
Relative expression
1.2
1
0.8
0.6
0.4
0.2
0
**
NS GIPZ
RSPO2
CMYC
AXIN2
LEF1
CCND1
BIRC5
F
Cell Viability
Relative Absorbance
0.6
0.5
0.4
0.3
0.2
0.1
0
-0.1
*
S462 NS GIPZ
S462 RSPO2 shRNA
T=0
T=24 hr
T= 48 hr
T=72 hr
T= 96 hr
T=120 hr

Figure 7: β-catenin inhibitors are effective *in vitro* and synergize with RAD-001. A. IC50 concentrations (uM) of two immortalized human cell lines (iHSC1λ and iHSC2λ) and 5 human MPNST cell lines (S462, S462-TY, ST8814, T265, STS-26T) for the mTOR inhibitor RAD-001 (Everolimus) and two Wnt signaling inhibitors, IWR-1 and XAV-939. B. Induction of apoptosis in NF1-associated MPNST cell lines (S462, T265) and the sporadic MPNST cell line (STS-26T) as determined by the percentage of TUNEL positive cells that were treated with IC50 concentrations of RAD-001, IWR-1 and XAV-939 shows that these single drug treatments are largely cytostatic. When treated with IC25 concentrations of RAD-001 in combination with IWR-1 or XAV-939, a synergistic increase in apoptosis is often observed. No treatment (No Tx) and 50uM DNase1 were used as positive and negative controls, respectively. C. Representative images of S462 cells treated with RAD-001, IWR-1 or combination of RAD-001 and IWR-1. Cells were stained with TUNEL (green) and DAPI (blue), images taken at 20X magnification. Error bars represent SEM.

Figure 7

A

IC50 (uM)	iHSC1L	iHSC2L	S462	S462-TY	ST8814	T265	STS-26T
RAD-001	2.64	2.70	0.97	1.87	2.12	1.46	1.36
XAV-939	N/A	85.5	0.047	2.22	0.243	1.22	0.048
IWR-1	N/A	N/A	186.87	26.14	0.055	9.79	0.90

B

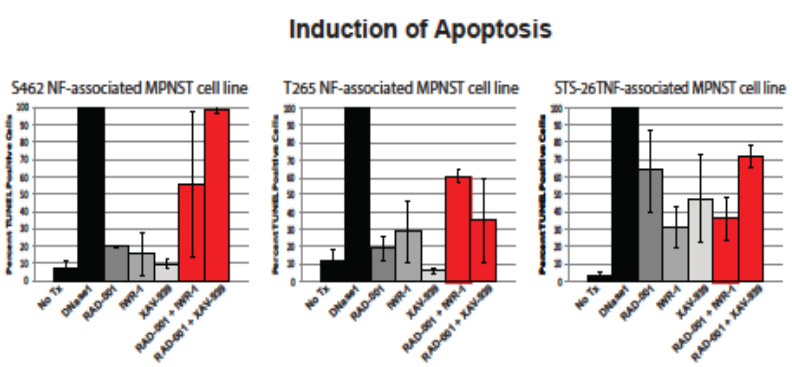

C

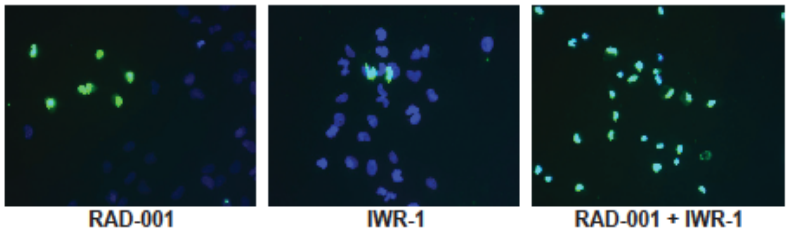

Supplementary Figure 1: Human tissue microarray shows that C-MYC staining intensity increases with tumor progression. A. The intensity of C-MYC staining increases from benign neurofibromas to plexiform neurofibromas and is the greatest in MPNSTs. B. Example of C-MYC staining intensity.

Supplementary Figure 1

A

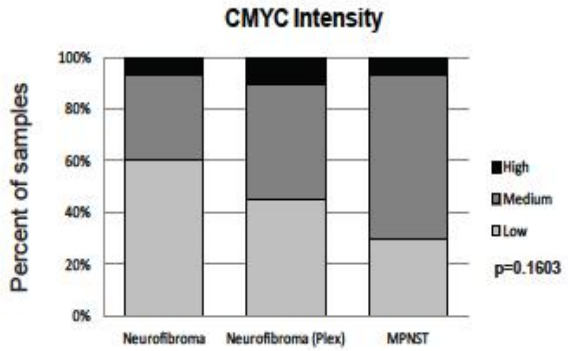

B CMYC Intensity

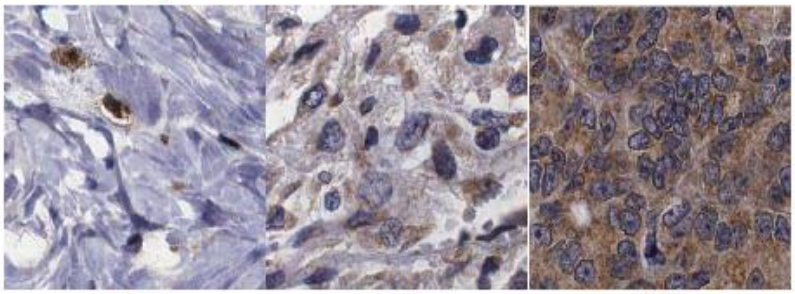

Supplementary Figure 2: Overexpression of activated *β-catenin* and knockdown of *AXIN1* or *GSK3B* results in increased Wnt signaling and an induction of oncogenic properties in immortalized human Schwann cells. A-B. Expression of *CTNNB1*^{S33Y} increases the expression of *β-catenin*, and known β-catenin co-activated genes *MYC, AXIN2, CCND1, LEF1,* and *BIRC5*. C. Immortalized human Schwann cells expressing shRNAs against *AXIN1* (iHSC1λ AXIN 84 and iHSC2λ AXIN 67) show a reduction in AXIN1 protein levels compared to cell lines expressing a non-silencing shRNA (NS GIPZ). D-E. Knockdown of *AXIN1* increases the expression of Wnt signaling outputs *MYC, AXIN2, LEF1, CCND1,* and *BIRC5* in both iHSC1λ and iHSC2λ cell lines. F. Knockdown of *GSK3B* in immortalized human Schwann cells (iHSC1λ GSK3B 91 and iHSC2λ GSK3B 90) results in a decrease in GSK3B protein levels compared to cells expressing a non-silencing shRNA (NS GIPZ). G-H. *GSK3B* knockdown increases Wnt signaling as shown by an increase in *MYC, AXIN2, LEF1, CCND1,* and *BIRC5* expression. I. Immortalized human Schwann cells (iHSC1λ) transduced with shRNA against *AXIN1* (AXIN 84) or *GSK3B* (GSK3β 91) show a decrease in expression level of *AXIN1* and *GSK3B* transcripts, respectively, by QPCR compared to cells treated with a non-silencing shRNA (NS GIPZ). J. shRNA knockdown of either *AXIN1* or *GSK3B* in iHSC1λ cells increases cell viability. K. iHSC1λ cell with knockdown of *AXIN1* or *GSK3B* show an increase in soft agar colony formation. * $p<0.05$, **$p<0.0001$ unpaired T-test. Error bars represent SEM.

Supplementary Figure 2

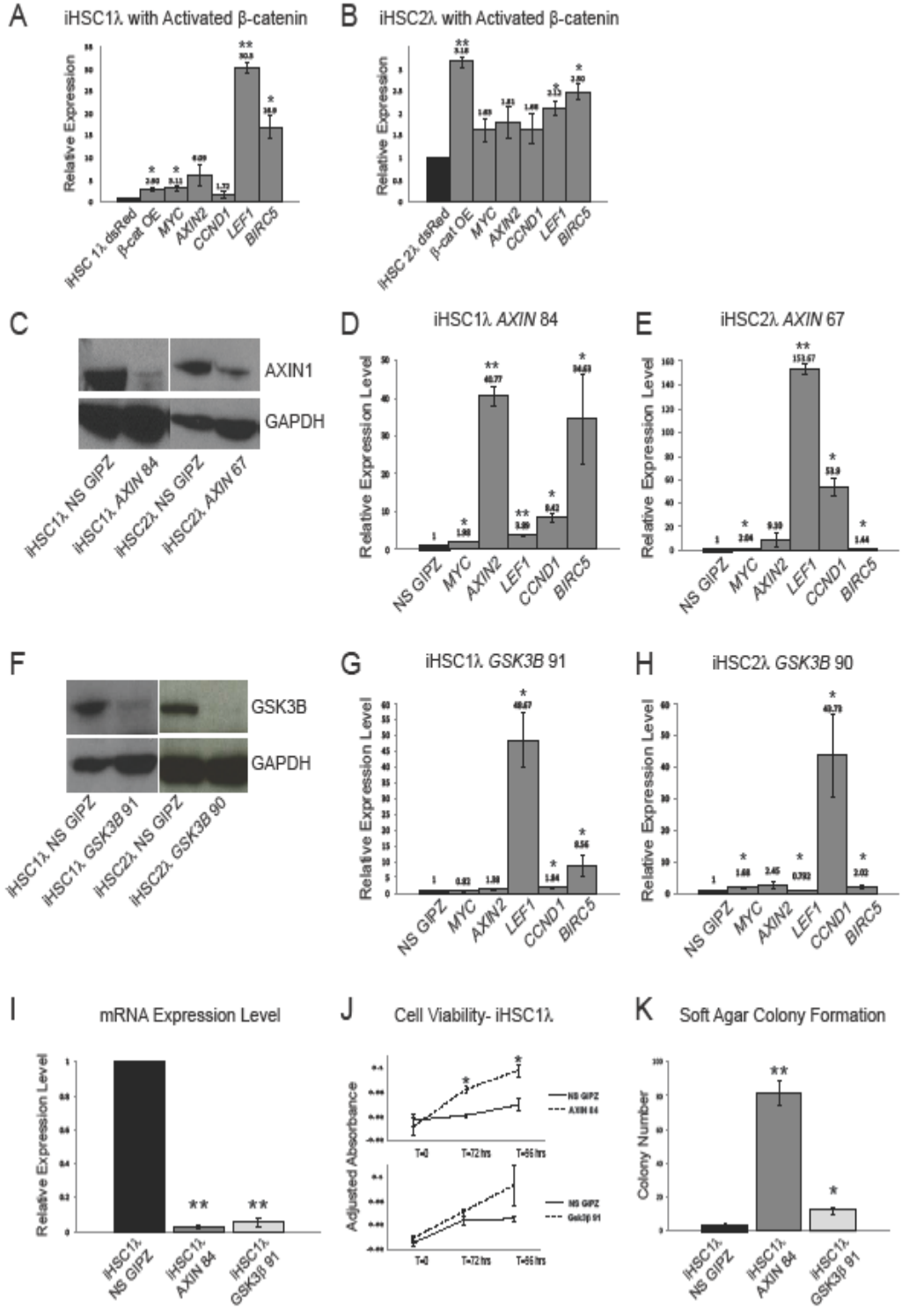

Supplementary Figure 3: Knockdown of *β-catenin* or *TNKS* and overexpression of *GSK3B* results in decreased Wnt signaling in MPNST cell lines. A-B. Knockdown of *β-catenin* in an NF1-associated MPNST cell line (S462-TY β-cat #23) and a sporadic MPNST cell line (STS-26T β-cat #22) results in a reduction in Wnt signaling as shown by reduced expression of *MYC, AXIN2, CCND1, LEF1,* and *BIRC5.* C-D. Knockdown of *TNKS* in an NF1-associated MPNST cell line (S462-TY TNKS #920) and a sporadic MPNST cell line (STS-26T TNKS #920) results in a reduction in Wnt signaling as shown by reduced expression of *MYC, AXIN2, CCND1, LEF1,* and *BIRC5.* E-F. *GSK3B* overexpression in S462-TY and STS-26T cell lines results in a decrease in the expression of Wnt pathway outputs *MYC, AXIN2, CCND1, LEF1,* and *BIRC5* * $p<0.05$, ** $p<0.0001$ unpaired T-test. Error bars represent SEM.

Supplementary Figure 3

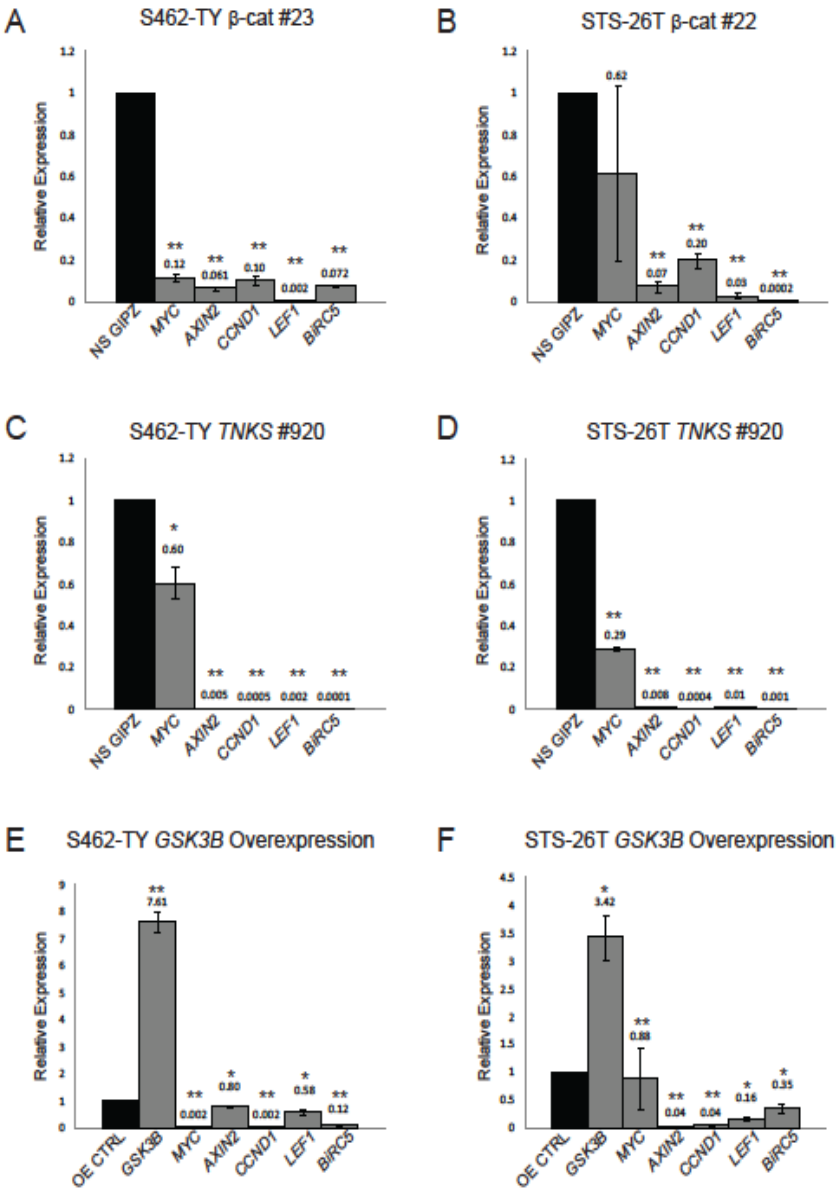

Supplementary Figure 4: Reduction of Wnt signaling by *β-catenin* knockdown or *GSK3B* overexpression reduces tumor growth in xenograft models. A. Reduction in *β-catenin* expression in the NF1-associated MPNST cell line (S462-TY) by shRNA (β-cat 23) results in a reduction in the rate of xenograft tumor growth compared to non-silencing shRNA (NS GIPZ) expressing cells. B-C. Tumors expressing a *β-catenin* shRNA are reduced in size and show a reduction in Ki67 positivity compared to NS GIPZ expressing cells. D. Overexpression of *GSK3B* in the sporadic MPNST cell line (STS-26T), results in a delay in xenograft tumor formation and reduction in the rate of xenograft tumor growth compared to cells expressing *GFP/Luciferase* (OE CTRL). E-F. Tumors overexpressing *GSK3B* are reduced in size and show a reduction in Ki67 positivity compared to cells expressing *GFP/Luciferase* (OE CTRL). Error bars represent SEM.

Supplementary Figure 4

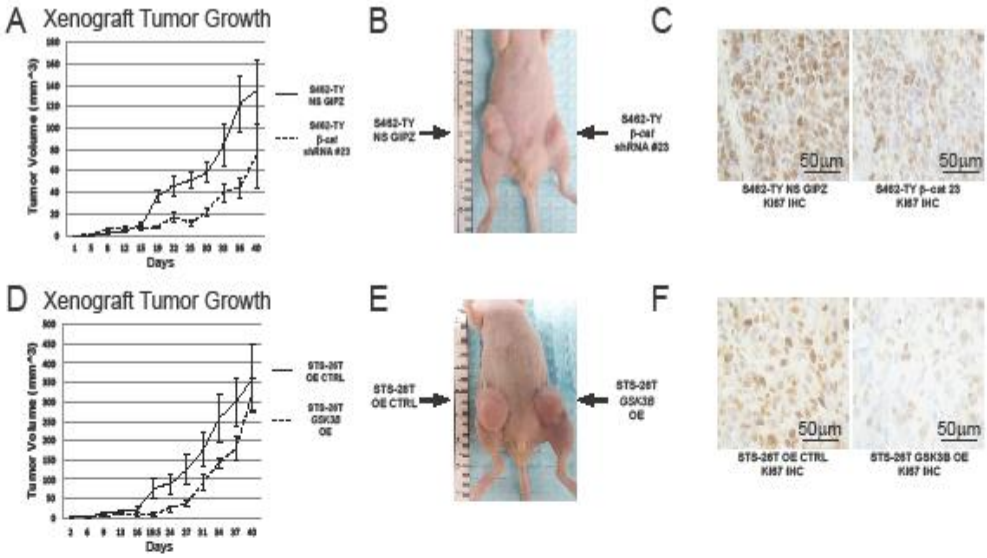

Supplementary Table 1: *SB* mutagenesis implicates Wnt/β-catenin signaling in neurofibroma and MPNST development in mice. Genes listed were identified in a murine *SB* screen for drivers of Schwann cell tumorigenesis, and all have known roles in canonical Wnt/β-catenin signaling. Listed is the percentage of neurofibromas or MPNSTs with an *SB* insertion within or near the gene listed, as well as the total number of tumors within a given gene.

Gene	Regulation of Wnt Signaling	Percentage of neuro-fibromas with SB insertion *N*= 276	Total number of neuro-fibromas with *SB* insertion *N*= 276	Percentage of MPNSTs with *SB* insertion *N*= 106	Total number of MPNSTs with *SB* insertion *N*= 106
Ctnnb1	Positive	2.54*	7	0*	0
Tnks	Positive	15.22	42	5.66*	6
Crebbp	Positive	15.58	43	21.70	23
Pak7	Positive	6.52*	18	6.60*	7
Gsk3b	Negative	17.75	49	9.43	10
Axin1	Negative	7.25	20	2.83*	3
Pten	Negative	15.94	44	50.00	53
Cav1	Negative	2.17*	6	1.89*	2

N, total number of tumors analyzed for *SB* insertions; *, denotes non-significant CIS.

Supplementary Table 2: QPCR primer sequences

Target	Primer 1 (5' to 3')	Primer 2 (3' to 5')	Reference
AXIN1	CCGGAAGACTCCCTCAGAA	AATAGGGGTTGACTGGCTCC	(Cui et al., 2007)
AXIN2	CTCCCCACCTTGAATGAAGA	TGGCTGGTGCAAAGACATAG	(Biechele et al., 2009)
ACTB	CACAGGGGAGGTGATAGCAT	CTCAAGTTGGGGGACAAAAA	---
CTNNB1	ATTGTCCACGCTGGATTTTC	AGGTCTGAGGAGCAGCTTCA	(Cui et al., 2007)
MYC	CACCGAGTCGTAGTCGAGGT	GCTGCTTAGACGCTGGATTT	(Cui et al., 2007)
CCND1	TGAGGCGGTAGTAGGACAGG	GACCTTCGTTGCCCTCTGT	(Cui et al., 2007)
GSK3B	CCACTGTTGTCACCTTGCTG	GAGTGATCATGTCAGGGCG	(Cui et al., 2007)
LEF1	GACGAGATGATCCCCTTCAA	AGGGCTCCTGAGAGGTTTGT	(Biechele et al., 2009)
BIRC5	AGCCCTTTCTCAAGGACCAC	GCACTTTCTTCGCAGTTTCC	(Emami et al., 2004)
TNKS	GCAGCTTCTAGGAGTTCGTCTT	GACCCAAACATTCGGAACAC	(Cui et al., 2007))

Chapter 3: Co-Targeting the MAPK and PI3K/AKT/MTOR Pathways in Two Genetically Engineered Mouse Models of Schwann Cell Tumors

Adrienne L. Watson[1,2,3,4], Vincent W. Keng[1,2,3,4,10] , Eric P. Rahrmann[1,2,3,4], Leah K. Anderson[2], Andrew D. Greeley[1,2], Amanda L. Halfond[5], Margaret H. Collins[7], Tilat Rizvi[7], Margaret R. Wallace[9], Nancy Ratner[6,8], and David A. Largaespada[1,2,3,4]

[1]Masonic Cancer Center, [2]Department of Genetics, Cell Biology and Development, [3]Center for Genome Engineering, [4]Brain Tumor Program, [5]Health and Natural Sciences Department, University of Minnesota, Minneapolis, MN 55455, USA. [6]Division of Experimental Hematology and Cancer Biology, [7]Division of Pathology and Laboratory Medicine, [8]Department of Pediatrics, Cincinnati Children's Hospital Medical Center, Cincinnati, OH 45229, USA. [9]Department of Molecular Genetics and Microbiology, University of Florida, Gainesville, FL 32611, USA. [10]Department of Applied Biology and Chemical Technology, The Hong Kong Polytechnic University, Hung Hom, Kowloon, Hong Kong.

This work was supported by the National Institutes of Health (P50 NS057531), The Children's Tumor Foundation, The Zachary NF Fund, and The Jacqueline Dunlap NF Fund. A.L.W is funded by the 2011 Children's Tumor Foundation Young Investigators Award (2011-01-018).

Correspondence should be addressed to David A. Largaespada (larga002@umn.edu)

Keywords: Malignant peripheral nerve sheath tumors, Schwann cells, neurofibromatosis type 1 syndrome, neurofibromin 1, neurofibromatosis 1, PI3K/AKT/mTOR signaling, MAPK signaling, targeted therapies, genetically engineered mouse models

Conflict of interest statement: Dr. Largaespada is the co-founder and part owner of two biotechnology companies, NeoClone Biotechnology, Inc. and Discovery Genomics, Inc. No company resources or personnel were involved in this research, which is unrelated to the goals of these companies.

Author Contributions:

Adrienne L. Watson: Her work contributed to the majority of the data published. She designed and optimized the majority of the experiments including the *in vitro* and *in vitro* drug studies. She performed the majority of the *in vitro* work, mouse maintenance, drug administration, preparation of histology, and tumor analysis by western bot. She also did the majority of data analysis and writing of the manuscript.

Vincent W. Keng: He designed, developed, and provided two novel mouse models of MPNST used in this work. He also assisted with drug administration.

Eric P. Rahrmann: He assisted in experimental design and interpretation. He also assisted with mouse necropsies and tumor analysis.

Leah K. Anderson: She helped with mouse maintenance, drug administration, tumor analysis, and western blot analyses.

Andrew D. Greeley: He maintained mice and performed immunohistochemistry on the mouse tumors.

Amanda L. Halfond: She maintained cells in culture and assisted in drug administration.

Margaret H. Collins: She performed all pathological analyses of all mouse Schwann tumors.

Tilat Rizvi: She assisted in the pathological analyses of all mouse tumors.

Margaret R. Wallace: She made and provided the immortalized human Schwann cells used in this work.

Nancy Ratner: She was a co-principal investigator on the grant for this work.

David A. Largaespada: He was a co-principal investigator on the grant for this work.

Malignant Peripheral Nerve Sheath Tumors (MPNSTs) are soft tissue sarcomas originating in Schwann cells or Schwann cell precursors, that can occur spontaneously or in the context of the genetic disorder Neurofibromatosis Type 1. The 5-year survival rate for patients that develop an MPNST is less than 25% and remains the leading cause of death for patients with NF1. With an incomplete understanding of the genetic drivers of MPNSTs, the current standard treatment remains surgical resection, high-dose chemotherapy, and radiation. Recently, several studies have suggested that the mTOR and MAPK pathways may be involved in the formation and progression of MPNSTs, and both of these pathways can be targeted with drugs that inhibit these pathways and are currently in use for other tumor types. *In vitro*, MPNST cell lines are more sensitive to inhibition of cell growth by RAD-001 and PD-901, inhibitors of the mTOR and MAPK pathways, respectively, while immortalized human Schwann cells are less sensitive. In combination, these drugs are also synergistic at inhibiting proliferation and inducing apoptosis. To better study the therapeutic potential of these drugs, we tested the efficacy in two mouse models of MPNSTs. One model closely resembles the genetic changes (*Pten* loss, *EGFR* overexpression) and histological features of human spontaneous MPNSTs, while the other models the NF1-associated form of MPNSTs (*Pten* loss, *NF1* loss). RAD-001 or PD-901 treatment alone moderately reduced tumor burden and size, and extended lifespan in these models. However, pharmacodynamic analysis showed that long term

treatment of a single agent resulted in the development of resistance, leading us to hypothesize that targeting both pathways in combination may be more effective. We found synergistic effects on reducing tumor burden and size, and a significant increase in lifespan when RAD-001 and PD-901 are given in combination. The synergy seen is due to the combination therapy allowing for persistent and prolonged reduction in signaling through both pathways, without a subsequent increase in signaling through one pathway, as seen in single agent treatments. These data suggest that co-targeting the mTOR and MAPK pathways could potentially be an effective treatment for patients with sporadic or NF1-associated MPNSTs.

I. Introduction

Malignant peripheral nerve sheath tumors (MPNSTs) are soft tissue sarcomas that occur in 50% of patients with Neurofibromatosis Type 1 (NF1) and can also occur spontaneously in the general population (Carroll and Ratner, 2008). These tumors are derived from Schwann cells and/or their precursors and are found to be highly associated with peripheral nerves throughout the body (Carroll and Ratner, 2008). The current standard of care for patients with MPNSTs is surgery, radiation, and/or chemotherapy (Widemann, 2009). Unfortunately, surgery is often not an option, as these tumors are highly associated with nerves and often infiltrative in nature (Packer and Rosser, 2002). MPNSTs are also highly aggressive and often chemo-resistant, making these tumors notoriously difficult to treat (Franz and Weiss, 2012). Even when surgery in combination with radiation or chemotherapy is used, the local recurrence rate is 40-65%, with distant recurrence occurring 40-68% of the time, and chemotherapy treatment on distant metastases does not improve survival rates (Hruban et al., 1990; Kourea et al., 1998; Wong et al., 1998). With the current treatment strategies used, the 5-year survival rate for patients with MPNSTs is less than 25% and remains the leading cause of death for patients with NF1 (Katz et al., 2009; Widemann, 2009). Current research in the field has been to identify the genetic changes and molecular pathways that drive MPNST formation in hopes of identifying targeted therapies that can be used to treat these tumors more

effectively, with fewer side effects (Katz et al., 2009; Packer et al., 2002; Packer and Rosser, 2002).

In NF1 patients, it is clear that loss of the *Neurofibromin 1* gene (*NF1*) is sufficient for benign neurofibroma formation, but other genetic changes are required for transformation into MPNSTs (Carroll, 2012). For example, in chimeric mice with loss of *Nf1*, benign, grade 1 neurofibromas will form, but if *Tp53* is also lost, these tumors present as high grade MPNSTs (Cichowski et al., 1999; Vogel et al., 1999). When *Nf1* is biallelically inactivated in Schwann cells, grade 1 neurofibromas occur, but when *Pten* is also lost, these mice form numerous, grade 2-3 MPNSTs (Keng et al., 2012a; Wu et al., 2008). Consistent with this observation, MPNSTs from human patients often have reduced *PTEN* expression compared to normal nerve or benign neurofibromas (Keng et al., 2012a). Less is known about the genetics changes that occur in spontaneous MPNST formation (Widemann, 2009). Some of the genetic changes that have been characterized are over expression of *EGFR,* loss of *PTEN,* and loss of *CDKN2A* (Carroll, 2012; Holtkamp et al., 2008; Keng et al., 2012b; Nielsen et al., 1999).

Despite the wide variety of genetic changes seen in both NF1-associated and spontaneous MPNSTs, one clear feature of many of these tumors is activation of the MAPK and PI3K/AKT/mTOR pathways (Brems et al., 2009; Franz and Weiss, 2012; Johannessen et al., 2005). *NF1* encodes the protein Neurofibromin,

which is a Ras GTPase activating protein (Ras-GAP) (Cichowski and Jacks, 2001). When *NF1* is lost, Ras is held in its GTP-bound, active state, and results in hyperactive signaling through both the MAPK and PI3K pathway (Cichowski and Jacks, 2001). While loss of *NF1* results in increased signaling through the PI3K pathway, data suggest that additional changes occur to further activate signaling through this pathway. For example, approximately 75% of MPNSTs have expression of the Epidermal Growth Factor Receptor (EGFR), which when stimulated by Epidermal Growth Factor (EGF), results in hyperactivation of PI3K signaling (Holtkamp et al., 2008; Ling et al., 2005; Tabone-Eglinger et al., 2008; Tawbi et al., 2008). It has also been shown in mouse models of Schwann cell tumors that loss of *Nf1* is sufficient for benign neurofibroma formation, but loss of *Pten* is both necessary and sufficient for malignant transformation (Keng et al., 2012a; Wu et al., 2008). Additionally, a *Sleeping Beauty* forward genetic screen carried out in our lab demonstrated that while both benign neurofibromas had insertions in either *Nf1* or *Pten*, these mutations only co-occurred in MPNSTs (Rahrmann et al., 2013).

With PI3K/AKT/mTOR and MAPK signaling being implicated in MPNST development and neurofibroma progression, therapies that target these pathways have been of interest, and have been studied both pre-clinically and in clinical trials (Chappell et al., 2011; Franz and Weiss, 2012; Grant, 2008). Many inhibitors have been developed to target the PI3K/AKT/mTOR pathway, and the

most clinically successful drugs have been inhibitors of mTOR itself, including sirolimus (Rapamycin) and its derivative, everolimus (RAD-001) (Chiang and Abraham, 2007; Gurk-Turner et al., 2012). Currently, RAD-001 is FDA approved for kidney cancer, subependymal glial cell astrocytomas, pancreatic cancer and certain subtypes of breast cancer (Populo et al., 2012). There are phase III clinical trials in progress for gastric cancer, hepatocellular carcinoma, and lymphoma (Populo et al., 2012).

Many preclinical studies have been conducted for Schwann cell tumors using mTOR inhibitors that have suggested varied efficacy. In MPNST xenograft studies, RAD-001 significantly, but transiently delayed tumor growth (Johansson et al., 2008). In a genetically engineered mouse model in which *Nf1* is biallelically inactivated in Schwann cell and their precursors (*Nf1 flox/flox; DhhCre*), which models grade 1 neurofibromas, RAD-001 was ineffective at decreasing tumor volume (Wu et al., 2012). In a mouse MPNST model in which *Nf1* and *p53* are deleted in *cis*, Rapamycin treatment resulted in delayed tumor formation (Johannessen et al., 2008). Based on these studies, phase II clinical trials are currently in progress using the mTOR inhibitor Rapamycin in the treatment of plexiform neurofibromas (Widemann, 2009).

PD0325901 (PD-901) is a potent and highly specific inhibitor of MEK (Wang et al., 2007). It is currently in clinical trials for non-small cell lung cancer and other advanced cancers (Thompson and Lyons, 2005). Compared to other

MEK inhibitors, PD-901 is more potent, exhibits effects with a longer duration, and has increased bioavailability and metabolic stability (Bain et al., 2007). In preclinical studies, PD-901 has shown efficacy in human MPNST xenograft models, where tumor growth was reduced and survival was prolonged, although tumor growth was not completely suppressed (Jessen et al., 2013). In the genetically engineered mouse model of neurofibromas (*Nf1 flox/flox; DhhCre*), PD-901 reduced tumor volume, but did not result in the induction of apoptosis of tumor cells (Jessen et al., 2013).

To date, no clinical trials evaluating molecularly targeted therapies has prevented neurofibromas formation, stopped the growth of neurofibromas, or caused prolonged arrest of MPNST growth (Huson et al., 2011). In preclinical studies using RAD-001 or PD-901, it has been shown that while these drugs can be either modestly or transiently effective, in most cases, each inhibitor acts cytostatically and does not induce apoptosis (Carli et al., 2005). It is thought that this could be due to the effect of negative feedback, or due to the need to inhibit multiple pathways to induce a cytotoxic response (Chappell et al., 2011; Grant, 2008). In light of these findings, we sought to address whether co-targeting the mTOR and MAPK pathways would be more effective in treating MPNSTs than targeting either pathway alone. We addressed this by testing the effect of each of these drugs alone and in combination in two genetically engineered mouse models of MPNSTs. One model represents NF1-associated MPNSTs, in which both *Nf1*

and *Pten* are biallelically deleted in Schwann cells and their precursors (*Dhh-Cre; Nf1 flox/flox; Pten flox/flox*) (Keng et al., 2012a). The other models spontaneous MPNSTs in which *Pten* is biallelically inactivated in Schwann cells and *EGFR* is overexpressed (*Dhh-Cre; Pten flox/flox; CNPase-hEGFR*) (Keng et al., 2012b).

We believe that this study has many advantages over previous pre-clinical studies. First, it is likely that the use of genetically engineered mouse models reflects patient outcomes better than *in vitro* and xenograft studies, as these tumors model the genetic changes, location, pathology, and histology of human tumors (Sharpless and Depinho, 2006). In addition, as these tumors form *in situ*, the contribution of other cell types can be evaluated (Sharpless and Depinho, 2006). This is especially important in studying Schwann cell tumors, as these tumors are quite angiogenic, contain fibroblasts and mast cells, and are highly associated with peripheral nerves (Brossier and Carroll, 2012; Carroll and Ratner, 2008). Another advantage of our models is that these mice rapidly and uniformly form high grade MPNSTs (Keng et al., 2012a; Keng et al., 2012b). Other models have evaluated the pre-clinical efficacy of targeted therapies in neurofibromas, but it is important to evaluate these therapies in mouse models of MPNSTs, as clinical trials are likely to evaluate these therapies in malignant tumors. This study also evaluated the efficacy of these therapies in two mouse models, one that represents NF1-associated MPNSTs and one that represents spontaneous MPNSTs. The 5-year survival rate for metastatic MPNSTs treated with

chemotherapy is 17.6% for patients with NF1 versus 55% in sporadic cases (Carli et al., 2005). It is important to evaluate efficacy in both types of MPNSTs, as clearly, they may respond differently to therapy. Finally, theses mouse models have advantages for pre-clinical drug testing, as the mice rapidly form tumors, with 100% penetrance, and multiple tumors per animal (Keng et al., 2012a; Keng et al., 2012b).

Here we show that targeting the MAPK pathway with the MEK inhibitor PD-901 and targeting the PI3K/AKT/mTOR pathway with the mTOR inhibitor RAD-001 is effective at inhibiting cellular proliferation in both NF1-assscociated and spontaneous MPNST cell lines *in vitro,* although these inhibitors appear to be cytostatic. When given in combination, RAD-001 and PD-901 synergistically inhibit proliferation and effectively induce apoptosis in MPNST cell lines. Based on this *in vitro* data, we tested the efficacy of these inhibitors as single agents and in combination in two genetically engineered mouse models of NF1-associated MPNSTs and spontaneous MPNSTs. While RAD-001 and PD-901 alone are moderately effective at reducing tumor burden and/or grade, the combination of these two drugs is much more effective, resulting in a reduction in tumor burden, size and grade as well as an increase in survival in both mouse models. When given as single agents, these drugs are initially effective at reducing signaling through their respective pathways, but long term treatment results in the development of drug resistance. In contrast, when RAD-001 and PD-901 are

given simultaneously, signaling through both the PI3K and MAPK pathway remains effectively and persistently inhibited.

II. Results

RAD-001 and PD-901 are effective at inhibiting cellular proliferation in both NF1-associated and spontaneous MPNST cell lines

To assess the therapeutic potential of inhibiting the PI3K/AKT/mTOR and MAPK pathways in human MPNSTs, a panel of two immortalized human Schwann cell lines (iHSC1λ and iHSC2λ, (Watson et al., 2013)) and 5 human MPNST cell lines (S462 (Frahm et al., 2004), S462-TY (Mahller et al., 2008), ST8814 (Fletcher et al., 1991), T265 (Badache and De Vries, 1998), and STS-26T (Dahlberg et al., 1993)) were exposed to the mTOR inhibitor RAD-001 and the MEK inhibitor PD-901. When exposed to RAD-001, the two immortalized Schwann cell lines were more resistant to inhibition of proliferation than the 5 MPNST cell lines, with inhibitory concentrations of 50% (IC50s) of 2.64uM to 2.70uM versus 0.97 to 2.12uM in the MPNST cell lines (**Figure 1A)**. Similarly, PD-901 IC50s were 134.01uM to 147.11uM in the immortalized human Schwann cell lines versus 1.25uM to 127.84uM in the MPNST cell lines. These data suggest that malignant Schwann cells are more sensitive to inhibition of mTOR and MAPK pathways than untransformed Schwann cells.

In addition to inhibiting proliferation at relatively low IC50s in MPNST cell lines as single agents, RAD-001 and PD-901 also act synergistically to inhibit cellular proliferation. MPNST cell lines treated with varying dilutions of RAD-001 and PD-901 at their respective IC50s resulted in combination indices of 0.02

to 0.107. (**Figure 1B**). Combination indices of below 1.0 as calculated using the software Calcusyn ©, suggest that in MPNST cell lines, RAD-001 and PD-901 function to inhibit cellular proliferation synergistically.

Inhibiting the mTOR and MAPK pathways in combination induces apoptosis in MPNST cell lines

To further understand how RAD-001 and PD-901 function to inhibit proliferation synergistically, we exposed the S462 MPNST cell line to the IC50 doses of RAD-001 and PD-901 and assessed apoptosis. In both cases, treatment with a single agent at a concentration that inhibits 50% proliferation results in less than 50% apoptosis, showing that these drugs function largely cytostatically (**Figure 1C**). In contrast, when the S462 cells were treated with the IC25 doses of RAD-001 and PD-901 in combination, the percentage of cells that are undergoing apoptosis is nearly 70%. These data suggest that co-targeting the mTOR and MAPK pathway results in a synergistic induction of apoptosis.

RAD-001 and PD-901 as single agents are moderately effective at reducing disease in two genetically engineered mouse models of MPNSTs

To test the efficacy of targeting the PI3K/AKT/mTOR and MAPK pathways for MPNSTs *in vivo,* two genetically engineered mouse models were treated with RAD-001 and PD-901. In a mouse model of MPNSTs that represents

NF1-associated Schwann cell tumors, the *Desert Hedgehog* promoter was used to drive *Cre Recombinase* (*Dhh-Cre*) resulting in *Cre Recombinase* expression in Schwann cells and their precursors (**Figure 2A**). (Jaegle et al., 2003). Combined with floxed alleles of *Nf1*(*Nf1 fl/fl*) and *Pten* (*Pten fl/fl*), expression of *Dhh-Cre* results in the biallelic inactivation of both *Nf1* and *Pten* in Schwann cells and their precursors (Xiao et al., 2005; Zhu et al., 2005). This genetically engineered mouse model has advantages for *in vivo* drug testing including severe and fully penetrant peripheral nerve disease, a short lifespan of approximately 15 days, and an average tumor burned on 21.8 high grade peripheral nerve sheath tumors per animal (**Figure 2B**). The breeding scheme and drug schedule are shown in **Figure 2C**. Briefly, pups were divided into 4 cohorts and given DMSO (vehicle control), 10mg/kg/day of RAD-001, 5 mg/kg/day of PD-901, or a combination of 5mg/kg/day of RAD-001 and 2.5 mg/kg/day of PD-901. In the mouse model that represents spontaneous MPNSTs, *Dhh-Cre* is again used to biallelically inactivate *Pten*, and human *EGFR* is expressed under the control of the *2', 3' cyclic nucleotide 3/phosphodiesterase* promoter, which results in the overexpression of EGFR in Schwann cells (**Figure 3A**) (Jaegle et al., 2003; Ling et al., 2005; Xiao et al., 2005). This mouse model has an average lifespan of 28 days, with 100% penetrance of high grade tumors and approximately 13.7 tumors per animal (**Figure 3B**). The breeding scheme and drug schedule is shown in **Figure 3C**.

Pups were separated into the same 4 cohorts described above for the NF1-associated mouse model.

When the NF1-associated MPNST mouse model was treated with RAD-001 or PD-901, survival was significantly prolonged from an average of 15.8 days with DMSO treatment, to 22.4 days with RAD-001 and 19.5 days with PD-901 (p=0.032 and p=0.036, respectively) (**Figure 4A**). Similarly, when the spontaneous MPNST mouse model was treated with RAD-001 or PD-901, survival was also extended from an average of 29.4 days with DMSO to 39.8 days with RAD-001 and 48 days with PD-901 (p=0.109 and p=0.019, respectively) (**Figure 4B**). Although RAD-001 extended lifespan in the NF1-associated mouse model, the number of tumors per animal was not significantly reduced at the time of necropsy (**Figure 4C**). PD-901 treatment in the NF1-associated mouse model did significantly reduce tumor burden from 20.6 tumors per animal with DMSO treatment to 12.8 tumors per animal with PD-901 treatment (p=0.0002) (**Figure 4C**). In contrast to the NF1-associated model, when the spontaneous mouse model was treated with RAD-001, the number of tumors per animal was reduced from 15.4 tumors per animal in the DMSO treated cohort versus 10.6 tumors per animals treated with RAD-001 (p= 0.0189) (**Figure 4D**). PD-901 did not significantly reduce tumor burned in the spontaneous mouse model (**Figure 4D**).

Tumors treated with each drug were histologically analyzed for tumor grade as previously described (Stemmer-Rachamimov et al., 2004; Weiss et al., 2002). Briefly, hematoxylin and eosin (H & E) staining was performed to assess cellularity and mitotic index, immunohistochemistry for S100 confirmed the Schwann cell origin of thee tumors, and Ki67 immunohistochemistry demonstrated the amount of cellular proliferation. Although the number of tumors per animal in the NF1-associated mouse model was not reduced, tumor grade was much lower with RAD-001 treatment (**Figure 5A)**. Tumors from mice treated with DMSO were mostly grade 2, with some being grade 1 peripheral nerve sheath tumors. When these mice were treated with RAD-001, there was a dramatic reduction in the fraction of grade 2 tumors, with most tumors being grade 1. While PD-901 treatment dramatically reduced tumor burden in this model, all tumors analyzed were grade 2. **Figure 5B** shows examples of the dorsal root ganglia (DRG) tumors in each of the treatment groups. DMSO treated mice have nearly every DRG nerve enlarged at only 15 days. In contrast, RAD-001 and PD-901 treatment resulted in fewer and smaller tumors at later time points (day 23 and 25, respectively). In the spontaneous MPNST mouse model, DMSO treated animals had tumors that varied between grade 1 and 3, with the majority of tumors being grade 3, 2/3, and 2 (**Figure 6A**). When these mice were treated with RAD-001, tumor grade was reduced, with the majority of tumors being grade 2, and some enlarged DRGs even being graded as peripheral nerve

hyperplasia. PD-901 was also effective at reducing tumor grade, with no tumors seen as grade 3. **Figure 6B** shows examples of DRG tumors with each treatment. DMSO treated animals have nearly every DRG nerve extremely enlarged, while mice treated with RAD-001 and PD-901 had fewer and/or smaller DRG tumors.

Simultaneously inhibiting both mTOR and MEK in vivo is very effective in both NF1-associated and spontaneous MPNST mouse models.

Co-targeting mTOR and MEK in both mouse models resulted a significant increase in survival compared to vehicle control (DMSO) treated animals (23.5 days, p=0.025 in the NF1-asociated model and 42.3 days, p= 0.002 in the spontaneous model), although the extension in lifespan was similar to treatment with RAD-001 or PD-901 alone (**Figure 4A & B**). Importantly, the combination treatment was given at half the doses of single treatments (5mg/kg/day RAD-001 and 2.5 mg/kg/day), as treatment with higher doses resulted in significant toxicity (data not shown). In addition, both mouse models had a significant reduction in tumor burden when both drugs were given (7.5 tumors per animal in the NF1-asociated model, p <0.0001 and 11.8 tumors per animal in the spontaneous model, p=0.0474) (**Figure 4C & D**).

Treatment with RAD-001 and PD-901 in combination in the NF1-asssociated mouse model extended lifespan and dramatically reduced tumor burden, all tumors that were analyzed at necropsy were grade 2 (**Figure 5A**),

although the DRG tumors from mice treated with the combination therapy appeared smaller at necropsy (**Figure 5B**). In contrast, combination treatment of RAD-001 and PD-901 in the spontaneous mouse model resulted in all grade 2 or grade 1/2 tumors (**Figure 6A**). Additionally, fewer enlarged DRG nerves were observed, and those seen in this model were quite small (**Figure 6B**).

Inhibiting mTOR or MAPK signaling results in the development of drug resistance and increased signaling through each respective pathway

To assess the ability of these drugs to inhibit their respective pathways *in vivo,* we assessed the level of p-AKT, p-4EBP, and p-ERK in tumors from animals treated with RAD-001 or PD-901. As expected, in mice treated with RAD-001, the levels of p-AKT and p-4EBP were reduced at early time points (day 24) at which there were few tumors, all of which were quite small (**Figure 7A, B, & C**). At later time points (day 55), tumors from RAD-001 treated mice were more numerous and larger, and western blot analysis shows that both p-AKT and p-4EBP were elevated, suggesting that long term treatment of RAD-001 results in the development of drug resistance (**Figure 7 A, B, & C**). Similarly, tumors from mice treated with PD-901 at early time points (day 25) have a reduced level of p-ERK (**Figure 7D & E**). At later time points (day 45), the level of p-ERK has strongly increased, again suggesting that long term PD-901 treatment results in the development of resistance.

Co-targeting mTOR and MAPK pathways results in prolonged and persistent inhibition of signaling through both pathways

After finding that long term treatment with RAD-001 or PD-901 results in reactivation of the PI3K/AKT/mTOR and MAPK pathways, we sought to determine if the increased efficacy of the combination therapy was due to persistent pathway inhibition. When mice were treated with RAD-001 and PD-901 in combination, p-AKT, p-4EBP, and p-ERK all remained inhibited at both early and late time points (**Figure 8 A, B, C & D**). This suggests that co-targeting PI3K/AKT/mTOR and MAPK pathways *in vivo* results in prolonged and persistent pathway inhibition, resulting in an effective combinational targeted therapy.

Iii. Materials and Methods

Tissue culture reagents and cell lines

Cultured immortalized Schwann cells (iHSC1λ and iHSC2λ) were both derived from a patient's normal sciatic nerve, are *NF1* wild-type, and were immortalized by *hTERT* and $CDK4^{R24C}$ to allow *in vitro* studies (Watson et al., 2013). Immortalized human Schwann cell and MPNST cell lines (S462 (Frahm et al., 2004), S462-TY (Mahller et al., 2008), ST8814 (Fletcher et al., 1991), T265 (Badache and De Vries, 1998), and STS-26T (Dahlberg et al., 1993)) were maintained in Dulbecco's Modification of Eagle Medium (DMEM) supplemented with 10% fetal bovine serum and penicillin/streptomycin (Cellgro) and cultured on tissue culture-treated plates under standard conditions of 37 degrees Celsius and 5% CO2.

In Vitro Drug Studies to Determine IC50 and CI

RAD-001, and PD-901 were solubilized in DMSO and then subsequently diluted in sterile PBS. 1,200 cells per well of a 96-well plate were treated with varying concentration of drug in quadruplicate and assayed for cell viability using the MTS assay (Promega) to determine the IC50 values. All data analysis was done using Calcusyn software (CalcuSyn Version 2.1, BioSoft). A combination of

RAD-001 and PD-901 at varying dilutions of their IC50 concentration were used to determine the combination index (CI) using Calcusyn software (CalcuSyn © Version 2.1, BioSoft).

Generation of Transgenic Animals and PCR Genotyping

Generation of transgenic animals and PCR genotyping were done as previously described (Keng et al., 2012a; Keng et al., 2012b).

In Vivo Drug Studies

RAD-001, and PD-901 were solubilized in DMSO and then subsequently diluted in PBS and sterilized. Mice were weighed daily and given 10 mg/kg/day of RAD-001 or 5 mg/kg/day of PD-901. For combination studies mice were given 5 mg/kg/day of RAD-001 and 2.5 mg/kg/day of PD-901. Mice were weighed and monitored daily and sacrificed when they became moribund. Tumors, nerves and organs were harvested for immunohistochemistry and western blot analysis. All animal work was conducted according to the University of Minnesota's approved animal welfare protocol.

Peripheral nerve tumor analysis

Tumors were carefully removed from the sacrificed animal under a dissecting microscope (Leica), washed and placed in cold phosphate buffered saline (PBS). Sciatic nerves, brachial plexi, sacral plexi, trigeminal nerves, spinal cord, brain, and liver were also removed and observed for any abnormalities. The number of enlarged dorsal root ganglia was counted for the whole spinal cord. All reasonably sized tumor nodules (>1 mm in diameter) were carefully removed from the spinal cord.

Hematoxylin and eosin staining

Tissues were fixed in 10% formalin, routinely processed and embedded in paraffin. Sections for histology were cut at 5 microns from the paraffin blocks using a standard microtome (Leica), mounted and heat fixed onto glass slides. Slides were stained with hematoxylin and eosin (H&E) using standard protocols.

Mouse Tumor Immunohistochemistry (IHC)

Immunohistochemistry was done as previously described (Keng et al., 2012a; Keng et al., 2012b). Briefly, formalin fixed, paraffin embedded tissues were sectioned at 5 microns, mounted, and heat-fixed onto glass slides to be used for IHC analyses. The glass section slides were de-waxed and rehydrated through a gradual decrease in ethanol concentration. The antigen epitopes on the tissue sections were then unmasked using a commercially available unmasking solution

(Vector Laboratories) according to the manufacturer's instructions. The tissue section slides were then treated with 3% hydrogen peroxide to remove endogenous peroxidases. Blocking was performed at room temperature in normal goat serum (5% serum in PBS) in a humidified chamber for one hour. Sections were then incubated overnight at 4°C in a humidified chamber with primary antibody (S100 (Santa Cruz 1:100), Ki67 (Novocastra 1:200)). After primary incubation, sections were washed thoroughly in PBS before incubating with goat anti-rabbit horseradish peroxidase conjugated-secondary antibody (Santa Cruz Biotechnology). After 3 washes with PBS, the sections were treated with freshly prepared DAB substrate (Vector Laboratories) and allowed to develop before stopping the reaction in water once adequate signal was obtained. Finally, sections were then lightly counter-stained with hematoxylin, dehydrated through gradual increase in ethanol concentration, cleared in Citrosol (Fisher Scientific) and mounted in Permount (Fisher Scientific).

Histologic evaluation

Sections stained with H&E, Ki67 and S100 were evaluated for all tumors. Each sample was graded using established criteria for tumors arising in genetically engineered mice (Stemmer-Rachamimov et al., 2004; Weiss et al., 2002). Briefly, low-grade PNSTs exhibited low cellularity with little if any nuclear atypia and

mitotic activity. High-grade PNSTs were increasingly cellular with increasing nuclear atypia and increasing mitotic activity.

Immunofluorescence and TUNEL staining

For immunofluorescence assays, cells were grown to 80% confluency on 8 chambered slides (Lab-TekII). Cells were fixed in 10% formalin and washed with phosphate-buffered saline (PBS) with 0.1% Tween-20 (PBST). TUNEL staining was performed using the In Situ Cell Death Detection Kit, POD (Roche). Slides were mounted using Prolong Gold Antifade Reagent with DAPI (Invitrogen) and images using a Zeiss Axiovert 25 inverted microscope. For analysis of cell death, total cells and TUNEL positive cells were counted and averaged over three independent frames with 50-100 cells per frame.

Western blot analysis

1 million cells were lysed using an NP-40 buffer (50mM Tris-HCl pH 7.6, 150mM NaCl, 1% NP-40, 5mM NaF, 1mM EDTA) containing a protease inhibitor (Roche) and phosphatase inhibitors (Sigma). Whole cell lysates were cleared by centrifugation. Protein samples were prepared in an SDS solution with reducing agent (Invitrogen) and run on 10% Bis-Tris pre-made gels (NuPage,

Invitrogen). Gels were transferred onto PVDF membranes using the iBlot system (Invitrogen) and activated in 100% methanol. Membranes were blocked in filtered 5% Bovine Serum Albumin (BSA) for 2 hours at room temp followed by a 4 degrees Celsius overnight incubation in primary antibody. The primary antibodies used in this study were: p-AKT S473 (Cell Signaling 1:100), p-4EBP (Cell Signaling 1:500), p-ERK (Cell Signaling 1:1000), GAPDH (Cell Signaling 1:2000). Following primary antibody incubation, membranes were thoroughly washed in Tris Buffered Saline (TBS) with 0.1% Tween-20 (TBST) and incubated in goat anti-rabbit IgG-HRP conjugated secondary antibody (Santa Cruz, 1:4000 in 0.5% BSA, 1 hour at room temperature). Blots were thoroughly washed in TBST and developed using the SuperSignal WestPico Chemiluminescence Detection Kit (Thermo Scientific). Densitometry quantification was done using ImageJ software and normalized to GAPDH (Rasband, 1997-2012).

IV. Discussion

Analysis of human Schwann cell tumors and mouse models of neurofibromas and MPNST have demonstrated the functional importance of both PI3K/AKT/mTOR and MAPK pathway activation (Cichowski and Jacks, 2001; Johannessen et al., 2005). Importantly, both of these pathways can be targeted by small molecule inhibitors (Chappell et al., 2011; Grant, 2008). While the functional consequence of targeting either of these pathways alone in preclinical models has shown moderate efficacy, we show that co-targeting mTOR and MAPK is more effective both *in vitro* and *in vivo,* than targeting either pathway alone. In MPNST cell lines, we show that a combination of the mTOR inhibitor, RAD-001, and the MAPK inhibitor, PD-901, act synergistically to inhibit proliferation and induce apoptosis (**Figure 1**). While many targeted therapies, including these, have been shown to act cytostatically, it is of clinical importance that in combination, these inhibitors act cytotoxically (Chappell et al., 2011; Grant, 2008).

Another important aspect of this preclinical study is that targeting the PI3K/AKT/mTOR and MAPK pathways alone and in combination was studied in two preclinical mouse models that represent two subsets of Schwann cell tumors, those that form in the context of NF1 and those that form spontaneously (**Figure 2 & 3**) (Keng et al., 2012a; Keng et al., 2012b). We show that survival is significantly increased in both mouse models when the mice are treated with

RAD-001, PD-901, or the combination of both (**Figure 4**). In the NF1-associated mouse model, the combination of RAD-001 and PD-901 significantly decreased tumor burden and size, although tumor grade remained high (**Figure 4 & 5**). Tumor burden, size, and grade were all significantly decreased when RAD-001 and PD-901 were administered in combination in the spontaneous MPNST mouse model (**Figure 4 & 6**). By showing efficacy of these targeted therapies in two different genetically engineered mouse models, we believe that there is an increased likelihood of success in human clinical trials.

The development of resistance to targeted therapies in cancer has been well documented (Chappell et al., 2011; Ellis and Hicklin, 2009; Sierra et al., 2010). We show that when mice are treated with either RAD-001 or PD-901 as single agents over a long period of time, resistance does indeed develop, and the PI3K/AKT/mTOR and MAPK pathways become reactivated (**Figure 7**). In contrast, when mTOR and MAPK are co-targeted in these two mouse models, both signaling pathways remain inhibited over the course of treatment (**Figure 8**). This likely accounts for the reason that single drug treatments do not show the efficacy that the combination therapy shows in these two mouse models and may explain why either of these drugs given alone in other models have only showed modest efficacy (Jessen et al., 2013; Johansson et al., 2008; Wu et al., 2012). It is also likely that mice treated with RAD-001 and PD-901 in combination may also be developing resistance, although more delayed than with single treatments,

through different mechanisms, as eventually these mice succumb to their tumors. Future work will be required to determine if other pathways become activated, allowing for tumor cells to escape inhibition from RAD-001 and PD-901.

The two genetically engineered mouse models used in this study are the most rapid models of high grade peripheral nerve tumors available. These models may not be the best representation of the human disease, due to the rapid formation of a large tumor burden, but showing efficacy in this model is significant, as these mice model the genetic changes often seen in human tumors (Keng et al., 2012a; Keng et al., 2012b). It will be important to study the effect of co-targeting mTOR and MAPK in other less severe models of neurofibromas or MPNST development, including other genetically engineered mouse models as well as xenograft models. In fact, in slower developing tumor models, these drugs may be more effective, as they have more time to effectively inhibit these pathways and control cellular proliferation and transformation.

Future work will need to be done to determine the safety and efficacy of co-targeting the PI3K/AKT/mTOR and MAPK pathways in human patients. In preclinical mouse models, it may be necessary to test the efficacy of these targeted therapies in combination with chemotherapy, as clinical trials will likely be designed to incorporate the current standard of therapy for these patients. It is also of interest to study whether the combination of RAD-001 and PD-901 could be used to treat plexiform neurofibromas in an attempt to prevent transformation

to MPNSTs. This could be done in the *Dhh-Cre; Nf1 flox/flox* model (Wu et al., 2008). One difficulty that could arise that we and others have demonstrated is that long term treatment with RAD-001 causes immunosuppresion, which could add a layer of complexity to the use of this drug in a clinical setting over a long period of time for plexiform neurofibromas (Eisen et al., 2003). Additionally, it has become clear that the immune system can play an important role in cancer, so immune system suppression may not be desirable (Hanahan and Weinberg, 2011). While there are challenges with implementing new targeted therapies in the clinic, the data presented here demonstrates that co-targeting PI3K/AKT/mTOR and MAPK may be beneficial for patients suffering from Schwann cell tumors.

Figure 1: RAD-001 and PD-901 are effective at inhibiting human MPNST cell proliferation and are synergistic at inhibiting proliferation and inducing apoptosis *in vitro*. A. Inhibitory concentrations of 50% (IC50) for RAD-001 and PD-901 in two immortalized human Schwann cell lines (iHSC1λ, iHSC2λ) and 5 MPNST cell lines (S462, S462-TY, ST8814, T265, and STS-26T) were determined using the MTS assay for proliferation and calculated using Calcusyn software ©. Immortalized Schwann cells are more resistant to inhibition of proliferation by RAD-001 and PD-901, while the MPNST cell lines are much more sensitive as shown by their lower IC50 values. B. The combination index (CI) for RAD-001 and PD-901 was determined using MTS proliferation data for the combination of drugs at varying IC50 dilutions. A combination index of less than 1 suggests that the two drugs act synergistically to inhibit proliferation in all 5 MPNST cell lines. C. In the S462 MPNST cell line treated with IC50 doses of RAD-001 or PD-901 as single agents, the percentage of cell undergoing apoptosis is less than 50%, suggesting that these drugs are acting cytostatically. In contrast, when RAD-001 and PD-901 are given in combination at their IC25 doses, the percentage of apoptosis is nearly 70%, suggesting that in combination, these drugs act synergistically to induce apoptosis. Example images are shown of S462 cells stained with DAPI (blue) to allow total cell counts and TUNEL (green) to determine cells undergoing apoptosis. Error bars represent SEM.

Figure 1

A

	Immortalized Human Schwann Cells		MPNST Cell Lines				
	iHSC1λ	iHSC2λ	S462	S462-TY	ST8814	T265	STS26T
RAD-001 IC50	2.64 μM	2.70 μM	0.97 μM	1.87 μM	2.12 μM	1.46 μM	1.36 μM
PD-901 IC50	134.01 μM	147.11 μM	1.61 μM	9.28 μM	65.97μM	1.25 μM	127.84 μM

B

	S462	S462-TY	ST8814	T265	STS26T
RAD-001 & PD-901 Combination Index	0.076	0.107	0.056	0.02	0.054

CI <1 Synergistic CI=1 Additive CI> Antagonistic

C

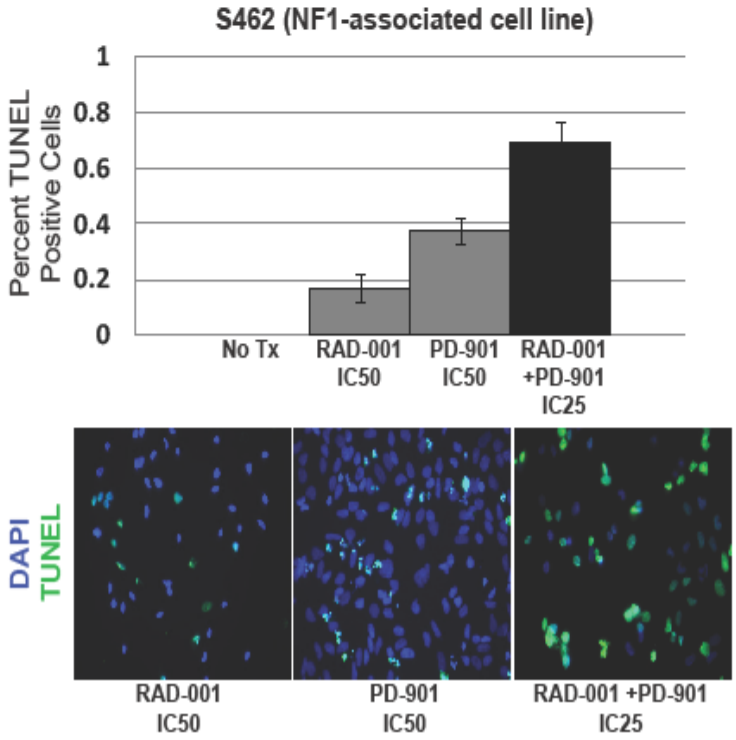

Figure 2: Breeding scheme and drug schedule for the NF1-associated MPNST mouse model. A. In the NF1-associated MPNST mouse model, mice contain a transgene with the *Desert Hedgehog* promoter driving *Cre Recombinase* (*Dhh-Cre)* (Jaegle et al., 2003). This transgene results in *Cre Recombinase* expression in Schwann cells and their precursors, the cell of origin for MPNSTs. In this model, *Cre Recombinase* allows for biallelic deletion of exons 31 and 32 of the *Nf1* gene (*Nf1 fl/fl*) and exons 4 and 5 of the *Pten* gene (*Pten fl/fl*) (Xiao et al., 2005; Zhu et al., 2005). B. Table describing the phenotype of *Dhh-Cre; Nf1 fl/fl; Pten fl/fl* mice (Keng et al., 2012a). C. Breeding scheme and drug schedule for the NF1-associated MPNST model.

Figure 2

A

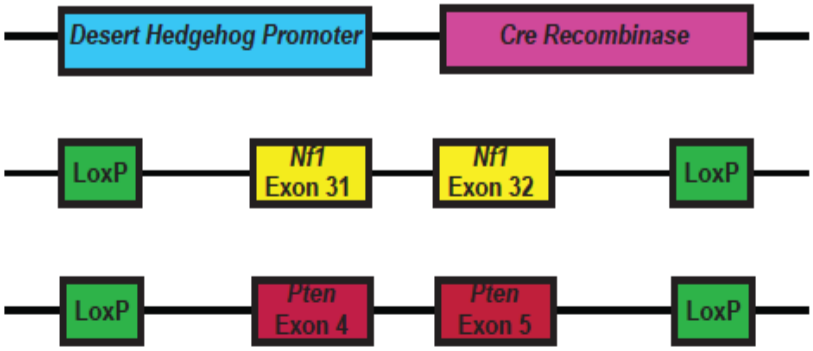

B

Median Lifespan	15 days
Average Tumor Burden	21.8
Tumor Location	Dorsal root ganglion, brachial plexus, lumbar plexus, intercostal nerves
Tumor Grade	2-3
Other Phenotypes	Severe mobility and coordination problems, enlarged nerves

C

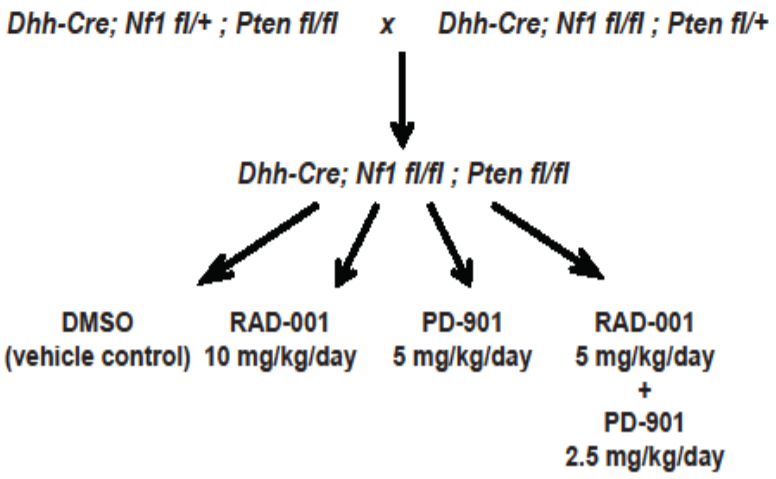

Figure 3: Breeding scheme and drug schedule for the spontaneous MPNST mouse model. A. In the spontaneous MPNST mouse model, mice contain a transgene with the *Desert Hedgehog* promoter driving *Cre Recombinase* (*Dhh-Cre)* (Jaegle et al., 2003). This transgene results in *Cre Recombinase* expression in Schwann cells and their precursors, the cell of origin for MPNSTs. In this model, *Cre Recombinase* allows for biallelic deletion of exons 4 and 5 of the *Pten* gene (*Pten fl/fl*) (Xiao et al., 2005). These mice also contain a transgene that uses *the 2', 3' cyclic nucleotide 3/ phosphodiesterase* promoter (*CNP*) to drive overexpression of human *EGFR* in the Schwann cell lineage (Ling et al., 2005). B. Table describing the phenotype of *Dhh-Cre; Pten fl/fl; EGFR* mice (Keng et al., 2012b). C. Breeding scheme and drug schedule for the spontaneous MPNST model.

Figure 3

A

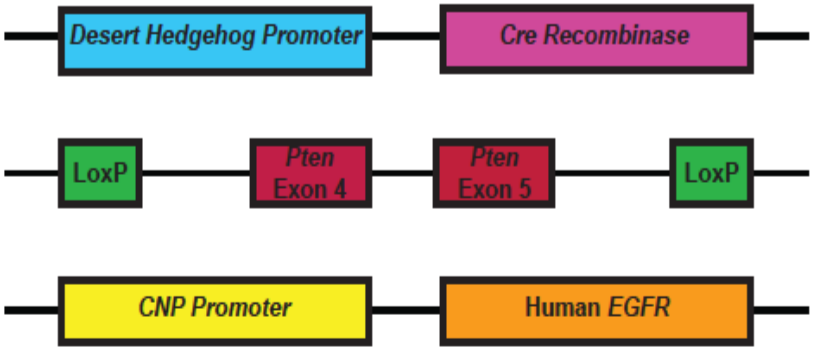

B

Median Lifespan	28 days
Average Tumor Burden	13.7
Tumor Location	Dorsalroot ganglion, brachial plexus, lumbar plexus, intercostal nerves
Tumor Grade	2-3
Other Phenotypes	Minor mobility problems, enlarged nerves

C

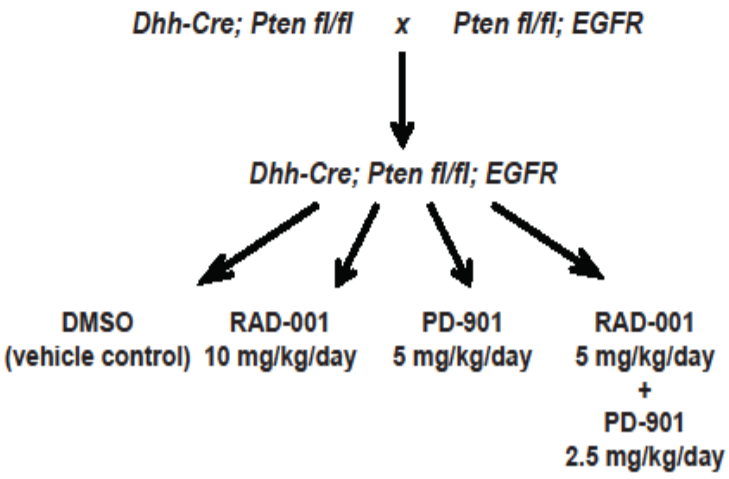

Figure 4: RAD-001 and PD-901 alone and in combination can increase survival and reduce tumor burden in both the NF1-associated and spontaneous MPNST mouse models. A. In the NF1-asociated MPNST mouse model, treatment with RAD-001 or PD-901 as single agents are able to extend lifespan as well as the combination therapy. B. In the spontaneous MPNST mouse model, RAD-001, PD-901, and the combination treatment were all able to extend the lifespan of mice. C. Tumor burden is reduced in the NF1-associated mouse model when treated with PD-901 or a combination of both RAD-001 and PD-901. D. Tumor burden is reduced in the spontaneous MPNST mouse model when treated with RAD-001 or a combination of both RAD-001 and PD-901.

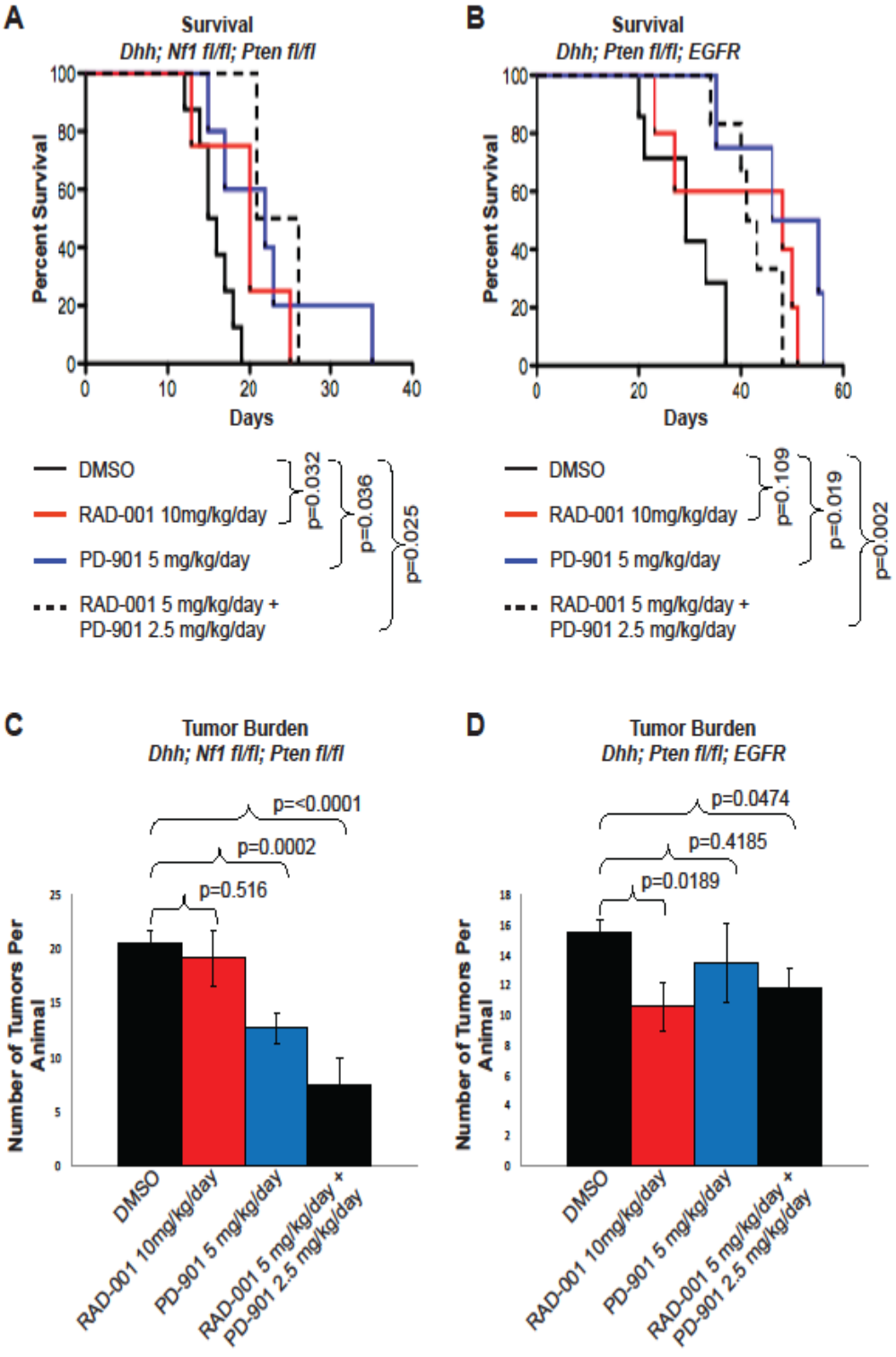
A
Survival
Dhh; Nf1 fl/fl; Pten fl/fl
Percent Survival
Days
DMSO
RAD-001 10mg/kg/day
PD-901 5 mg/kg/day
RAD-001 5 mg/kg/day +
PD-901 2.5 mg/kg/day
p=0.032
p=0.036
p=0.025
B
Survival
Dhh; Pten fl/fl; EGFR
Percent Survival
Days
DMSO
RAD-001 10mg/kg/day
PD-901 5 mg/kg/day
RAD-001 5 mg/kg/day +
PD-901 2.5 mg/kg/day
p=0.109
p=0.019
p=0.002
C
Tumor Burden
Dhh; Nf1 fl/fl; Pten fl/fl
Number of Tumors Per Animal
p=<0.0001
p=0.0002
p=0.516
DMSO
RAD-001 10mg/kg/day
PD-901 5 mg/kg/day
RAD-001 5 mg/kg/day +
PD-901 2.5 mg/kg/day
D
Tumor Burden
Dhh; Pten fl/fl; EGFR
Number of Tumors Per Animal
p=0.0474
p=0.4185
p=0.0189
DMSO
RAD-001 10mg/kg/day
PD-901 5 mg/kg/day
RAD-001 5 mg/kg/day +
PD-901 2.5 mg/kg/day

Figure 5: Tumor grade, burden, and size change when the NF1-associated MPNST mouse model is treated with RAD-001, PD-901, or a combination of RAD-001 and PD-901. A. The majority of tumors from mice treated with the vehicle control (DMSO) are grade 2, with the rest being grade 1. When mice were treated with RAD-001, tumor grade was reduced, with the majority of tumors being grade 1. When mice were treated with PD-901 or the combination of RAD-001 and PD-901, despite having a reduced number of tumors, all tumors were grade 2. B. Example images of dorsal root ganglia (DRG) tumors in the NF1-associated mouse model with various treatments. DMSO treated mice have nearly every DRG highly enlarged, while RAD-001 or PD-901 treatments reduce the size and number of enlarged DRGs. The combination treatment of RAD-001 and PD-901 most effectively reduces the number and size of DRGs in the NF1-associated mouse model.

Figure 5

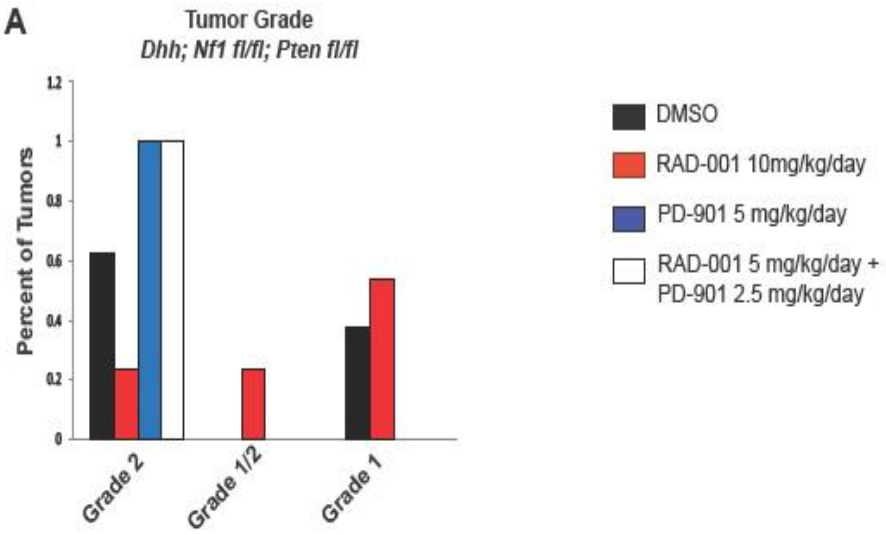
A
Tumor Grade
Dhh; Nf1 fl/fl; Pten fl/fl
Percent of Tumors
1.2
1
0.8
0.6
0.4
0.2
0
Grade 2
Grade 1/2
Grade 1
DMSO
RAD-001 10mg/kg/day
PD-901 5 mg/kg/day
RAD-001 5 mg/kg/day +
PD-901 2.5 mg/kg/day

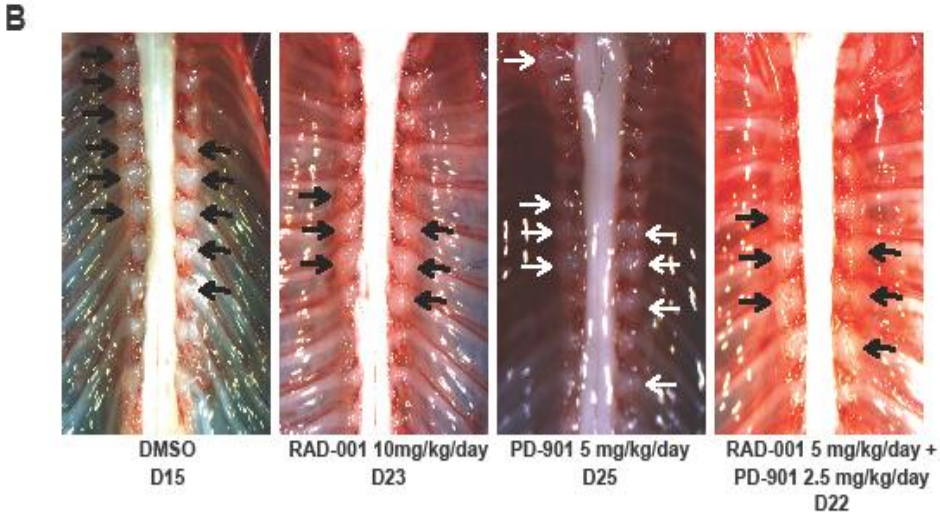
B
DMSO
D15
RAD-001 10mg/kg/day
D23
PD-901 5 mg/kg/day
D25
RAD-001 5 mg/kg/day +
PD-901 2.5 mg/kg/day
D22

Figure 6: Tumor grade is reduced when the spontaneous MPNST mouse model is treated with RAD-001 and PD-901 in combination. A. Vehicle control (DMSO) treated mice have grade 1-3 tumors, with the majority being grade 2, 2/3, or 3. Treatment with RAD-001 reduces the fraction of grade 3 and 2/3 tumors and increases the fraction of lower grade 1 tumors. Some enlarged dorsal root ganglia were even categorized as nerve hyperplasia. Treatment with PD-901 resulted in no tumors that were grade 3 and an increase in grade 2/3 and 1/2. Treatment with the combination of RAD-001 and PD-901 most dramatically reduced tumor grade resulting in only grade 2 and 1/2 tumors. B. Example images of dorsal root ganglia (DRG) tumors in the spontaneous MPNST mouse model with various treatments. DMSO treated mice have nearly every DRG highly enlarged, while RAD-001 or PD-901 treatments reduce the size and number of enlarged DRGs. The combination treatment of RAD-001 and PD-901 most effectively reduces the size of DRGs in the spontaneous MPNST mouse model.

Figure 6

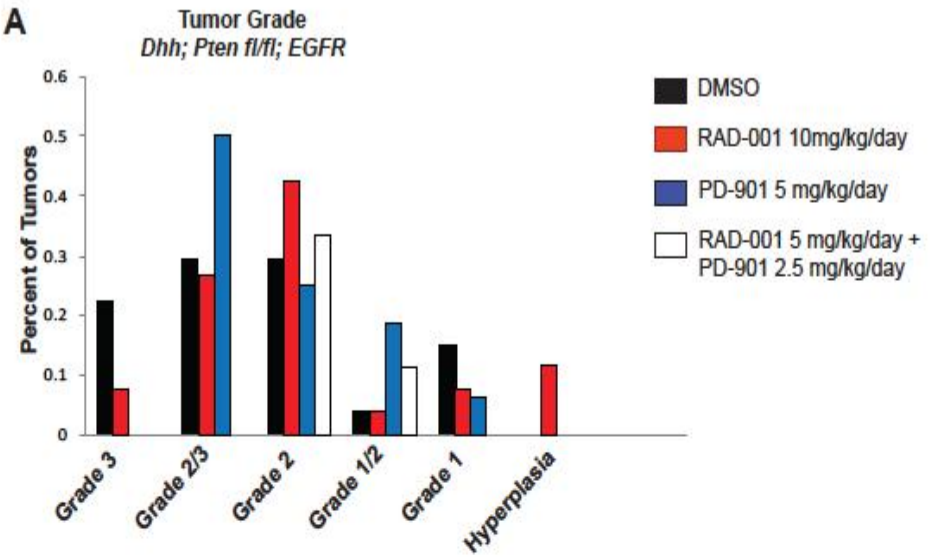
A
Tumor Grade
Dhh; Pten fl/fl; EGFR
Percent of Tumors
0.6
0.5
0.4
0.3
0.2
0.1
0
Grade 3
Grade 2/3
Grade 2
Grade 1/2
Grade 1
Hyperplasia
DMSO
RAD-001 10mg/kg/day
PD-901 5 mg/kg/day
RAD-001 5 mg/kg/day +
PD-901 2.5 mg/kg/day

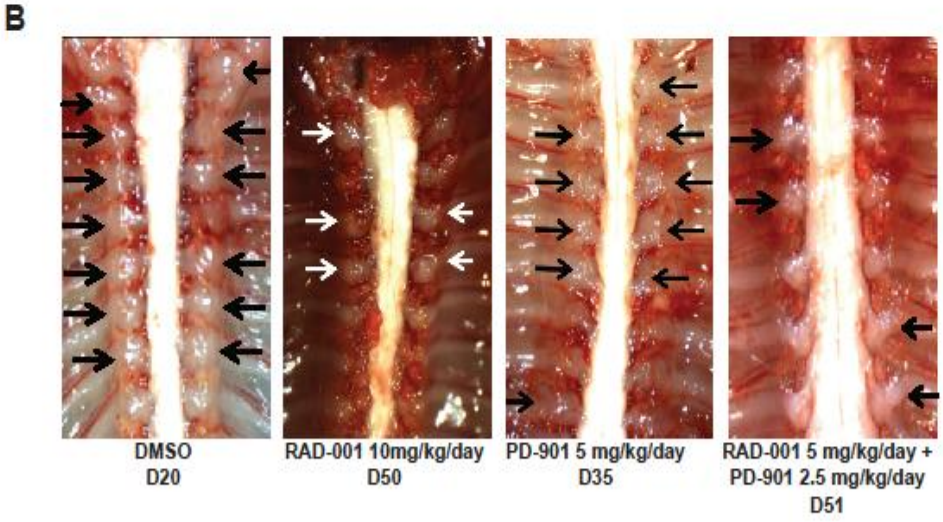
B
DMSO
D20
RAD-001 10mg/kg/day
D50
PD-901 5 mg/kg/day
D35
RAD-001 5 mg/kg/day +
PD-901 2.5 mg/kg/day
D51

Figure 7: Treatment with RAD-001 or PD-901 as single agents is effective at early time points, but resistance develops at later time points. A. Western blot analysis of p-AKT and p-4EBP in DRG tumors from animals treated with DMSO or RAD-001 at early and later time points. B. Quantification of the western blot in A shows that at early time points, RAD-001 effectively reduces p-AKT levels, but at later time points, the level of p-AKT is very high. C. Quantification of the western blot in A shows that at early time points, RAD-001 also effectively reduces p-4EBP levels, but at later time points, the level of p-4EBP is very high, suggesting the development of resistance to RAD-001 treatment. D. Western blot analysis of p-ERK levels in DRG tumors from animals treated with DMSO or PD-901 at early and later time points. E. Quantification of the western blot in D shows that at early time points, p-ERK is inhibited, but at later time points the level of p-ERK increases suggesting that these mice are becoming resistant to PD-901 treatment.

Figure 7

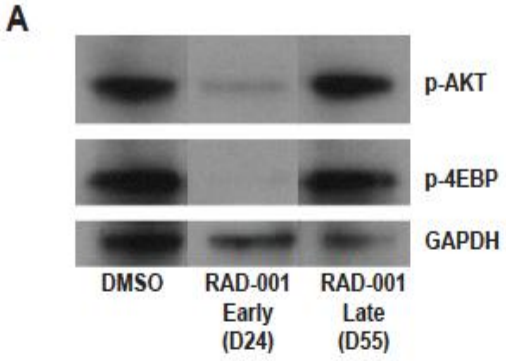
A
p-AKT
p-4EBP
GAPDH
DMSO
RAD-001 Early (D24)
RAD-001 Late (D55)

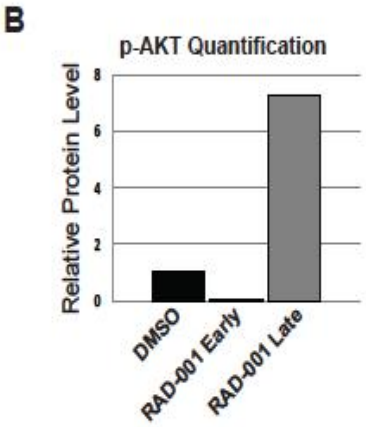
B
p-AKT Quantification
Relative Protein Level
0
2
4
6
8
DMSO
RAD-001 Early
RAD-001 Late

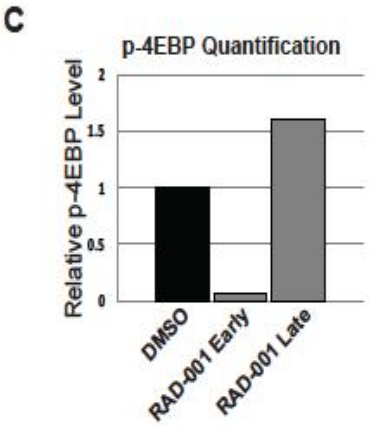
C
p-4EBP Quantification
Relative p-4EBP Level
0
0.5
1
1.5
2
DMSO
RAD-001 Early
RAD-001 Late

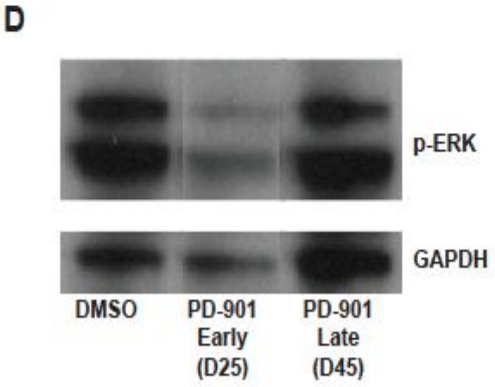
D
p-ERK
GAPDH
DMSO
PD-901 Early (D25)
PD-901 Late (D45)

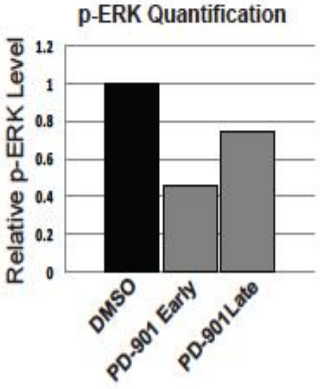
E
p-ERK Quantification
Relative p-ERK Level
0
0.2
0.4
0.6
0.8
1
1.2
DMSO
PD-901 Early
PD-901 Late

Figure 8: Treating mice with a combination of RAD-001 and PD-901 results in persistent and prolonged inhibition of signaling through the MAPK and PI3K pathways. A. Western blot analysis of DRG tumors treated with DMSO, RAD-001, PD-901, or a combination of RAD-001 and PD-901 at late time points. B. Quantification of western blot shown in A demonstrates that at late time points, the level of p-AKT is elevated in RAD-001 treated animals, but remains low when animals are treated with a combination of RAD-001 and PD-901. C. Similarly, the level of p-4EBP remains lowest when mice are given the combination treatment. D. p-ERK levels also remain lowest when mice are given RAD-001 and PD-901 in combination.

Figure 8

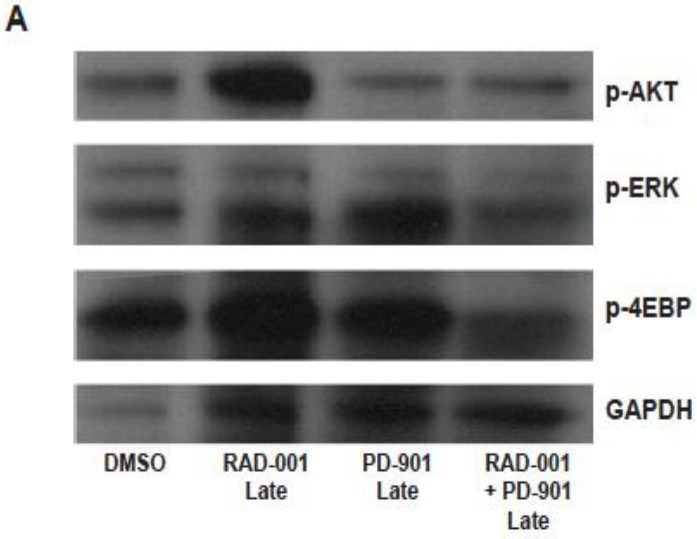
A
p-AKT
p-ERK
p-4EBP
GAPDH
DMSO
RAD-001 Late
PD-901 Late
RAD-001 + PD-901 Late
B
p-AKT Quantification
Relative Protein Level
2
1.5
1
0.5
0
DMSO
RAD001
PD-901
RAD001+ PD-901
C
p-4EBP Quantification
Relative Protein Level
1.2
1
0.8
0.6
0.4
0.2
0
DMSO
RAD001
PD-901
RAD001+ PD-901
D
p-ERK Quantification
Relative Protein Level
1.2
1
0.8
0.6
0.4
0.2
0
DMSO
RAD001
PD-901
RAD001+ PD-901

Chapter 4: Conclusions and Future Directions

I. *Sleeping Beauty* mutagenesis has uncovered novel genes, pathways, and drug targets for Schwann cell tumors

The *Sleeping Beauty* (*SB*) screen that we performed identified hundreds of genes that are predicted to drive the formation, progression, and maintenance of neurofibromas and malignant peripheral nerve sheath tumors (MPNSTs) (Rahrmann et al., 2013). From these genes, we were able to validate the contribution that many played in both human and mouse Schwann cell tumorigenesis, identify the corresponding pathways that were modulated by these genetic changes, and use this information to design rational targeted therapies.

Many genes that were identified by *SB* mutagenesis play a role in the Wnt/β-Catenin signaling pathway (Watson et al., 2013). These genes included tumor suppressor genes that were disrupted by the *T2/Onc* mutagenic transposon such as *Axin and Gsk3β* and oncogenes that were activated by *T2/Onc* such as *Tnks* (Watson et al., 2013). Once we had identified these genes, we verified that Wnt signaling was in fact activated in many human MPNSTs (Watson et al., 2013). Further, we showed that that activating Wnt signaling in immortalized human Schwann cells was sufficient to induce transformative properties to these cells, and that inhibiting Wnt signaling in human MPNST cell lines was sufficient to reduce the oncogenic phenotype of these cells (Watson et al., 2013). In addition, genetically inhibiting Wnt signaling reduced tumor growth in MPNST

xenograft models (Watson et al., 2013). Based on these genetic data, we hypothesized that pharmacological inhibition of Wnt signaling may be effective in preclinical models of MPNSTs (Watson et al., 2013). We found that MPNST cell lines are much more sensitive to small molecules that inhibit Wnt signaling than are immortalized human Schwann cells (Watson et al., 2013). Further, after screening for other small molecule inhibitors that synergize with Wnt inhibitors, we identified RAD-001, and mTOR inhibitor that is currently in clinical trials for Schwann cell tumors (Watson et al., 2013). The combination of Wnt and mTOR pathway inhibition dramatically induced MPNST cell death, and may be potential avenues for targeted therapy in the clinic (Watson et al., 2013).

Another interesting finding that came out of the *SB* screen was the implication of both PI3K/AKT/mTOR and MAPK signaling pathways in the progression from neurofibromas to MPNST (Rahrmann et al., 2013). While both of these pathways have been implicated in Schwann cell tumors, the *SB* screen showed that while benign neurofibromas has *SB* insertions in either *Nf1*, a negative regulator of MAPK signaling, or *Pten*, a negative regulator of PI3k/AKT/mTOR signaling, nearly every tumor that had co-insertions in *Nf1* and *Pten*, were MPNSTs (Keng et al., 2012a). This observation led us to design and create two new genetically engineered mouse models of MPNSTs (Keng et al., 2012a; Keng et al., 2012b). The first model used the *Dessert Hedgehog (Dhh)* promoter to drive *Cre Recombinase (Cre)* expression in Schwann cells and their

precursors, which then resulted in the biallelic deletion of both *Nf1* and *Pten* (Jaegle et al., 2003; Keng et al., 2012a; Xiao et al., 2005; Zhu et al., 2005). This mouse model resulted in severe peripheral nerve disease, with greater than 20 tumors per animal, hyperplastic peripheral nerves, problems with mobility and coordination, and a highly reduced lifespan of approximately 15 days (Keng et al., 2012a). In an attempt to model spontaneous MPNSTs that do not occur in the context of NF1, we designed a mouse model in which *Dhh-Cre* was used to biallelically knock out *Pten*, in the context of EGFR overexpression (Jaegle et al., 2003; Keng et al., 2012b; Ling et al., 2005; Xiao et al., 2005). This mouse model also resulted in severe peripheral nerve disease, with 10-15 tumors per animal, hyperplastic peripheral nerves, problems with mobility and coordination, and a highly reduced lifespan of approximately 28 days (Keng et al., 2012b).

After validating the importance of activation of PI3K/AKT/mTOR and MAPK signaling by creating two new genetically engineered mouse models, we hypothesized that since activation of both of these pathways leads to the formation of MPNSTs, then co-targeting both of these pathways may be effective in treating MPNSTs. To this end, we found that *in vitro*, the mTOR inhibitor, RAD-001, and the MAPK inhibitor, PD-901 were both effective at inhibiting cellular proliferation in 5 MPNST cell lines at relatively low concentrations, with little effect on immortalized human Schwann cells. Further, RAD-001 and PD-

901 function synergistically in MPNST cell lines to inhibit proliferation and induce apoptosis.

To further investigate co-targeting the PI3K/AKT/mTOR and MAPK pathways as therapeutic targets in Schwann cell tumors, we conducted a preclinical study using RAD-001and PD-901 in the two new mouse models of MPNSTs that were developed in our lab (Keng et al., 2012a; Keng et al., 2012b). We found that both RAD-001 and PD-901 were effective as single agents in the NF1-associated and spontaneous mouse models at increasing survival and reducing tumor burden and/or grade. Unfortunately, but consistent with other studies, we found that mice soon developed resistance to treatment with single agents, and the respective signaling pathway that was targeted would become re-activated with long-term treatment. In an attempt to avoid resistance and find a more effective treatment for MPNSTs, we tested the efficacy of blocking both pathways by using RAD-001 and PD-901 in combination. In both models, the combination was much more effective at reducing peripheral nerve disease. While survival was similar to single agent treatments, there were much fewer tumors, which were much smaller than seen when RAD-001 or PD-901 were used alone. In the spontaneous MPNST mouse model, tumor grade was dramatically reduced with the combination treatment.

The findings of the *SB* screen described above resulted in the identification of hundreds of genes that may play a role in Schwann cell

tumorigenesis (Rahrmann et al., 2013). From this large gene list, we have identified and validated the contribution of 3 signaling pathways, namely the Wnt/β-catenin, PI3K/AKT/mTOR, and MPAK pathways as being important in tumor initiation, progression and maintenance (Keng et al., 2012a; Keng et al., 2012b; Watson et al., 2013). Importantly, these pathways are all able to be targeted with small molecule inhibitors, and have shown efficacy in preclinical studies for MPNSTs (Curtin and Lorenzi, 2010; Grant, 2008; Watson et al., 2013). In addition to the data presented here, there are many other genes that have come out of the *SB* screen that are being studied for their potential contribution and therapeutic impact in Schwann cell tumors (Rahrmann et al., 2013). These include *Caveolin-1,* a known tumor suppressor gene in other tumor types, which may regulate growth factor receptor trafficking, and *FoxR2,* a transcription factor that may have influence the gene expression of a wide variety of genes, some of which may be targetable by drugs (Rahrmann et al., 2013).

II. Targeted therapies are likely to make progress clinically in treating Schwann cell tumors

The current standard treatment for Schwann cell tumors is surgery, non-specific chemotherapy, and high dose radiation (Widemann, 2009). These treatments have been largely ineffective, and the 5-year survival rate for MPNSTs is less than 25% (Widemann, 2009). In addition, MPNSTs remain the leading

cause of death for patients with NF1 (Widemann, 2009). These data exemplify the need for new, better treatments for patients, and targeted therapies may hold the key for treating these deadly tumors.

Unfortunately, to date, no targeted therapies that have entered clinical trials for neurofibromas or MPNSTs have been as successful as hoped for (Packer and Rosser, 2002; Widemann, 2009). These include the phase II clinical trial of either the maturation agent *cis*-retinoic acid or the anti-angiogenic interferon-α, in which 86% of patients on retinoic acid and 96% of patients on interferon-α were stable, but no patients demonstrated a radiographic response. (Packer et al., 2002). Another anti-angiogenic agent, thalidomide entered a phase I clinical trial, although out of 20 patients, only 4 patients showed a decrease in tumor size, and five patients had symptomatic improvements (Gupta et al., 2003). Another phase I clinical trial tested the use of a farnesyl protein transferase inhibitor, in an attempt to block the function of RAS proteins and no patients showed a radiographic response (Yan et al., 1995).

The results of these clinical trials has demonstrated the urgent need to both identify better drugable targets, as well as design better drugs to target the molecular changes seen in these tumors (Packer and Rosser, 2002). With the advent and implementation of new technologies to understand the changes that occur in normal Schwann cells as they become malignant, it is highly likely that

new, more effective targeted therapies will become available in the near future. Method such as gene expression microarrays, whole exome sequencing, methylome analysis and RNA sequencing are being implemented in the clinic for many tumor types, including Schwann cell tumors (Feber et al., 2011; Hummel et al., 2010; Kobayashi et al., 2006; Lee et al., 2004; Levy et al., 2004; Miller et al., 2009; Miller et al., 2006). With this technology advancing, and methods to quickly and efficiently analyze the large amount of data that is generated, personalized medicine is becoming a reality (Gonzalez de Castro et al., 2013). It is the hope of doctors and researchers, that for each tumor biopsied in the clinic, an analysis of the molecular changes will be conducted, the changes that can be targeted by drugs and biologic therapies will be identified, and the efficacy of these targeted therapies will dramatically improve tumor response and quality of life for patients (Gonzalez de Castro et al., 2013).

III. New avenues to explore in the treatment of Schwann cell tumors

While targeted therapies hold the promise of better and more effective ways to treat Schwann cell tumors, there are many new avenues that need to be explored in treating these aggressive and deadly tumors. For example, improving methods to identify and diagnose these tumors is critical (Akin et al., 2012). The earlier tumors can be identified, the sooner therapeutic intervention can be implemented, and the better chance these patients have for survival (Akin et al., 2012). If benign neurofibromas can be detected early, they can be monitored for

changes, so that progression can be detected and managed early. Further, if diagnostic methods can be improved, plexiform neurofibromas can more easily be detected, as these neurofibromas are much more likely to progress.

In addition to identifying these tumors early, it is critical to have better diagnostic markers to both identify tumors as Schwann cell-derived tumor and characterize these tumors molecularly to determine treatments that are likely to be more effective. For example, many MPNSTs are chemotherapy and radiation resistant, and if there were diagnostic markers to suggest that a specific tumor may not respond well to these treatments, other therapies could be pursued (Packer et al., 2002; Widemann, 2009). This would also limit the number of chemotherapy and radiation-induced mutations that can drive plexiform neurofibromas into malignant transformation, or make MPNSTs more aggressive (Packer and Rosser, 2002).

New technologies to molecularly characterize tumors are becoming widely available and are being implemented in the clinic for many tumor types, including Schwann cell tumors. These methods include gene expression microarray analysis, whole exome sequencing, methylome analysis and RNA-sequencing (Feber et al., 2011; Hummel et al., 2010; Kobayashi et al., 2006; Lee et al., 2004; Levy et al., 2004; Miller et al., 2009; Miller et al., 2006). With these methods, one can identify the molecular changes that occur in a tumor and may function to drive tumorigenesis, such as gene overexpression, gene mutations, alternatively

spliced gene products, and gene copy number changes. Once these changes are identified, molecularly targeted therapies can be implemented. For example, if a tumor begins abnormally expressing a growth factor receptor, such as the case of *EGFR* expression in nearly 75% of MPNSTs, patients could be given Erlotinib, a monoclonal antibody that targets *EGFR* (Holtkamp et al., 2008). This type of personalized medicine will likely be a very effective way to implement targeted therapies in the clinic (Gonzalez de Castro et al., 2013).

In addition to identifying molecular targets in tumors, there are many ways to improve targeted therapies that are currently available or being developed. For example, toxicity remains a problem in patients that are given small molecule inhibitors, and more research defining what causes this toxicity and how to avoid it is needed. The most problematic aspect of targeted therapy is the development of resistance, which almost always occurs when a single targeted agent is given (Ellis and Hicklin, 2009; Sierra et al., 2010). Research on the mechanism of resistance is ongoing and needs to continue so that targeted therapies or combination of targeted therapies can be developed that avoid this phenomenon (Ellis and Hicklin, 2009). Finally, the use of targeted therapies in combination with chemotherapy has been largely understudied. With the design of clinical trials in the U.S., it is likely that any targeted therapy that will be used in the clinic to treat Schwann cell tumors will be given in combination with the current standard of therapy, which is chemotherapy. The effect of these combinations

needs to be further investigated to determine targeted therapies that work as well or better in the context of non-specific chemotherapy for the benefit of patients.

Another avenue of clinical investigation for Schwann cell tumors is targeting tumor-associated cells and the tumor stroma. The contribution of normal cells to tumor growth and progression is becoming quite clear, and targeting these cellular interactions has been an effective method for the treatment of several tumor types (Hanahan and Weinberg, 2011). For example, neurofibromas have been shown to be composed of both tumor cells and fibroblasts, and gene expression microarray shows overexpression of fibroblast growth factor and platelet-derived growth factor in several plexiform neurofibromas (Brossier and Carroll, 2012; Packer et al., 2002). In addition, these tumors have an abundant extracellular matrix composed of collagen fibers (Packer et al., 2002). Based on these observations, 5-methyl-1-phenyl-2-(I*H*)-pyridone (Pirfenidone), an antifibrotic drug that inhibits cytokines and inhibits the growth of fibroblasts has been used in both Phase I and Phase II clinical trials for plexiform neurofibromas (Gurujeyalakshmi et al., 1999; Iyer et al., 1999; Raghu et al., 1999). Of 24 patients, 4 patients had a 15% or more decrease in tumor volume by three-dimensional MRI, and 17 patients remained stable (Babovic-Vuksanovic et al., 2006; Babovic-Vuksanovic et al., 2007). We have recently observed that murine Schwann cell tumors are extremely hypovascular with collapsed blood vessels with no clear luminal space (unpublished data). This finding may explain why

these tumors are highly resistant to both chemo- and targeted therapies. Further, we found that these murine tumors stain highly positive for hyluronic acid (HA). It has been show that the hypovascularity and non-functional vessel phenotype seen in mouse models of pancreatic cancer are also due to the high expression of HA, and can be targeted by a drug that breaks down HA, resulting in an increase in functional blood vessels and improved efficacy of chemotherapeutic agents to treat these tumors (Provenzano et al., 2012). Targeting the tumor stroma is an interesting avenue of therapy that will continue to be pursued in the future.

The interaction between the immune system and cancer has been recognized for a long time, and immunotherapy is becoming widely used in cancer treatment (Miller et al., 2013). The contribution of the immune system to cancer was first recognized when it was shown that mice deficient for the Recombinase-activating gene (*Rag2*) are unable to rearrange antigen receptors and are therefore functionally T and B cell deficient and have a higher susceptibility to cancer (Shankaran et al., 2001). Another study showed that colorectal cancer can be stratified based on the number of immune cells within a tumor, and this stratification correlates with survival (Galon et al., 2006). With the importance of the immune system established, many therapies that target the immune system have emerged. There are two general types of immunotherapy: to enhance a pre-existing immune response, and to create a *de novo* immune response. Enhancing pre-existing immune response can be done by using drugs

that inhibit immune system checkpoints such as CTLA4 or PD-1 inhibitors (Hodi et al., 2010; Topalian et al., 2012). The CTLA4 inhibitor, ipilimumab was FDA approved in 2011 for malignant melanoma, a tumor type that has been shown to be highly immunogenic, although this type of therapy often shows toxicity in patients due to an enhancement of all T cells, not just tumor specific lymphocytes (Hodi et al., 2010). A more novel type of immunotherapy involves creating a *de novo* immune response that is tumor specific, such as cancer vaccines and adoptive immunotherapy (Kantoff et al., 2010). Cancer vaccines drive tumor specific T cell responses *in vivo*, but despite much effort, the only successful vaccine has been Provenge which was recently FDA approved for prostate cancer (Kantoff et al., 2010). Adoptive immunotherapy is the infusion of T cells into the patient which have been manipulated *ex vivo* (Payne et al., 2012). A hallmark example of adoptive immunotherapy is the use of chimeric antigen receptors (CARs) to treat B cell malignancies. CARs are genetically engineered T cells that have an artificial, high affinity receptor for B cells (Porter et al., 2011). The result of CAR therapy is the complete loss of B cells in the patient, and has been a very effective therapy for B cell malignancies (Porter et al., 2011). Adoptive immunotherapy can also be performed by autologous transplant of tumor infiltrating lymphocytes (TILs) (Restifo et al., 2012). This type of immunotherapy involves culturing T cells from a patient's tumor *ex vivo*, expanding T cells in culture, irradiating the patient, and re-infusing the T cells back into the patient

(Restifo et al., 2012). TIL therapy has been quite successful in malignant melanoma, with 30% of patients surviving greater than 5 years (Rosenberg, 2011). While immunotherapy has yet to be tried in Schwann cell tumors, these tumors may be good candidates for this type of therapy. It has been widely demonstrated that neurofibromas and MPNSTs are characterized by mast cell infiltration, suggesting that the immune system does in fact play a role in this type of cancer, and immune checkpoint inhibitors may be efficacious in enhancing a preexisting immune response (Levy et al., 2004; Zhu et al., 2002). Further, whole exome sequencing has demonstrated that these tumors have a number of mutations that could potentially be used to develop a cancer vaccine against (Brekke et al., 2010; Frahm et al., 2004; Kobayashi et al., 2006). With advances in immunotherapy being rapidly made, this type of cancer therapy may show promise for treating Schwann cell tumors in the future.

IV. Summary

Despite decades of research on Schwann cell tumors, MPNSTs continue to have very poor 5-year survival rates and are the leading cause of death in patients with NF1. A major difficulty in treating these tumors is due to lack of complete understanding of the genetic drivers of Schwann cell tumors, and currently, there are no effective targeted therapies available for these tumors. Using the *SB* system in mice, we identified hundreds of genes that could potentially be drivers of Schwann cell tumor initiation, progression, and maintenance. Among these genes,

the canonical Wnt/b-catenin, mTOR/PI3K/AKT and MAPK pathways were highly represented, and often found co-mutated. Here, I have demonstrated the identification and validation of canonical Wnt/β-catenin signaling in human neurofibromas and MPNSTs. This pathway has shown pre-clinical efficacy when inhibited alone and in combination with mTOR inhibition, where co-targeting these pathways induces cell death. I have also demonstrated the importance of co-targeting the mTOR/PI3K/AKT and MAPK pathways in both a panel of human MPNST cell lines, and in two genetically engineered mousse models of Schwann cell tumors. The combination therapy of RAD-001 and PD-901 not only extends lifespan and reduces tumor burden, but also avoids the rapid development of resistance that is seen when single therapies are used. The data presented here gives pre-clinical evidence for the use of novel targeted therapy combinations that will hopefully have success in clinical trials that is desperately needed for patients suffering from Schwann cell tumors.

Bibliography

Adams, G. P., and Weiner, L. M. (2005). Monoclonal antibody therapy of cancer. Nature biotechnology *23*, 1147-1157.

Akin, O., Brennan, S. B., Dershaw, D. D., Ginsberg, M. S., Gollub, M. J., Schoder, H., Panicek, D. M., and Hricak, H. (2012). Advances in oncologic imaging: update on 5 common cancers. CA: a cancer journal for clinicians *62*, 364-393.

Albertson, D. G., Collins, C., McCormick, F., and Gray, J. W. (2003). Chromosome aberrations in solid tumors. Nature genetics *34*, 369-376.

Ames, B. N. (1979). Identifying environmental chemicals causing mutations and cancer. Science *204*, 587-593.

Armitage, P., and Doll, R. (2004). The age distribution of cancer and a multi-stage theory of carcinogenesis. British journal of cancer *91*, 1983-1989.

Babovic-Vuksanovic, D., Ballman, K., Michels, V., McGrann, P., Lindor, N., King, B., Camp, J., Micic, V., Babovic, N., Carrero, X., *et al.* (2006). Phase II trial of pirfenidone in adults with neurofibromatosis type 1. Neurology *67*, 1860-1862.

Babovic-Vuksanovic, D., Widemann, B. C., Dombi, E., Gillespie, A., Wolters, P. L., Toledo-Tamula, M. A., O'Neill, B. P., Fox, E., MacDonald, T., Beck, H., and Packer, R. J. (2007). Phase I trial of pirfenidone in children with neurofibromatosis 1 and plexiform neurofibromas. Pediatric neurology *36*, 293-300.

Badache, A., and De Vries, G. H. (1998). Neurofibrosarcoma-derived Schwann cells overexpress platelet-derived growth factor (PDGF) receptors and are induced to proliferate by PDGF BB. Journal of cellular physiology *177*, 334-342.

Bain, J., Plater, L., Elliott, M., Shpiro, N., Hastie, C. J., McLauchlan, H., Klevernic, I., Arthur, J. S., Alessi, D. R., and Cohen, P. (2007). The selectivity of protein kinase inhibitors: a further update. The Biochemical journal *408*, 297-315.

Barker, N. (2008). The canonical Wnt/beta-catenin signalling pathway. Methods in molecular biology *468*, 5-15.

Bergers, G., and Benjamin, L. E. (2003). Tumorigenesis and the angiogenic switch. Nature reviews Cancer *3*, 401-410.

Bhatheja, K., and Field, J. (2006). Schwann cells: origins and role in axonal maintenance and regeneration. The international journal of biochemistry & cell biology *38*, 1995-1999.

Biechele, T. L., Adams, A. M., and Moon, R. T. (2009). Transcription-based reporters of Wnt/beta-catenin signaling. Cold Spring Harbor protocols *2009*, pdb prot5223.

Bignell, G. R., Greenman, C. D., Davies, H., Butler, A. P., Edkins, S., Andrews, J. M., Buck, G., Chen, L., Beare, D., Latimer, C., *et al.* (2010). Signatures of mutation and selection in the cancer genome. Nature *463*, 893-898.

Bird, A. (2007). Perceptions of epigenetics. Nature *447*, 396-398.

Blasco, M. A. (2005). Telomeres and human disease: ageing, cancer and beyond. Nature reviews Genetics *6*, 611-622.

Brawer, M. K. (2006). Hormonal therapy for prostate cancer. Reviews in urology *8 Suppl 2*, S35-47.

Brekke, H. R., Ribeiro, F. R., Kolberg, M., Agesen, T. H., Lind, G. E., Eknaes, M., Hall, K. S., Bjerkehagen, B., van den Berg, E., Teixeira, M. R., *et al.* (2010). Genomic changes in chromosomes 10, 16, and X in malignant peripheral nerve sheath tumors identify a high-risk patient group. Journal of clinical oncology : official journal of the American Society of Clinical Oncology *28*, 1573-1582.

Brems, H., Beert, E., de Ravel, T., and Legius, E. (2009). Mechanisms in the pathogenesis of malignant tumours in neurofibromatosis type 1. The lancet oncology *10*, 508-515.

Brossier, N. M., and Carroll, S. L. (2012). Genetically engineered mouse models shed new light on the pathogenesis of neurofibromatosis type I-related neoplasms of the peripheral nervous system. Brain research bulletin *88*, 58-71.

Bucci, M. K., Bevan, A., and Roach, M., 3rd (2005). Advances in radiation therapy: conventional to 3D, to IMRT, to 4D, and beyond. CA: a cancer journal for clinicians *55*, 117-134.

Cappuzzo, F., Hirsch, F. R., Rossi, E., Bartolini, S., Ceresoli, G. L., Bemis, L., Haney, J., Witta, S., Danenberg, K., Domenichini, I., *et al.* (2005). Epidermal growth factor receptor gene and protein and gefitinib sensitivity in non-small-cell lung cancer. Journal of the National Cancer Institute *97*, 643-655.

Carli, M., Ferrari, A., Mattke, A., Zanetti, I., Casanova, M., Bisogno, G., Cecchetto, G., Alaggio, R., De Sio, L., Koscielniak, E., *et al.* (2005). Pediatric malignant peripheral nerve sheath tumor: the Italian and German soft tissue sarcoma cooperative group. Journal of clinical oncology : official journal of the American Society of Clinical Oncology *23*, 8422-8430.

Carroll, S. L. (2012). Molecular mechanisms promoting the pathogenesis of Schwann cell neoplasms. Acta neuropathologica *123*, 321-348.

Carroll, S. L., and Ratner, N. (2008). How does the Schwann cell lineage form tumors in NF1? Glia *56*, 1590-1605.

Chappell, W. H., Steelman, L. S., Long, J. M., Kempf, R. C., Abrams, S. L., Franklin, R. A., Basecke, J., Stivala, F., Donia, M., Fagone, P., *et al.* (2011). Ras/Raf/MEK/ERK and PI3K/PTEN/Akt/mTOR inhibitors: rationale and importance to inhibiting these pathways in human health. Oncotarget *2*, 135-164.

Chiang, G. G., and Abraham, R. T. (2007). Targeting the mTOR signaling network in cancer. Trends in molecular medicine *13*, 433-442.

Cichowski, K., and Jacks, T. (2001). NF1 tumor suppressor gene function: narrowing the GAP. Cell *104*, 593-604.

Cichowski, K., Shih, T. S., Schmitt, E., Santiago, S., Reilly, K., McLaughlin, M. E., Bronson, R. T., and Jacks, T. (1999). Mouse models of tumor development in neurofibromatosis type 1. Science *286*, 2172-2176.

Collier, L. S., and Largaespada, D. A. (2005). Hopping around the tumor genome: transposons for cancer gene discovery. Cancer research *65*, 9607-9610.

Croce, C. M. (2008). Oncogenes and cancer. The New England journal of medicine *358*, 502-511.

Cui, W., Taub, D. D., and Gardner, K. (2007). qPrimerDepot: a primer database for quantitative real time PCR. Nucleic acids research *35*, D805-809.

Curtin, J. C., and Lorenzi, M. V. (2010). Drug discovery approaches to target Wnt signaling in cancer stem cells. Oncotarget *1*, 563-577.

D'Andrea, A. D. (2010). Susceptibility pathways in Fanconi's anemia and breast cancer. The New England journal of medicine *362*, 1909-1919.

Dahlberg, W. K., Little, J. B., Fletcher, J. A., Suit, H. D., and Okunieff, P. (1993). Radiosensitivity in vitro of human soft tissue sarcoma cell lines and skin fibroblasts derived from the same patients. International journal of radiation biology *63*, 191-198.

Dai, M., Wang, P., Boyd, A. D., Kostov, G., Athey, B., Jones, E. G., Bunney, W. E., Myers, R. M., Speed, T. P., Akil, H., *et al.* (2005). Evolving gene/transcript definitions significantly alter the interpretation of GeneChip data. Nucleic acids research *33*, e175.

Daub, H., Specht, K., and Ullrich, A. (2004). Strategies to overcome resistance to targeted protein kinase inhibitors. Nature reviews Drug discovery *3*, 1001-1010.

de Vries, A., Flores, E. R., Miranda, B., Hsieh, H. M., van Oostrom, C. T., Sage, J., and Jacks, T. (2002). Targeted point mutations of p53 lead to dominant-negative inhibition of wild-type p53 function. Proceedings of the National Academy of Sciences of the United States of America *99*, 2948-2953.

DeRycke, M. S., Andersen, J. D., Harrington, K. M., Pambuccian, S. E., Kalloger, S. E., Boylan, K. L., Argenta, P. A., and Skubitz, A. P. (2009). S100A1 expression in ovarian and endometrial endometrioid carcinomas is a prognostic indicator of relapse-free survival. American journal of clinical pathology *132*, 846-856.

DeVita, V. T., Jr., and Chu, E. (2008). A history of cancer chemotherapy. Cancer research *68*, 8643-8653.

Downward, J. (2003). Targeting RAS signalling pathways in cancer therapy. Nature reviews Cancer *3*, 11-22.

Dupuy, A. J., Rogers, L. M., Kim, J., Nannapaneni, K., Starr, T. K., Liu, P., Largaespada, D. A., Scheetz, T. E., Jenkins, N. A., and Copeland, N. G. (2009). A modified sleeping beauty transposon system that can be used to model a wide variety of human cancers in mice. Cancer research *69*, 8150-8156.

Eisen, H. J., Tuzcu, E. M., Dorent, R., Kobashigawa, J., Mancini, D., Valantine-von Kaeppler, H. A., Starling, R. C., Sorensen, K., Hummel, M., Lind, J. M., *et al.* (2003). Everolimus for the prevention of allograft rejection and vasculopathy in cardiac-transplant recipients. The New England journal of medicine *349*, 847-858.

Ellis, L. M., and Hicklin, D. J. (2009). Resistance to Targeted Therapies: Refining Anticancer Therapy in the Era of Molecular Oncology. Clinical cancer research : an official journal of the American Association for Cancer Research *15*, 7471-7478.

Emami, K. H., Nguyen, C., Ma, H., Kim, D. H., Jeong, K. W., Eguchi, M., Moon, R. T., Teo, J. L., Kim, H. Y., Moon, S. H., *et al.* (2004). A small molecule inhibitor of beta-catenin/CREB-binding protein transcription [corrected]. Proceedings of the National Academy of Sciences of the United States of America *101*, 12682-12687.

Esteller, M. (2008). Epigenetics in cancer. The New England journal of medicine *358*, 1148-1159.

Fearon, E. R. (2011). Molecular genetics of colorectal cancer. Annual review of pathology *6*, 479-507.

Feber, A., Wilson, G. A., Zhang, L., Presneau, N., Idowu, B., Down, T. A., Rakyan, V. K., Noon, L. A., Lloyd, A. C., Stupka, E., *et al.* (2011). Comparative methylome analysis of benign and malignant peripheral nerve sheath tumors. Genome research *21*, 515-524.

Ferner, R. E. (2010). The neurofibromatoses. Practical neurology *10*, 82-93.

Fletcher, J. A., Kozakewich, H. P., Hoffer, F. A., Lage, J. M., Weidner, N., Tepper, R., Pinkus, G. S., Morton, C. C., and Corson, J. M. (1991). Diagnostic relevance of clonal cytogenetic aberrations in malignant soft-tissue tumors. The New England journal of medicine *324*, 436-442.

Frahm, S., Mautner, V. F., Brems, H., Legius, E., Debiec-Rychter, M., Friedrich, R. E., Knofel, W. T., Peiper, M., and Kluwe, L. (2004). Genetic and phenotypic characterization of tumor cells derived from malignant peripheral nerve sheath tumors of neurofibromatosis type 1 patients. Neurobiology of disease *16*, 85-91.

Franz, D. N., and Weiss, B. D. (2012). Molecular therapies for tuberous sclerosis and neurofibromatosis. Current neurology and neuroscience reports *12*, 294-301.

Galon, J., Costes, A., Sanchez-Cabo, F., Kirilovsky, A., Mlecnik, B., Lagorce-Pages, C., Tosolini, M., Camus, M., Berger, A., Wind, P., *et al.* (2006). Type, density, and location of immune cells within human colorectal tumors predict clinical outcome. Science *313*, 1960-1964.

Gambacorti-Passerini, C. B., Gunby, R. H., Piazza, R., Galietta, A., Rostagno, R., and Scapozza, L. (2003). Molecular mechanisms of resistance to imatinib in Philadelphia-chromosome-positive leukaemias. The lancet oncology *4*, 75-85.

Gehrke, I., Gandhirajan, R. K., and Kreuzer, K. A. (2009). Targeting the WNT/beta-catenin/TCF/LEF1 axis in solid and haematological cancers: Multiplicity of therapeutic options. European journal of cancer *45*, 2759-2767.

Gera, J. F., Mellinghoff, I. K., Shi, Y., Rettig, M. B., Tran, C., Hsu, J. H., Sawyers, C. L., and Lichtenstein, A. K. (2004). AKT activity determines sensitivity to mammalian target of rapamycin (mTOR) inhibitors by regulating cyclin D1 and c-myc expression. The Journal of biological chemistry *279*, 2737-2746.

Gerlinger, M., Rowan, A. J., Horswell, S., Larkin, J., Endesfelder, D., Gronroos, E., Martinez, P., Matthews, N., Stewart, A., Tarpey, P., *et al.* (2012). Intratumor heterogeneity and branched evolution revealed by multiregion sequencing. The New England journal of medicine *366*, 883-892.

Gilman, A. (1963). The initial clinical trial of nitrogen mustard. American journal of surgery *105*, 574-578.

Gonsalves, F. C., Klein, K., Carson, B. B., Katz, S., Ekas, L. A., Evans, S., Nagourney, R., Cardozo, T., Brown, A. M., and DasGupta, R. (2011). An RNAi-based chemical genetic screen identifies three small-molecule inhibitors of the Wnt/wingless signaling pathway. Proceedings of the National Academy of Sciences of the United States of America *108*, 5954-5963.

Gonzalez de Castro, D., Clarke, P. A., Al-Lazikani, B., and Workman, P. (2013). Personalized cancer medicine: molecular diagnostics, predictive biomarkers, and drug resistance. Clinical pharmacology and therapeutics *93*, 252-259.

Grant, S. (2008). Cotargeting survival signaling pathways in cancer. The Journal of clinical investigation *118*, 3003-3006.

Gregorian, C., Nakashima, J., Dry, S. M., Nghiemphu, P. L., Smith, K. B., Ao, Y., Dang, J., Lawson, G., Mellinghoff, I. K., Mischel, P. S., *et al.* (2009). PTEN dosage is essential for neurofibroma development and malignant transformation. Proceedings of the National Academy of Sciences of the United States of America *106*, 19479-19484.

Gupta, A., Cohen, B. H., Ruggieri, P., Packer, R. J., and Phillips, P. C. (2003). Phase I study of thalidomide for the treatment of plexiform neurofibroma in neurofibromatosis 1. Neurology *60*, 130-132.

Gurk-Turner, C., Manitpisitkul, W., and Cooper, M. (2012). A comprehensive review of everolimus clinical reports: a new mammalian target of rapamycin inhibitor. Transplantation *94*, 659-668.

Gurujeyalakshmi, G., Hollinger, M. A., and Giri, S. N. (1999). Pirfenidone inhibits PDGF isoforms in bleomycin hamster model of lung fibrosis at the translational level. The American journal of physiology *276*, L311-318.

Gutmann, D. H., Hunter-Schaedle, K., and Shannon, K. M. (2006). Harnessing preclinical mouse models to inform human clinical cancer trials. The Journal of clinical investigation *116*, 847-852.

Hanahan, D., and Weinberg, R. A. (2000). The hallmarks of cancer. Cell *100*, 57-70.

Hanahan, D., and Weinberg, R. A. (2011). Hallmarks of cancer: the next generation. Cell *144*, 646-674.

Hartline, D. K., and Colman, D. R. (2007). Rapid conduction and the evolution of giant axons and myelinated fibers. Current biology : CB *17*, R29-35.

Hassold, T., and Hunt, P. (2001). To err (meiotically) is human: the genesis of human aneuploidy. Nature reviews Genetics *2*, 280-291.

Henderson, I. C., and Canellos, G. P. (1980). Cancer of the breast: the past decade (first of two parts). The New England journal of medicine *302*, 17-30.

Hirsch, J. (2006). An anniversary for cancer chemotherapy. JAMA : the journal of the American Medical Association *296*, 1518-1520.

Hodi, F. S., O'Day, S. J., McDermott, D. F., Weber, R. W., Sosman, J. A., Haanen, J. B., Gonzalez, R., Robert, C., Schadendorf, D., Hassel, J. C., *et al.* (2010). Improved survival with ipilimumab in patients with metastatic melanoma. The New England journal of medicine *363*, 711-723.

Holtkamp, N., Malzer, E., Zietsch, J., Okuducu, A. F., Mucha, J., Mawrin, C., Mautner, V. F., Schildhaus, H. U., and von Deimling, A. (2008). EGFR and erbB2 in malignant peripheral nerve sheath tumors and implications for targeted therapy. Neuro-oncology *10*, 946-957.

Houlston, R. S., Collins, A., Slack, J., and Morton, N. E. (1992). Dominant genes for colorectal cancer are not rare. Annals of human genetics *56*, 99-103.

Hruban, R. H., Shiu, M. H., Senie, R. T., and Woodruff, J. M. (1990). Malignant peripheral nerve sheath tumors of the buttock and lower extremity. A study of 43 cases. Cancer *66*, 1253-1265.

Hu, T., and Li, C. (2010). Convergence between Wnt-beta-catenin and EGFR signaling in cancer. Molecular cancer *9*, 236.

Huang, L., Snyder, A. R., and Morgan, W. F. (2003). Radiation-induced genomic instability and its implications for radiation carcinogenesis. Oncogene *22*, 5848-5854.

Huang, S. M., Mishina, Y. M., Liu, S., Cheung, A., Stegmeier, F., Michaud, G. A., Charlat, O., Wiellette, E., Zhang, Y., Wiessner, S., *et al.* (2009). Tankyrase inhibition stabilizes axin and antagonizes Wnt signalling. Nature *461*, 614-620.

Hummel, T. R., Jessen, W. J., Miller, S. J., Kluwe, L., Mautner, V. F., Wallace, M. R., Lazaro, C., Page, G. P., Worley, P. F., Aronow, B. J., *et al.* (2010). Gene expression analysis identifies potential biomarkers of neurofibromatosis type 1 including adrenomedullin. Clinical cancer research : an official journal of the American Association for Cancer Research *16*, 5048-5057.

Huson, S. M., Acosta, M. T., Belzberg, A. J., Bernards, A., Chernoff, J., Cichowski, K., Gareth Evans, D., Ferner, R. E., Giovannini, M., Korf, B. R., *et al.* (2011). Back to the future: proceedings from the 2010 NF Conference. American journal of medical genetics Part A *155A*, 307-321.

Ischenko, I., Seeliger, H., Schaffer, M., Jauch, K. W., and Bruns, C. J. (2008). Cancer stem cells: how can we target them? Current medicinal chemistry *15*, 3171-3184.

Iyer, S. N., Gurujeyalakshmi, G., and Giri, S. N. (1999). Effects of pirfenidone on procollagen gene expression at the transcriptional level in bleomycin hamster model of lung fibrosis. The Journal of pharmacology and experimental therapeutics *289*, 211-218.

Jaegle, M., Ghazvini, M., Mandemakers, W., Piirsoo, M., Driegen, S., Levavasseur, F., Raghoenath, S., Grosveld, F., and Meijer, D. (2003). The POU proteins Brn-2 and Oct-6 share important functions in Schwann cell development. Genes & development *17*, 1380-1391.

Jansson, M. D., and Lund, A. H. (2012). MicroRNA and cancer. Molecular oncology *6*, 590-610.

Jessen, K. R., and Mirsky, R. (2005). The origin and development of glial cells in peripheral nerves. Nature reviews Neuroscience *6*, 671-682.

Jessen, W. J., Miller, S. J., Jousma, E., Wu, J., Rizvi, T. A., Brundage, M. E., Eaves, D., Widemann, B., Kim, M. O., Dombi, E., *et al.* (2013). MEK inhibition exhibits efficacy in human and mouse neurofibromatosis tumors. The Journal of clinical investigation *123*, 340-347.

Jiang, B. H., and Liu, L. Z. (2009). PI3K/PTEN signaling in angiogenesis and tumorigenesis. Advances in cancer research *102*, 19-65.

Jin, Y. R., and Yoon, J. K. (2012). The R-spondin family of proteins: emerging regulators of WNT signaling. The international journal of biochemistry & cell biology *44*, 2278-2287.

Johannessen, C. M., Johnson, B. W., Williams, S. M., Chan, A. W., Reczek, E. E., Lynch, R. C., Rioth, M. J., McClatchey, A., Ryeom, S., and Cichowski, K. (2008). TORC1 is essential for NF1-associated malignancies. Current biology : CB *18*, 56-62.

Johannessen, C. M., Reczek, E. E., James, M. F., Brems, H., Legius, E., and Cichowski, K. (2005). The NF1 tumor suppressor critically regulates TSC2 and mTOR. Proceedings of the National Academy of Sciences of the United States of America *102*, 8573-8578.

Johansson, G., Mahller, Y. Y., Collins, M. H., Kim, M. O., Nobukuni, T., Perentesis, J., Cripe, T. P., Lane, H. A., Kozma, S. C., Thomas, G., and Ratner, N. (2008). Effective in vivo targeting of the mammalian target of rapamycin pathway in malignant peripheral nerve sheath tumors. Molecular cancer therapeutics *7*, 1237-1245.

Jones, K. L., and Buzdar, A. U. (2004). A review of adjuvant hormonal therapy in breast cancer. Endocrine-related cancer *11*, 391-406.

Kantoff, P. W., Higano, C. S., Shore, N. D., Berger, E. R., Small, E. J., Penson, D. F., Redfern, C. H., Ferrari, A. C., Dreicer, R., Sims, R. B., *et al.* (2010). Sipuleucel-T immunotherapy for castration-resistant prostate cancer. The New England journal of medicine *363*, 411-422.

Katz, D., Lazar, A., and Lev, D. (2009). Malignant peripheral nerve sheath tumour (MPNST): the clinical implications of cellular signalling pathways. Expert reviews in molecular medicine *11*, e30.

Keng, V. W., Rahrmann, E. P., Watson, A. L., Tschida, B. R., Moertel, C. L., Jessen, W. J., Rizvi, T. A., Collins, M. H., Ratner, N., and Largaespada, D. A. (2012a). PTEN and NF1 Inactivation in Schwann Cells Produces a Severe Phenotype in the Peripheral Nervous System That Promotes the Development and Malignant Progression of Peripheral Nerve Sheath Tumors. Cancer research.

Keng, V. W., Watson, A. L., Rahrmann, E. P., Li, H., Tschida, B. R., Moriarity, B. S., Choi, K., Rizvi, T. A., Collins, M. H., Wallace, M. R., *et al.* (2012b). Conditional Inactivation of Pten with EGFR Overexpression in Schwann Cells Models Sporadic MPNST. Sarcoma *2012*, 620834.

Klein, C. A. (2008). Cancer. The metastasis cascade. Science *321*, 1785-1787.

Kobayashi, C., Oda, Y., Takahira, T., Izumi, T., Kawaguchi, K., Yamamoto, H., Tamiya, S., Yamada, T., Oda, S., Tanaka, K., *et al.* (2006). Chromosomal aberrations and microsatellite instability of malignant peripheral nerve sheath tumors: a study of 10 tumors from nine patients. Cancer genetics and cytogenetics *165*, 98-105.

Kong, D., Li, Y., Wang, Z., and Sarkar, F. H. (2011). Cancer Stem Cells and Epithelial-to-Mesenchymal Transition (EMT)-Phenotypic Cells: Are They Cousins or Twins? Cancers *3*, 716-729.

Kourea, H. P., Bilsky, M. H., Leung, D. H., Lewis, J. J., and Woodruff, J. M. (1998). Subdiaphragmatic and intrathoracic paraspinal malignant peripheral nerve sheath tumors: a clinicopathologic study of 25 patients and 26 tumors. Cancer *82*, 2191-2203.

Kourea, H. P., Cordon-Cardo, C., Dudas, M., Leung, D., and Woodruff, J. M. (1999a). Expression of p27(kip) and other cell cycle regulators in malignant peripheral nerve sheath tumors and neurofibromas: the emerging role of p27(kip) in malignant transformation of neurofibromas. The American journal of pathology *155*, 1885-1891.

Kourea, H. P., Orlow, I., Scheithauer, B. W., Cordon-Cardo, C., and Woodruff, J. M. (1999b). Deletions of the INK4A gene occur in malignant peripheral nerve sheath tumors but not in neurofibromas. The American journal of pathology *155*, 1855-1860.

Kurzrock, R., Kantarjian, H. M., Druker, B. J., and Talpaz, M. (2003). Philadelphia chromosome-positive leukemias: from basic mechanisms to molecular therapeutics. Annals of internal medicine *138*, 819-830.

Lappe-Siefke, C., Goebbels, S., Gravel, M., Nicksch, E., Lee, J., Braun, P. E., Griffiths, I. R., and Nave, K. A. (2003). Disruption of Cnp1 uncouples oligodendroglial functions in axonal support and myelination. Nature genetics *33*, 366-374.

Largaespada, D. A. (2009). Transposon-mediated mutagenesis of somatic cells in the mouse for cancer gene identification. Methods *49*, 282-286.

Laycock-van Spyk, S., Thomas, N., Cooper, D. N., and Upadhyaya, M. (2011). Neurofibromatosis type 1-associated tumours: their somatic mutational spectrum and pathogenesis. Human genomics *5*, 623-690.

Lee, P. R., Cohen, J. E., Tendi, E. A., Farrer, R., GH, D. E. V., Becker, K. G., and Fields, R. D. (2004). Transcriptional profiling in an MPNST-derived cell line and normal human Schwann cells. Neuron glia biology *1*, 135-147.

Levy, P., Vidaud, D., Leroy, K., Laurendeau, I., Wechsler, J., Bolasco, G., Parfait, B., Wolkenstein, P., Vidaud, M., and Bieche, I. (2004). Molecular profiling of malignant peripheral nerve sheath tumors associated with neurofibromatosis type 1, based on large-scale real-time RT-PCR. Molecular cancer *3*, 20.

Ling, B. C., Wu, J., Miller, S. J., Monk, K. R., Shamekh, R., Rizvi, T. A., Decourten-Myers, G., Vogel, K. S., DeClue, J. E., and Ratner, N. (2005). Role for the epidermal growth factor receptor in neurofibromatosis-related peripheral nerve tumorigenesis. Cancer cell *7*, 65-75.

MacDonald, B. T., Tamai, K., and He, X. (2009). Wnt/beta-catenin signaling: components, mechanisms, and diseases. Developmental cell *17*, 9-26.

Mahller, Y. Y., Vaikunth, S. S., Ripberger, M. C., Baird, W. H., Saeki, Y., Cancelas, J. A., Crombleholme, T. M., and Cripe, T. P. (2008). Tissue inhibitor of metalloproteinase-3 via oncolytic herpesvirus inhibits tumor growth and vascular progenitors. Cancer research *68*, 1170-1179.

Mawrin, C. (2010). Critical role of PTEN for development and progression of nerve sheath tumors in neurofibromatosis type 1. Future oncology *6*, 499-501.

Mayes, D. A., Rizvi, T. A., Cancelas, J. A., Kolasinski, N. T., Ciraolo, G. M., Stemmer-Rachamimov, A. O., and Ratner, N. (2011). Perinatal or adult Nf1

inactivation using tamoxifen-inducible PlpCre each cause neurofibroma formation. Cancer research *71*, 4675-4685.

Miller, M. J., Foy, K. C., and Kaumaya, P. T. (2013). Cancer immunotherapy: present status, future perspective, and a new paradigm of peptide immunotherapeutics. Discovery medicine *15*, 166-176.

Miller, S. J., Jessen, W. J., Mehta, T., Hardiman, A., Sites, E., Kaiser, S., Jegga, A. G., Li, H., Upadhyaya, M., Giovannini, M., *et al.* (2009). Integrative genomic analyses of neurofibromatosis tumours identify SOX9 as a biomarker and survival gene. EMBO molecular medicine *1*, 236-248.

Miller, S. J., Rangwala, F., Williams, J., Ackerman, P., Kong, S., Jegga, A. G., Kaiser, S., Aronow, B. J., Frahm, S., Kluwe, L., *et al.* (2006). Large-scale molecular comparison of human schwann cells to malignant peripheral nerve sheath tumor cell lines and tissues. Cancer research *66*, 2584-2591.

Mo, W., Chen, J., Patel, A., Zhang, L., Chau, V., Li, Y., Cho, W., Lim, K., Xu, J., Lazar, A. J., *et al.* (2013). CXCR4/CXCL12 Mediate Autocrine Cell- Cycle Progression in NF1-Associated Malignant Peripheral Nerve Sheath Tumors. Cell *152*, 1077-1090.

Moses, M. A., Brem, H., and Langer, R. (2003). Advancing the field of drug delivery: taking aim at cancer. Cancer cell *4*, 337-341.

Murphree, A. L., and Benedict, W. F. (1984). Retinoblastoma: clues to human oncogenesis. Science *223*, 1028-1033.

Nielsen, G. P., Stemmer-Rachamimov, A. O., Ino, Y., Moller, M. B., Rosenberg, A. E., and Louis, D. N. (1999). Malignant transformation of neurofibromas in

neurofibromatosis 1 is associated with CDKN2A/p16 inactivation. The American journal of pathology *155*, 1879-1884.

Noble, C. O., Kirpotin, D. B., Hayes, M. E., Mamot, C., Hong, K., Park, J. W., Benz, C. C., Marks, J. D., and Drummond, D. C. (2004). Development of ligand-targeted liposomes for cancer therapy. Expert opinion on therapeutic targets *8*, 335-353.

O'Brien, S. G., Guilhot, F., Larson, R. A., Gathmann, I., Baccarani, M., Cervantes, F., Cornelissen, J. J., Fischer, T., Hochhaus, A., Hughes, T., *et al.* (2003). Imatinib compared with interferon and low-dose cytarabine for newly diagnosed chronic-phase chronic myeloid leukemia. The New England journal of medicine *348*, 994-1004.

Packer, R. J., Gutmann, D. H., Rubenstein, A., Viskochil, D., Zimmerman, R. A., Vezina, G., Small, J., and Korf, B. (2002). Plexiform neurofibromas in NF1: toward biologic-based therapy. Neurology *58*, 1461-1470.

Packer, R. J., and Rosser, T. (2002). Therapy for plexiform neurofibromas in children with neurofibromatosis 1: an overview. Journal of child neurology *17*, 638-641; discussion 646-651.

Pardoll, D. M. (2012). The blockade of immune checkpoints in cancer immunotherapy. Nature reviews Cancer *12*, 252-264.

Payne, K. K., Toor, A. A., Wang, X. Y., and Manjili, M. H. (2012). Immunotherapy of cancer: reprogramming tumor-immune crosstalk. Clinical & developmental immunology *2012*, 760965.

Persad, S., Troussard, A. A., McPhee, T. R., Mulholland, D. J., and Dedhar, S. (2001). Tumor suppressor PTEN inhibits nuclear accumulation of beta-catenin

and T cell/lymphoid enhancer factor 1-mediated transcriptional activation. The Journal of cell biology *153*, 1161-1174.

Persidis, A. (1999). Cancer multidrug resistance. Nature biotechnology *17*, 94-95.

Populo, H., Lopes, J. M., and Soares, P. (2012). The mTOR Signalling Pathway in Human Cancer. International journal of molecular sciences *13*, 1886-1918.

Porter, D. L., Levine, B. L., Kalos, M., Bagg, A., and June, C. H. (2011). Chimeric antigen receptor-modified T cells in chronic lymphoid leukemia. The New England journal of medicine *365*, 725-733.

Prada, C. E., Jousma, E., Rizvi, T. A., Wu, J., Dunn, R. S., Mayes, D. A., Cancelas, J. A., Dombi, E., Kim, M. O., West, B. L., *et al.* (2013). Neurofibroma-associated macrophages play roles in tumor growth and response to pharmacological inhibition. Acta neuropathologica *125*, 159-168.

Provenzano, P. P., Cuevas, C., Chang, A. E., Goel, V. K., Von Hoff, D. D., and Hingorani, S. R. (2012). Enzymatic targeting of the stroma ablates physical barriers to treatment of pancreatic ductal adenocarcinoma. Cancer cell *21*, 418-429.

Raghu, G., Johnson, W. C., Lockhart, D., and Mageto, Y. (1999). Treatment of idiopathic pulmonary fibrosis with a new antifibrotic agent, pirfenidone: results of a prospective, open-label Phase II study. American journal of respiratory and critical care medicine *159*, 1061-1069.

Rahrmann, E. P., Watson, A. L., Keng, V. W., Choi, K., Moriarity, B. S., Beckmann, D. A., Wolf, N. K., Sarver, A., Collins, M. H., Moertel, C. L., *et al.* (2013). Forward genetic screen for malignant peripheral nerve sheath tumor

formation identifies new genes and pathways driving tumorigenesis. Nature genetics.

Rajagopalan, H., and Lengauer, C. (2004). Aneuploidy and cancer. Nature *432*, 338-341.

Rasband, W. S. (1997-2012). ImageJ.

Renan, M. J. (1993). How many mutations are required for tumorigenesis? Implications from human cancer data. Molecular carcinogenesis *7*, 139-146.

Restifo, N. P., Dudley, M. E., and Rosenberg, S. A. (2012). Adoptive immunotherapy for cancer: harnessing the T cell response. Nature reviews Immunology *12*, 269-281.

Riman, T., Persson, I., and Nilsson, S. (1998). Hormonal aspects of epithelial ovarian cancer: review of epidemiological evidence. Clinical endocrinology *49*, 695-707.

Rini, B. I. (2007). Vascular endothelial growth factor-targeted therapy in renal cell carcinoma: current status and future directions. Clinical cancer research : an official journal of the American Association for Cancer Research *13*, 1098-1106.

Rizzardi, A. E., Johnson, A. T., Vogel, R. I., Pambuccian, S. E., Henriksen, J., Skubitz, A. P., Metzger, G. J., and Schmechel, S. C. (2012). Quantitative comparison of immunohistochemical staining measured by digital image analysis versus pathologist visual scoring. Diagnostic pathology *7*, 42.

Rosenberg, S. A. (2011). Cell transfer immunotherapy for metastatic solid cancer--what clinicians need to know. Nature reviews Clinical oncology *8*, 577-585.

Ross, J. S., Schenkein, D. P., Pietrusko, R., Rolfe, M., Linette, G. P., Stec, J., Stagliano, N. E., Ginsburg, G. S., Symmans, W. F., Pusztai, L., and Hortobagyi, G. N. (2004). Targeted therapies for cancer 2004. American journal of clinical pathology *122*, 598-609.

Sarver, A. L., Erdman, J., Starr, T., Largaespada, D. A., and Silverstein, K. A. (2012). TAPDANCE: an automated tool to identify and annotate transposon insertion CISs and associations between CISs from next generation sequence data. BMC bioinformatics *13*, 154.

Sawyers, C. (2004). Targeted cancer therapy. Nature *432*, 294-297.

Seshagiri, S., Stawiski, E. W., Durinck, S., Modrusan, Z., Storm, E. E., Conboy, C. B., Chaudhuri, S., Guan, Y., Janakiraman, V., Jaiswal, B. S., *et al.* (2012). Recurrent R-spondin fusions in colon cancer. Nature *488*, 660-664.

Shankaran, V., Ikeda, H., Bruce, A. T., White, J. M., Swanson, P. E., Old, L. J., and Schreiber, R. D. (2001). IFNgamma and lymphocytes prevent primary tumour development and shape tumour immunogenicity. Nature *410*, 1107-1111.

Sharpless, N. E., and Depinho, R. A. (2006). The mighty mouse: genetically engineered mouse models in cancer drug development. Nature reviews Drug discovery *5*, 741-754.

Siegel, R., DeSantis, C., Virgo, K., Stein, K., Mariotto, A., Smith, T., Cooper, D., Gansler, T., Lerro, C., Fedewa, S., *et al.* (2012). Cancer treatment and survivorship statistics, 2012. CA: a cancer journal for clinicians *62*, 220-241.

Sierra, J. R., Cepero, V., and Giordano, S. (2010). Molecular mechanisms of acquired resistance to tyrosine kinase targeted therapy. Molecular cancer *9*, 75.

Sjoblom, T., Jones, S., Wood, L. D., Parsons, D. W., Lin, J., Barber, T. D., Mandelker, D., Leary, R. J., Ptak, J., Silliman, N., *et al.* (2006). The consensus coding sequences of human breast and colorectal cancers. Science *314*, 268-274.

Smith, N. D., Rubenstein, J. N., Eggener, S. E., and Kozlowski, J. M. (2003). The p53 tumor suppressor gene and nuclear protein: basic science review and relevance in the management of bladder cancer. The Journal of urology *169*, 1219-1228.

Spurlock, G., Knight, S. J., Thomas, N., Kiehl, T. R., Guha, A., and Upadhyaya, M. (2010). Molecular evolution of a neurofibroma to malignant peripheral nerve sheath tumor (MPNST) in an NF1 patient: correlation between histopathological, clinical and molecular findings. Journal of cancer research and clinical oncology *136*, 1869-1880.

Stegmeier, F., Warmuth, M., Sellers, W. R., and Dorsch, M. (2010). Targeted cancer therapies in the twenty-first century: lessons from imatinib. Clinical pharmacology and therapeutics *87*, 543-552.

Stemmer-Rachamimov, A. O., Louis, D. N., Nielsen, G. P., Antonescu, C. R., Borowsky, A. D., Bronson, R. T., Burns, D. K., Cervera, P., McLaughlin, M. E., Reifenberger, G., *et al.* (2004). Comparative pathology of nerve sheath tumors in mouse models and humans. Cancer research *64*, 3718-3724.

Sudhakar, A. (2009). History of Cancer, Ancient and Modern Treatment Methods. Journal of cancer science & therapy *1*, 1-4.

Tabone-Eglinger, S., Bahleda, R., Cote, J. F., Terrier, P., Vidaud, D., Cayre, A., Beauchet, A., Theou-Anton, N., Terrier-Lacombe, M. J., Lemoine, A., *et al.* (2008). Frequent EGFR Positivity and Overexpression in High-Grade Areas of Human MPNSTs. Sarcoma *2008*, 849156.

Tawbi, H., Thomas, D., Lucas, D. R., Biermann, J. S., Schuetze, S. M., Hart, A. L., Chugh, R., and Baker, L. H. (2008). Epidermal growth factor receptor expression and mutational analysis in synovial sarcomas and malignant peripheral nerve sheath tumors. The oncologist *13*, 459-466.

Thompson, N., and Lyons, J. (2005). Recent progress in targeting the Raf/MEK/ERK pathway with inhibitors in cancer drug discovery. Current opinion in pharmacology *5*, 350-356.

Topalian, S. L., Hodi, F. S., Brahmer, J. R., Gettinger, S. N., Smith, D. C., McDermott, D. F., Powderly, J. D., Carvajal, R. D., Sosman, J. A., Atkins, M. B., *et al.* (2012). Safety, activity, and immune correlates of anti-PD-1 antibody in cancer. The New England journal of medicine *366*, 2443-2454.

Uhlmann, E. J., and Plotkin, S. R. (2012). Neurofibromatoses. Advances in experimental medicine and biology *724*, 266-277.

Vincent W. Keng, A. L. W., Eric P. Rahrmann, Hua Li, Barbara R. Tschida, Branden S. Moriarity, Kwangmin Choi, Tilat A. Rizvi, Margaret H. Collins, Margaret R. Wallace, Nancy Ratner and David A. Largaespada (2012). Conditional inactivation of Pten together with EGFR overexpression in Schwann cells models sporadic MPNST. Sarcoma.

Vogel, K. S., Klesse, L. J., Velasco-Miguel, S., Meyers, K., Rushing, E. J., and Parada, L. F. (1999). Mouse tumor model for neurofibromatosis type 1. Science *286*, 2176-2179.

Wang, J. Y., Wilcoxen, K. M., Nomoto, K., and Wu, S. (2007). Recent advances of MEK inhibitors and their clinical progress. Current topics in medicinal chemistry *7*, 1364-1378.

Watson, A. L., Rahrmann, E. P., Moriarity, B. S., Choi, K., Conboy, C. B., Greeley, A. D., Halfond, A. L., Anderson, L. K., Wahl, B. R., Keng, V. W., *et al.* (2013). Canonical Wnt/beta-catenin Signaling Drives Human Schwann Cell Transformation, Progression, and Tumor Maintenance. Cancer discovery.

Weinberg, R. A. (1991). Tumor suppressor genes. Science *254*, 1138-1146.

Weiss, W. A., Israel, M., Cobbs, C., Holland, E., James, C. D., Louis, D. N., Marks, C., McClatchey, A. I., Roberts, T., Van Dyke, T., *et al.* (2002). Neuropathology of genetically engineered mice: consensus report and recommendations from an international forum. Oncogene *21*, 7453-7463.

Whiteside, T. L. (2006). Immune suppression in cancer: effects on immune cells, mechanisms and future therapeutic intervention. Seminars in cancer biology *16*, 3-15.

Widemann, B. C. (2009). Current status of sporadic and neurofibromatosis type 1-associated malignant peripheral nerve sheath tumors. Current oncology reports *11*, 322-328.

Wong, W. W., Hirose, T., Scheithauer, B. W., Schild, S. E., and Gunderson, L. L. (1998). Malignant peripheral nerve sheath tumor: analysis of treatment outcome. International journal of radiation oncology, biology, physics *42*, 351-360.

Wu, J., Dombi, E., Jousma, E., Scott Dunn, R., Lindquist, D., Schnell, B. M., Kim, M. O., Kim, A., Widemann, B. C., Cripe, T. P., and Ratner, N. (2012). Preclincial testing of sorafenib and RAD001 in the Nf(flox/flox) ;DhhCre mouse model of plexiform neurofibroma using magnetic resonance imaging. Pediatric blood & cancer *58*, 173-180.

Wu, J., Williams, J. P., Rizvi, T. A., Kordich, J. J., Witte, D., Meijer, D., Stemmer-Rachamimov, A. O., Cancelas, J. A., and Ratner, N. (2008). Plexiform and dermal neurofibromas and pigmentation are caused by Nf1 loss in desert hedgehog-expressing cells. Cancer cell *13*, 105-116.

Xiao, A., Yin, C., Yang, C., Di Cristofano, A., Pandolfi, P. P., and Van Dyke, T. (2005). Somatic induction of Pten loss in a preclinical astrocytoma model reveals major roles in disease progression and avenues for target discovery and validation. Cancer research *65*, 5172-5180.

Yan, N., Ricca, C., Fletcher, J., Glover, T., Seizinger, B. R., and Manne, V. (1995). Farnesyltransferase inhibitors block the neurofibromatosis type I (NF1) malignant phenotype. Cancer research *55*, 3569-3575.

Yao, H., Ashihara, E., and Maekawa, T. (2011). Targeting the Wnt/beta-catenin signaling pathway in human cancers. Expert opinion on therapeutic targets *15*, 873-887.

Zhang, W., and Liu, H. T. (2002). MAPK signal pathways in the regulation of cell proliferation in mammalian cells. Cell research *12*, 9-18.

Zhu, Y., Ghosh, P., Charnay, P., Burns, D. K., and Parada, L. F. (2002). Neurofibromas in NF1: Schwann cell origin and role of tumor environment. Science *296*, 920-922.

Zhu, Y., Harada, T., Liu, L., Lush, M. E., Guignard, F., Harada, C., Burns, D. K., Bajenaru, M. L., Gutmann, D. H., and Parada, L. F. (2005). Inactivation of NF1 in CNS causes increased glial progenitor proliferation and optic glioma formation. Development *132*, 5577-5588.

zur Hausen, H. (1991). Viruses in human cancers. Science *254*, 1167-1173.